PSERC

Avoiding and Suppressing Oscillations

Final Project Report

Power Systems Engineering Research Center

A National Science Foundation
Industry/University Cooperative Research Center
since 1996

Cornell • Arizona State • Berkeley • Carnegie Mellon • Colorado School of Mines
Georgia Tech • Illinois • Iowa State • Texas A&M • Washington State • Wisconsin

Avoiding and Suppressing Oscillations

Final Report

Research Team Faculty

Ian Dobson, Project Leader
Fernando L. Alvarado
Christopher L. DeMarco
University of Wisconsin-Madison

Peter W. Sauer
University of Illinois at Urbana-Champaign

Research Team Students

Scott Greene
Henrik Engdahl
Jianfeng Zhang

PSERC Publication 00-01

December 1999

Information about this Project

For information about this project contact:

Ian Dobson, Project Leader
Professor
Electrical and Computer Engineering
University of Wisconsin-Madison
1415 Engineering Drive
Phone: 607-262-2661
Fax: 607-262-1267
Email: dobson@engr.wisc.edu

Additional Copies of the Report

Copies of this report can be obtained from the Power Systems Engineering Research Center's website, www.pserc.wisc.edu. The PSERC publication number is 00-01. For additional information, contact:

Power Systems Engineering Research Center
Cornell University
428 Phillips Hall
Ithaca, New York 14853
Phone: 607-255-5601
Fax: 607-255-8871

Notice Concerning Copyright Material

Contents

1 Introduction

This is the final report for the 1997-99 PSerc project on interarea electric power system oscillations. The main project objective is to determine the feasibility of computations to avoid or suppress large scale system oscillations. Further project materials, including interim reports, software and test cases are available on the Pserc web site [60].

1.1 Main accomplishments

The main accomplishments of the project are

1. Discovery and initial analysis of a new mechanism for oscillations in which a strong resonance between two oscillatory modes is a precursor to the oscillations.

2. Assessment of the computational speed of advanced eigenvalue algorithms for oscillations and its scaling with system size.

3. Analysis of a steady state "angle collapse" instability preceded by resonance in a low frequency oscillatory mode and caused by increasing interarea transfer.

4. Improved eigenvalue sensitivity formulas taking account of the different time scales of oscillations and operator actions.

5. New methods for quantifying the robustness of eigenvalues to uncertainties such as poorly known load or generator data.

6. Nine, fourteen and thirty seven bus systems oscillation test cases.

7. Foundational work towards a new generation of dynamics software with algebraically assisted numerics.

8. Outline of an opportunity for the combined use of system measurements and model based software for real time control of oscillations.

9. Identification of key barriers to developing software to assist the real time suppression and avoidance of oscillations.

1.2 Background on oscillations

The power system may be thought of as a large, nonlinear system with many lightly damped electromechanical modes of oscillation. If the damping of these modes become too small or positive, then the resulting oscillations can cause equipment

damage or malfunction. Practical definitions of power system security often require sufficient damping of oscillatory modes [16] and power transfers on tie lines are sometimes limited by oscillations.

Power transactions are increasing in volume and variety in restructured power systems because of the large amounts of money to be made in exploiting geographic differences in power prices and costs. Restructured power systems are expected to be operated at a greater variety of operating points and closer to their operating constraints. The onset of low frequency interarea oscillations is one operational constraint which already limits bulk power transactions under some conditions [16, 32, 33]. Better methods of simulating and analyzing oscillations would lead to more accurate determination of these limits and the ability to operate the power system closer to these limits. In particular, the ability to use software to advise operators to better avoid or suppress oscillations in real time would allow the power system to be operated closer to oscillation limits.

For example, real time calculation of an oscillation limit would reduce the conservatism necessary when applying a limit derived off line to the necessarily different on line conditions. If the uncertainty in the limit calculation could also be quantified, this would allow improved and more defensible safety margins in transfer limits. Further, if an oscillation does occur, advice to operators about how to quickly suppress it would be very valuable. Past incidents such as the Rush Island incident in 1992 [37] have taken considerable time for operators to arrive at actions to suppress the oscillations. In general, confidence in being able to quickly suppress oscillations, particularly those oscillations which would be likely to occur if a fault occurred would enable the power system to be more fully utilized. There are substantial economic, social and environmental benefits to the utilities, the public and industry in operating the power system up to but not past its limits.

Interarea oscillations are observed as oscillations of real power flow between regions of a power system or groups of generators [33]. Voltages and current oscillate with the power swings. Sufficiently large oscillations trip, stress or damage equipment and can disrupt monitoring devices. In particular, oscillations can cause voltages to exceed limits causing protective devices to trip and forcing equipment outages. Thus oscillations play a role in the cascading outages causing blackouts.

Interarea oscillations are a complex phenomenon with potentially many contributing causes which can span the entire Eastern or Western interconnections of North America. This spanning of corporate and institutional boundaries puts a premium on understanding oscillations and arriving at defensible and reliable ways to avoid or suppress them.

Two prominent types of subsynchronous power system oscillations are

- Interarea oscillations: Power system areas swing against each other at frequen-

cies of 0.1 Hz to 1 Hz.

- Local oscillations: Typically one plant swinging against the rest of the system or several generators swinging against each other at frequencies of 1 Hz to 2 Hz.

Some of the project methods apply to both types of oscillations, but the project concentrates on interarea oscillations. Torsional oscillations involving interaction of generator shaft modes with the power system are not considered in this project.

The power system without controls has many lightly damped electromechanical modes. Much of the positive damping originates in the steam turbine driven generators and the loads. Power system controls significantly affect the damping and can contribute either positive or negative damping. Generation control and particularly the generator voltage regulation can be significant sources of negative damping. For weak tie lines and high power transfers, an oscillation in real power also causes an oscillation in voltage magnitudes and interaction with the generator voltage regulation. High gain in the generator voltage regulation can lead to poor or negative damping of the oscillation. This problem led to the deployment of power system stabilizers to modify the voltage regulation to damp these oscillations sufficiently. Power system stabilizers are effective, but the resulting higher limits on tie line transfers may still be associated with oscillations.

Three ways in which oscillations can arise are

- Spontaneous oscillations. Spontaneous oscillations arise when the mode damping becomes negative by a gradual change in system conditions. The oscillations grow and may reach a steady state in which the oscillations persist at constant amplitude.

- Oscillations due to a disturbance. Outage of a line or generator under unfavorable conditions can cause oscillations by suddenly reducing damping of a mode. If the mode damping becomes negative, sustained or increasing oscillations result. If the mode becomes poorly damped, the disturbance can excite the mode to cause a transient oscillation. These transient oscillations eventually decay, but can be of sufficient amplitude and duration to be harmful.

- Forced oscillations due to incomplete islanding or pulsating loads. Forced oscillations are not considered in this project.

1.3 Related work by others

This section reviews some work by others closely related or relevant to the project. Some useful references are indicated.

1.3.1 Avoiding oscillations by controller design

There is a large amount of valuable work done to avoid oscillations by design or redesign of system controls, including generator regulators such as power system stabilizers, FACTS devices such as SVC, and HVDC. Analytic methods used to help design these controls generally linearize a detailed power system dynamic model about an operating point and then apply control theory to the linearized model. The damping, frequency and form of the system modes can be studied with eigenanalysis. The choice of controller input and output signals is important and relies on concepts of modal controllability and observability. The possibilities of adverse interactions with other controls and the robustness of the control design to different operating conditions are considered.

The power system linearization at an operating point can vary in two ways:

1. Changing controller gains changes the formula for the linearization. System changes such as line outages or enabling or disabling controllers can also change the linearization formula.

2. Changing the operating point changes the linearization by changing where the formula for the linearization is evaluated. For example, operator actions such as changing the generator dispatch or switching capacitor banks change the operating point. Line outages also change the operating point.

The work on control system design focuses on adding controllers (e.g. PSS) or changing controller gains to affect the linearization formula. Changes in operating point are only considered at a later stage when testing the design for robustness. Note that changes in controller gains do not change the operating point.

In contrast, the work on this project focuses on how changes in the operating point change the linearization:

> *One of the themes of the project is to analyze how the change in operating point affects the linearization and hence the oscillatory mode damping and furthermore to exploit this relationship to suppress or avoid the oscillation.*

The relationship between the operating point and the linearization depends on the nonlinearity of the power system. Essentially we seek to exploit this nonlinearity to find changes in operating point which suppress oscillations.

1.3.2 Useful references

References [67, 41] include both contemporary and classical approaches to power system dynamic stability and machine modeling. The texts [81, 9, 42] all contain

informative descriptions of the Automatic Generation Control (AGC) and tie line bias control. The working group paper [34] and its many discussions provide an accurate assessment of current AGC practices and emphasize the time scale appropriate for AGC. Anderson and Fouad [7] is the classic text for power system control and stability.

In dynamical systems terminology, oscillations arise as Hopf bifurcations. The basic mathematical analysis of the Hopf bifurcation is well covered in [27] and computational methods to locate Hopf bifurcations are presented in [70]. Eigenvalue parametric sensitivity and generalized eigenvalue computation is addressed in [26]. Previous work concerning Hopf bifurcations in power systems includes [1], [21], [47] and [37]. [12] and [30] address saddle node bifurcation in systems of differential-algebraic equations. Applicable work regarding small signal stability and eigensensitivity includes [33], [50], [71].

Methods for computing eigenvalues and eigenvectors for power systems are presented in [50, 76, 82, 5] and for general sparse unsymmetric matrices in [25].

1.4 Summary guide to this report

Section 2 summarizes the power system test cases used in the project.

Section 3 illustrates various applications of the eigenvalue sensitivity computations that are a major tool in the project work. Oscillation test cases are presented and used to demonstrate the use of eigenvalue sensitivity methods to predict the effects of various operator controls and estimate the robustness to data. Model results are compared with PSS/E.

Section 4 discusses the modeling required to represent both the dynamics of oscillations and operator actions. The eigenvalue sensitivity formula is derived and several applications to optimum redispatch, quantifying eigenvalue uncertainty and margin sensitivity are discussed.

Section 5 examines the scaling of computational speed with system size for advanced eigenvalue algorithms. Special models with scalable size approximating realistic models for computational purposes are devised and tested. A typical result is that one can compute 5 eigenvalues of a power system with 300 seventh order generator models in less than one minute using Matlab on a 233 MHz Pentium II.

Section 6 reviews the software approaches used in the project and, based on this experience, suggests concepts and development directions for large scale dynamic software.

Section 7 reports a new mechanism for interarea oscillations involving resonance between closely spaced system modes. The new mechanism has been simulated on a 9 bus test system with detailed generator models. General mathematical considerations suggest that the new mechanism can occur in large scale practical power systems.

Section 8 Approximating generator models with swing equations allows oscillation modes which are primarily electromechanical to be studied in reduced equations which are of a modified Hamiltonian form. Using this approximation, a low frequency mode in a 14 bus system was observed to reduce to zero frequency and then cause a loss of steady state stability as an interarea transfer was increased. This event can be computed using the reduced model if the pattern of oscillation is known.

Section 9 reviews some work on real time power system measurements which complements the project work. In particular, the measurements could be used to help identify critical eigenvalues by estimating their frequencies.

Section 10 presents promising project ideas that were not fully pursued.

Section 11 outlines the principal barriers to computations assisting operators to suppress or avoid oscillations and discusses the prospects for overcoming these barriers.

Section 12 describes the project work statement, budgets and deliverables of the project.

1.5 Acknowledgments

The work described in this report was sponsored in part by the Power Systems Engineering Research Center (PSERC). We express our appreciation for the support provided by PSERC's industrial members and by the National Science Foundation through the following grants received under the Industry/University Cooperative Research Center program: NSF EEC 96-15792 (University of Illinois at Urbana-Champaign) and 96-15778 (University of Wisconsin-Madison).

Funding in part from NSF PYI grant ECS-9157192 is gratefully acknowledged. Chris DeMarco's work was also supported in part by the Western Area Power Administration. Henrik Engdahl gratefully acknowledges support in part from KTH (Royal Institute of Technology), Stockholm, Sweden and Elforsk AB, Sweden.

The 37 bus data was graciously provided by ESEERCO. We thank Graham Rogers for advice about generator modeling and Lawrence Jones and Göran Andersson for assistance in finding references by Seyranian.

2 Test systems

2.1 Assumption of a good dynamic model

One set of methods to avoiding or suppressing oscillations may be called exact. Exact methods assume that a dynamic power system model is available which corresponds sufficiently well with the real power system for the purpose of studying interarea oscillations or estimating suitable control actions. Uncertainties in satisfying this assumption include determining dynamic load models [48], verifying data for controls of generators and other devices, and ensuring that the model reflects the actual system configuration and control options. While satisfying this assumption may be challenging in practice, this assumption is made for much of the project for several reasons:

- it allows the computational limitations for the exact methods to be assessed by themselves, separate from modeling concerns.
- the models and analysis used for exact methods are essential for developing and testing approximate methods.
- analysis of models that are as accurate as possible is used to study oscillations offline in power systems and these models are improving. The project is aimed towards operator actions, but the methods developed are also useful offline.
- the modeling accuracy needed for estimating suitable operator control actions is not known and it is possible that the control actions could be insensitive to some of the modeling. For example, it is possible that the model could incorrectly predict the value of a modal damping, but correctly select a control action increasing that damping.

2.2 Model overview

The power system models for the exact methods need to be detailed and large enough to allow methods to be developed and assessed. The project works with models with up to 37 buses in order to assess the potential of methods for larger systems. However, some of the numerical experiments on computational speed have been performed on much larger networks. All work assumes that methods must ultimately be practical on larger systems.

The dynamic power system model represents many of the generators in detail with up to 12 states. An example of the generator modeling is a fourth-order synchronous machine (angle, speed, field flux, one damper winding) with an IEEE

type I excitation system (third order), and first-order models for the turbine, boiler, and governor.

Load modeling is done by specifying proportions of constant admittance, constant current, and constant power. Avoiding pure constant power loads could be sufficient to avoid singularity of the algebraic equations. Load modeling presents some significant uncertainties. The dynamics of loads do affect oscillations but the project will not represent these dynamics because of the difficulties of obtaining suitable data. However, the project has developed an efficient method to quickly quantify the robustness of eigenvalue calculations with respect to load data and the project methods are consistent with future elaboration of the load models.

Many of the project models are available on the Pserc web site [60].

2.2.1 3 bus test system

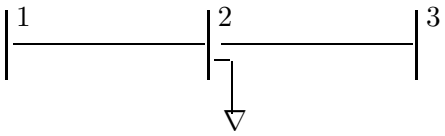

Figure 1: Three bus power system

The three bus system consists of generators at bus 1 and bus 3 and a constant power load at bus 2 as shown in Figure 1. One of the generators is a slack bus for load flow calculations. Both generators are modeled as round rotor generators with six dynamic states, accounting for both the transient and the subtransient impedances. The exciters are of IEEE type 1 with four dynamic states [31]. The load is modeled as a constant power load. The system parameters are reported in section A.1.

2.2.2 9 bus test system

The 9 bus test system has 3 generators and 27 dynamic states. The 9 bus test system is essentially the WSCC system from the text of Sauer and Pai [67] with some adjustment in loading. The generator models have been adjusted to match generator models available in the PSS/E software and the generator data is adapted from machines in the New York Power Pool 37 bus system. The generators are round rotor with d and q axis transient and subtransient effects and saturation effects represented. The exciters are IEEE type 1. Exciter saturation is represented but hard limits are not represented.

The real power portion of the loads are modeled as 60% admittance and 40% constant current. The reactive power portion of the loads are modeled as 50%

impedance and 50% constant current.

The 9 bus system can be viewed as representing a three area system with one generator per area and each area intertied to the other two areas. More details of the 9 bus system are given in section A.2.

2.2.3 14 bus test system

The 14 bus test system is a slightly modified version of the IEEE 14 bus system. The generators are modeled by classical swing equations with equal damping so that the model has a modified Hamiltonian structure. More details of the 14 bus system are given in section 8.

2.2.4 37 bus test system

The 37 bus test system has 28 generators and is based on a 37 bus equivalent of the New York Power Pool. The data includes many different generator models and was supplied by ESEERCO in PSS/E format. We first summarize the full model provided by ESEERCO: There are 37 generators, of which 11 are two axis round rotor machines with transient and subtransient effects, 3 are salient pole machines with transient and subtransient effects on the q axis only, and the remainder are classical swing equation models. There are 12 exciters of 6 different types and 6 stabilizers of 4 different types. One hydro unit has a governor represented. There are two SVC devices.

The following version of the full model was implemented: All 3 generator models are implemented without change. Two of the exciter models are implemented, in particular, IEEE Type 1 and IEEE Type ST1; this accounts for 7 of the exciters. Two other exciters are approximated by an IEEE Type 1. A third generic and simple exciter model is implemented to approximately represent the remaining 3 exciters. The stabilizers, hydro governor and SVCs are not represented. Quadratic saturation effects are represented throughout but hard limits are not represented. More details of the 37 bus system are given in section B.

3 Test cases showing application of sensitivities

One of the main themes of the project is computing and applying the sensitivity of eigenvalues to system parameters. This section illustrates the use of sensitivity calculations to suppress oscillations by suitable operator actions. The associated theory and algorithms are described in later sections. Many of the test cases are available on the Pserc web site [60].

3.1 Producing an unstable case for the 9 bus system

The first task is to modify the base case for the 9 bus system to produce an unstable case that has oscillations. The base case has parameters:

$pl1$	$ql1$	$pl2$	$ql2$	$pl5$	$ql5$	$pl6$	$ql6$
1.8	0.265	0.5	0.0	0.25	0.075	0.25	0.075
$pl8$	$ql8$	$v1$	$v2$	$v3$	$pg2$	$pg3$	
1.0	0.35	1.02	0.99	1.005	1.5	1.5	

All values are in per unit. The following parameter changes were implemented simultaneously and the eigenvalues computed at each step:

parameter	initial value	final value	increment
$pl5$	0.25	2.0	0.25
$pl6$	0.25	2.0	0.25
$pl8$	1.0	2.75	0.25
$pg2$	1.5	3.25	0.25
$pg3$	1.5	2.375	0.125

Figure 2 shows how some eigenvalues change with the parameters.

At the final value, an eigenvalue $\lambda = 0.1324 + 3.0767j$ is located in the right half plane (this oscillatory mode also has a complex conjugate eigenvalue at $\overline{\lambda} = 0.1324 - 3.0767j$). This unstable mode indicates oscillatory instability at 0.49 Hz. The objective of operator action is to suppress oscillation by stabilizing this unstable mode.

3.2 Sensitivity validation

This subsection validates eigenvalue sensitivity formula (64) which is derived and explained in section 4. Note that this procedure is evaluating analytically derived formulas and *not* simply incrementing the parameter, recomputing the eigenvalue, subtracting, and dividing by the parameter increment.

In the unstable case produced in subsection 3.1, the critical eigenvalue is $\lambda = 0.1324 + 3.0767j$ in the right half plane. We write $\lambda_p = \frac{\partial \lambda}{\partial p}$ for the sensitivity of

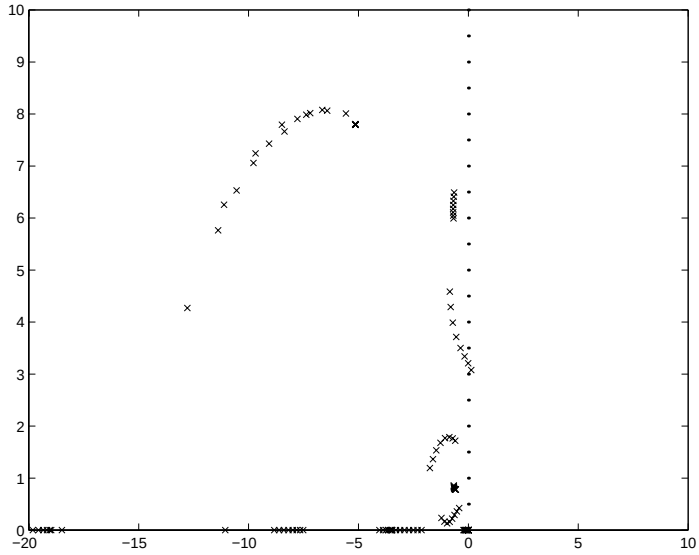

Figure 2: Change in eigenvalues as the parameters are changed from their base case values in the 9 bus system (case2).

eigenvalue λ with respect to p. To validate the formula (64) for λ_p, table 1 shows the real parts of λ_p, λ^+ and λ^* for several parameters p. λ^+ is the predicted eigenvalue

p	$pl2$	$ql2$	$pl8$	$ql8$	$v1$	$v2$	$v3$	$pg2$	$pg3$
λ_p	-0.8179	-0.7465	-0.8641	-0.5382	2.9667	-8.6458	-1.9151	1.8066	0.9920
λ^+	0.1316	0.1317	0.1315	0.1319	0.1354	0.1238	0.1305	0.1342	0.1334
λ^*	0.1316	0.1317	0.1315	0.1319	0.1354	0.1238	0.1305	0.1342	0.1334

Table 1: Validation of sensitivity to parameters

assuming that the parameter changed by 0.001 per unit, where the prediction is obtained using the computed value of λ_p:

$$\lambda^+ = \lambda + 0.001\lambda_p \tag{1}$$

λ^* is the eigenvalue recomputed assuming that the parameter changed by 0.001 per unit. The match between the real parts of λ^* and λ^+ validates the formula used for λ_p.

3.3 Control by redispatch

This subsection illustrates the control by redispatch to suppress an oscillation and the prediction of control effectiveness using eigenvalue sensitivities.

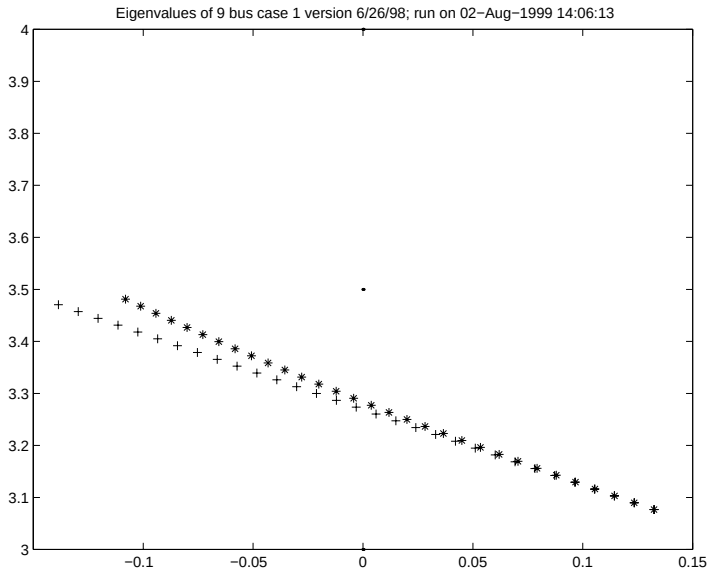

Figure 3: Eigenvalue variation with redispatch; +=predicted with sensitivity, *=actual

The unstable case produced in subsection 3.1 is assumed. Table 1 shows that decreasing generation at bus 2 and/or bus 3 will move the unstable eigenvalue to the left. The sensitivities show that decreasing generation at bus 2 is more effective. Figure 3 shows how the critical eigenvalue changes when $pg2$ is changed from 3.25 pu to 3.1 pu in steps of 0.005 pu. Points labeled + are the linear prediction of the eigenvalue using sensitivity, while points labeled * are the actual eigenvalues.

3.4 Control by adding reactive load

This subsection illustrates the selection of reactive compensation controls to suppress an oscillation and the prediction of control effectiveness using eigenvalue sensitivities.

The unstable case produced in subsection 3.1 is assumed. Table 1 shows that adding reactive load at bus 2 and/or bus 8 will move the unstable eigenvalue to the left. The sensitivities show that adding reactive load at bus 2 is more effective. Figure 4 shows how the critical eigenvalue changes when $ql2$ is changed from 0.0 pu to 0.29 pu in steps of 0.01 pu. Points labeled + are the linear prediction of the

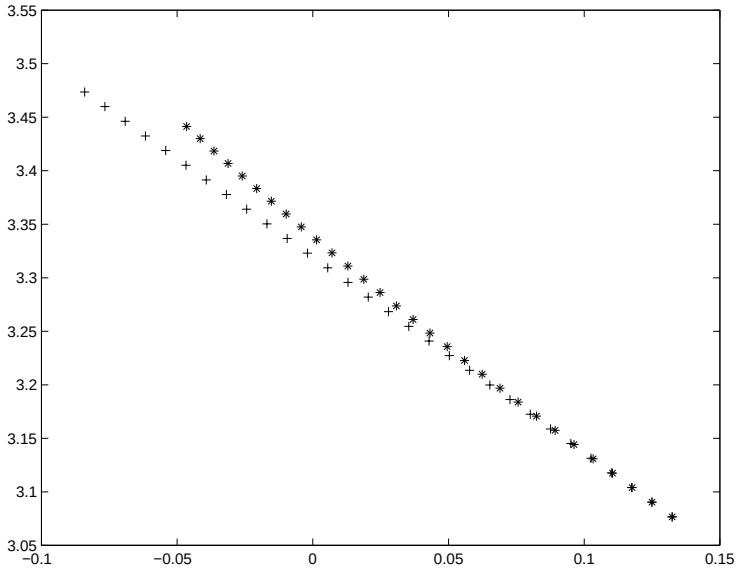

Figure 4: Eigenvalue variation with q2; +=predicted with sensitivity, *=actual

eigenvalue using sensitivity, while points labeled * are the actual eigenvalues.

3.5 Control by changing bus voltage

This subsection illustrates the selection of bus voltage changes to suppress an oscillation and the prediction of control effectiveness using eigenvalue sensitivities. In practice, the voltage at a generator bus would be changed by changing the voltage reference and the voltage at a load bus could be changed if a device such as an SVC were installed.

Table 1 shows that increasing the bus voltage at generator bus 2 will move the unstable eigenvalue to the left. Figure 5 shows how the eigenvalue changes when $v2$ is changed from 0.99 pu to 1.019 pu in step of 0.001 pu. Points labeled + are linear prediction of the eigenvalue using sensitivity, while points labeled * are the actual eigenvalues.

3.6 Control by setting an exciter to manual

One control available to operators is to manually set constant generator excitation. This subsection gives initial results on using eigenvalue sensitivities to rank the effectiveness of setting exciters to manual control in order to suppress an oscillation. The problem of predicting the effect of setting exciters to manual is more difficult than

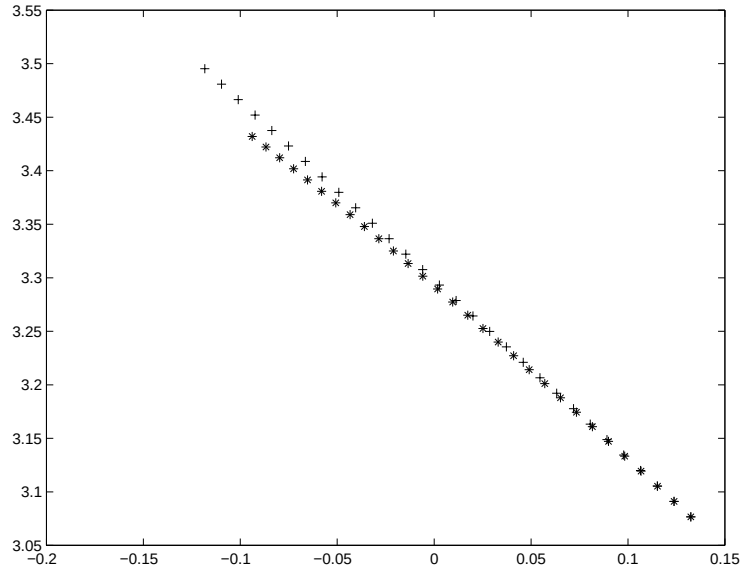

Figure 5: Eigenvalue variation with v2; +=predicted with sensitivity, *=actual

the predicting the effect of parameter changes because setting exciters to manual changes the form of the system equations instead of simply varying system parameters. Nevertheless, two methods of approximating the change to manual excitation by varying parameters are tested on the 9 bus system.

Each exciter is modeled as

$$
\begin{aligned}
T_E \frac{E_{fd}}{dt} &= \alpha \left[-(K_E + S_E(E_{fd}))E_{fd} + V_R \right] \\
T_F \frac{dR_f}{dt} &= \alpha \left[-R_f + \frac{K_F}{T_F} E_{fd} \right] \\
T_A \frac{dV_R}{dt} &= \alpha \left[-V_R + K_A R_f - \frac{K_A K_F}{T_F} E_{fd} + K_A (V_{ref} - V) \right]
\end{aligned}
$$

The idea is that when $\alpha = 1$ the exciter is enabled and that when $\alpha = 0$ the exciter is set to manual. Sensitivity of the critical eigenvalue to α at $\alpha = 1$ is used to attempt to predict the critical eigenvalue when $\alpha = 0$. Since this is a large signal change in α, a less accurate prediction is expected.

The sensitivities of the real part of the unstable eigenvalue λ to the parameter α in the unstable case produced in subsection 3.1 are shown in table 2. The eigenvalue changes in table 2 predicted by the eigenvalue sensitivity to α suggest that setting any of the exciters to manual will move the eigenvalue to the left and stabilize the eigenvalue, but that the most effective is exciter 3 and the least effective is exciter 1.

	exciter 1	exciter 2	exciter 3
λ_α	0.0174	0.0531	0.0907
predicted change	-0.0174	-0.0531	-0.0907
actual change	-0.0436	-0.1952	-0.2819

Table 2: Using sensitivities to rank exciters to be set to manual

The actual changes computed by altering the system equations and recomputing the eigenvalue are also shown in table 2. The numerical value of the actual changes is not accurately predicted by the sensitivities, but the *ranking* of the effectiveness is correctly predicted. These initial results giving the correct ranking suggest that further testing of this approach is warranted.

A second, simpler approach was to effectively remove the effect of α by setting $\alpha = 1$ and instead vary $\frac{1}{T_E}$. $\frac{1}{T_E}$ at its nominal value includes the exciter control whereas $\frac{1}{T_E} = 0$ removes the exciter control. The sensitivity to $\frac{1}{T_E}$ could be an index to select which exciters to remove. However, this approach did not give a good ranking result and we regard the first approach as more promising.

3.7 Redispatch to stabilize the 37 bus system

Figure 6 shows the eigenvalue movement when increasing the PQ load at bus 2855 from 166.0184+118.3536j to 170.49+121.08j in steps of 0.160+0.114j. The increased load is provided equally by all generators except those modeled with swing equations.

When load at bus 2855 is 170.33+121.43i pu, there is an unstable eigenvalue $0.0101 + 2.4053j$ with positive real part. Sensitivities of this real part to some of the parameters are listed in table 3.

$pg51$	$pg136$	$pg3814$	$pg1459$	$pg2855$	$pg3645$	$pg5890$	$pg5902$	$pg5903$
0.0100	0.0087	0.0003	0.0044	-0.0002	0.0003	0.0003	0.0003	0.0003
$pg5525$	$pg2458$	$pg4895$	$pg6321$	$pg1$	$pg2812$	$pg2833$	$pg2834$	$pg2864$
0.0003	0.0006	0.0003	0.0003	0.0122	-0.0004	-0.0002	-0.0002	-0.0004

Table 3: Sensitivity of real part of critical eigenvalue in 37 bus system

The sensitivities in table 3 predict that the unstable mode can be effectively stabilized by decreasing $pg1$ by 2.0 pu and increasing $pg2812$ by 2.0 pu. In particular, the sensitivities predict that this redispatch will change the damping to -0.0151. Simulation shows the damping actually moves to -0.0146.

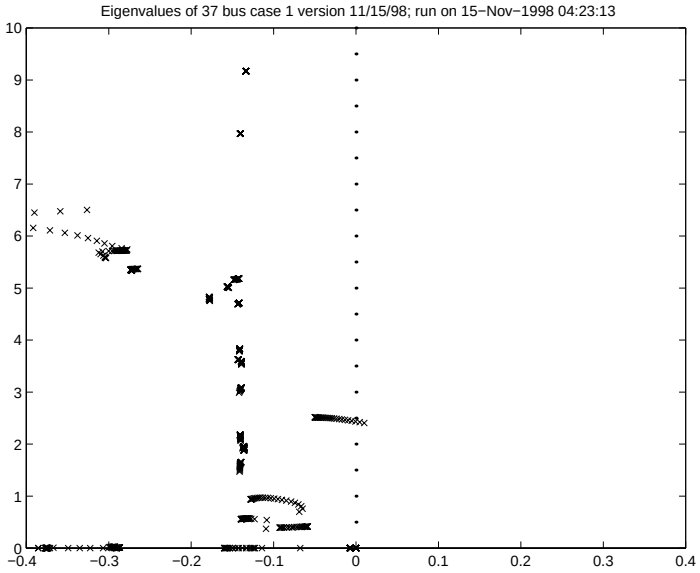

Figure 6: 37 bus eigenvalues as dispatch varies

3.8 Robustness with respect to data in 9 bus system

In the cases we have given, we calculated the eigenvalues based on some given parameters, such as time constants, etc. In practice, these parameters are uncertain due to a variety of sources of error. It is of engineering importance to quantify the uncertainty in the eigenvalues due to the uncertainty in the parameters. The parameter uncertainty is modeled by regarding the parameters as random variables with known mean and variance. Then the eigenvalues also become random variables. If there are many parameters, as is the case in practical power systems, and some technical conditions are satisfied, the eigenvalues are approximately Gaussian random variables and the standard deviation of the eigenvalues can be estimated by a simple calculation. The method is based on eigenvalue sensitivities and a central limit theorem explained in section 4.7; this section presents the results of applying the method.

We study the robustness of an eigenvalue in the 9 bus case with respect to uncertainty in the generator time constants of the three generators. The generator time constants are assumed to be random variables uniformly distributed over a range $\pm 5\%$ about their nominal values. The resulting means and standard deviations of the generator time constants are shown in table 4.

When all the generator time constants are at their mean or nominal values, the eigenvalues of the system are known. One of these eigenvalues has real part

p	mean	σ	λ_p
T'_{do1}	8.96	0.2587	-0.0005
T''_{do1}	0.31	0.0089	0.0220
T'_{qo1}	0.05	0.0014	-0.6521
T''_{qo1}	0.05	0.0014	-0.2830
T_{E1}	0.314	0.0091	-0.1257
T_{F1}	0.35	0.0101	0.0460
T_{A1}	0.2	0.0058	-0.1558
T''_{do2}	8.50	0.2454	0.0079
T''_{do2}	1.24	0.0358	0.0240
T'_{qo2}	0.037	0.0011	-3.1369
T''_{qo2}	0.074	0.0021	-0.9045
T_{E2}	0.314	0.0091	-0.1845
T_{F2}	0.35	0.0101	0.1033
T_{A2}	0.2	0.0058	-0.2514
T'_{do3}	3.27	0.0944	0.1069
T''_{do3}	0.31	0.0089	-0.0315
T'_{qo3}	0.032	0.0009	-5.6904
T''_{qo3}	0.079	0.0023	-1.0487
T_{E3}	0.314	0.0091	-0.4328
T_{F3}	0.35	0.0101	0.2290
T_{A3}	0.2	0.0058	-0.8183

Table 4: parameters in simulation

$\lambda^r = -0.8423$. The sensitivities of λ^r with respect to the generator time constants are computed using the eigenvalue sensitivity formula and shown in table 4. As explained in section 4.7, λ^r is approximately normally distributed and the standard deviation σ_{λ^r} of λ^r can be computed with the formula

$$\sigma_{\lambda^r} = \sqrt{\sum_i (\lambda^r_{p_i})^2 \sigma^2_{p_i}} \tag{2}$$

Using the data in table 4 in formula (2) yields $\sigma_{\lambda^r} = 0.0144$ and this, together with the approximately normal distribution of λ^r, quantifies the uncertainty in λ^r due to the uncertainty in the generator time constants.

For example, for any normally distributed random variable X of standard devi-

ation σ,

$$\text{Prob}\{X < \text{mean}(X) + 1.65\sigma\} = 0.9505 \tag{3}$$
$$\text{Prob}\{X < \text{mean}(X) + 2.33\sigma\} = 0.9901 \tag{4}$$
$$\text{Prob}\{X < \text{mean}(X) + 2.65\sigma\} = 0.9960 \tag{5}$$

and applying these results to λ^r, which has mean -0.8423 and estimated standard deviation $\sigma_{\lambda^r} = 0.0144$ yields

$$\text{Prob}\{\lambda^r < -0.8185\} = 0.9505 \tag{6}$$
$$\text{Prob}\{\lambda^r < -0.8087\} = 0.9901 \tag{7}$$
$$\text{Prob}\{\lambda^r < -0.8041\} = 0.9960 \tag{8}$$

We validated results (6), (7), (8) by running a Monte Carlo simulation with 10000 samples. The Monte Carlo results are

$$\text{Prob}\{\lambda^r < -0.8185\} = 0.9575 \tag{9}$$
$$\text{Prob}\{\lambda^r < -0.8087\} = 0.9943 \tag{10}$$
$$\text{Prob}\{\lambda^r < -0.8041\} = 0.9989 \tag{11}$$

which are satisfactorily close to (6), (7), (8).

3.9 Robustness with respect to load modeling in 37 bus system

There is significant uncertainty in load modeling which could be an important limiting factor in obtaining accurate enough stability results from a dynamic power system model. To show how to quantify this effect, we study the robustness of an eigenvalue in the 37 bus base case with respect to uncertainty in the load models. The 37 bus system has 32 loads and each of these loads is modeled as:

$$P_L = ir\,V + gg\,V^2 \tag{12}$$
$$Q_L = ii\,V + sus\,V^2 \tag{13}$$
$$\alpha_P P_{L0} = ir\,V \tag{14}$$
$$(1-\alpha_P)P_{L0} = gg\,V^2 \tag{15}$$
$$\alpha_Q Q_{L0} = ii\,V \tag{16}$$
$$(1-\alpha_Q)Q_{L0} = sus\,V^2 \tag{17}$$

The constants ir, gg, ii, sus, α_P, α_Q in the load model are defined in section A.2.2. The load model is the same as used in section A.2.2 except that it is assumed that there is no constant power portion of the load ($\beta_P = 1 - \alpha_P$ and $\beta_Q = 1 - \alpha_Q$).

The parameters of each load are $\alpha_P, \alpha_Q, P_{L0}$ and Q_{L0}. For the 37 bus base case, the nominal values of α_P and α_Q are $\alpha_P = 0.4$, $\alpha_Q = 0.5$ for all buses and the nominal values of P_{L0} and Q_{L0} are shown in Table 5.

The 37 bus base case has one eigenvalue with real part $\lambda^r = -0.0500$. The sensitivities of λ^r with respect to the all the load parameters are computed using the eigenvalue sensitivity formula (64) and are shown in Table 5. Obtaining this data by brute force computations would require successively changing from nominal each of the 128 load parameters and recomputing the eigenvalue 128 times. On the other hand, the analytic sensitivity formula essentially requires some Jacobians and a Hessian to be evaluated once.

It is apparent that several of the loads (e.g. buses 51,136, 3520, 3523) have parameters that have much greater effect on the eigenvalue damping. If the sensitivity of this eigenvalue to load parameters is a limiting factor in ensuring power system stability, then the sensitivities in Table 5 show where money should be spent in order to more accurately determine load parameters.

Now we show how to quantify the uncertainty in the eigenvalue damping due to the combined uncertainty in all the loads. To model the load uncertainty, we first assume that α_P, α_Q, P_{L0} and Q_{L0} are random variables uniformly distributed over a range $\pm 5\%$ about their nominal values. As explained in section 4.7, λ^r is approximately normally distributed and the standard deviation σ_{λ^r} of λ^r can be computed with the formula

$$\sigma_{\lambda^r} = \sqrt{\sum_i (\lambda^r_{p_i})^2 \sigma^2_{p_i}} \tag{18}$$

Using the sensitivity data in Table 5, formula (18) yields

$$\sigma_{\lambda^r} = 0.0120 \tag{19}$$

The standard deviation (19) together with the approximately normal distribution of λ^r quantifies the uncertainty in λ^r due to the uncertainty in the load models as:

$$\text{Prob}\{\lambda^r < 0\} = 0.99998 \tag{20}$$

$$\text{Prob}\{\lambda^r < -0.04\} = 0.7967 \tag{21}$$

The computation (19) assumed (rather optimistically) an uncertainty in the load parameters as a uniform distribution $\pm 5\%$ about nominal. It is simple to recalculate with different assumptions about the load parameter standard deviation without recomputing any sensitivities. For example, if the load parameters are assumed to have a uniform distribution $\pm 10\%$ about nominal, then the load parameter standard deviations are double those obtained in the $\pm 5\%$ case and formula (18) shows that

the standard deviation σ_{λ^r} is double that obtained in (19). Thus for the $\pm 10\%$ case we obtain

$$\sigma_{\lambda^r} = 0.0240 \tag{22}$$

and hence

$$\text{Prob}\{\lambda^r < 0\} = 0.9812 \tag{23}$$

$$\text{Prob}\{\lambda^r < -0.04\} = 0.6628 \tag{24}$$

Indeed, for the general case of load parameters uniformly distributed $\pm K\%$ about nominal, we obtain

$$\sigma_{\lambda^r} = 0.0024K \tag{25}$$

bus #	$\lambda^r_{\alpha_P}$	$\lambda^r_{\alpha_Q}$	P_L	λ^r_{PL}	Q_L	λ^r_{QL}
1	-0.0020	0.0003	23.51	-0.0103	12.39	0.0000
51	-0.0052	0.0148	20.55	-0.0060	32.39	-0.0005
136	-0.0121	0.0084	52.04	-0.0052	26.30	-0.0004
1377	0.0034	0.0022	27.11	-0.0031	20.10	-0.0001
2458	0.0001	0.0000	-14.92	0.0000	17.37	0.0000
2812	-0.0005	0.0001	206.2	0.0003	47.50	0.0000
2833	-0.0001	0.0000	222.4	0.0001	49.51	0.0000
2834	-0.0001	0.0000	221.8	0.0001	49.37	0.0000
2855	0.0001	0.0001	166.0	0.0001	118.4	0.0000
2864	-0.0020	0.0003	220.8	0.0004	49.30	0.0000
3517	0.0000	0.0000	232.3	0.0000	51.89	0.0000
3520	0.0044	-0.0006	230.7	-0.0002	52.65	0.0001
3523	0.0051	-0.0007	232.0	-0.0002	55.04	0.0001
3645	0.0000	0.0000	3.265	0.0000	3.510	0.0000
3814	0.0000	0.0000	230.3	0.0000	50.35	0.0000
3864	0.0000	0.0000	1.575	0.0000	0.9613	0.0000
4305	0.0000	0.0000	7.169	0.0000	16.63	0.0000
4383	0.0000	0.0003	2.490	0.0000	3.529	0.0000
4387	0.0000	0.0007	5.876	-0.0002	8.056	0.0000
4611	0.0000	0.0000	230.0	0.0001	50.00	0.0000
4656	-0.0001	0.0000	231.4	0.0001	51.21	0.0000
4895	0.0000	0.0000	15.82	0.0000	15.01	0.0000
5506	0.0000	0.0000	19.74	0.0000	28.33	0.0000
5525	0.0000	0.0000	10.06	0.0000	15.69	0.0000
5685	0.0000	0.0000	37.20	0.0000	27.99	0.0000
5686	0.0000	0.0000	26.45	0.0000	22.58	0.0000
6188	0.0000	0.0000	15.34	0.0000	11.23	0.0000
6597	-0.0001	0.0000	233.7	0.0000	52.49	0.0000
6632	0.0000	0.0000	234.1	0.0000	55.29	0.0000
6659	0.0000	0.0000	229.5	0.0000	49.83	0.0000
6660	0.0000	0.0000	229.5	0.0000	50.17	0.0000
9484	0.0000	0.0001	2.210	0.0001	3.614	0.0002

Table 5: Sensitivities of the real part of an eigenvalue with respect to all load parameters of the 37 bus system and the nominal values of the load parameters (the nominal values of α_P and α_Q are $\alpha_P = 0.4$ and $\alpha_Q = 0.5$ for all buses).

3.10 Validation with PSS/E

To validate the correctness of the project models, the matlab results are compared with PSS/E results for both the 9 bus and the 37 bus test systems. Matlab codes for both test systems give substantial, although not perfect agreement with PSS/E. Figure 7 and Figure 8 show the comparison of the eigenvalues for the base case of the 9 bus test system and the 37 bus test system, respectively.

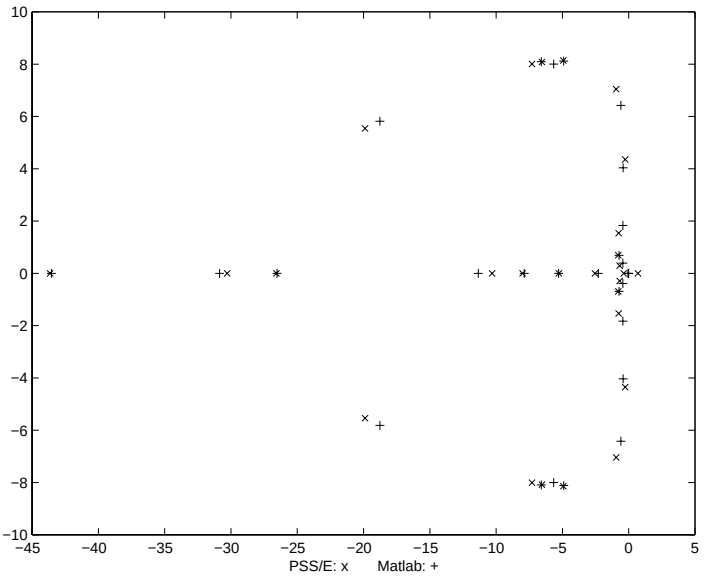

Figure 7: Eigenvalue comparison for 9 bus test system

3.11 Conclusion

This section shows the usefulness of the analytic formulas for eigenvalue sensitivity. These formulas allow

- selection of stabilizing controls
- estimates of control damping effectiveness
- estimates of robustness to model data
- a suggested method to select AVR to be set to manual.

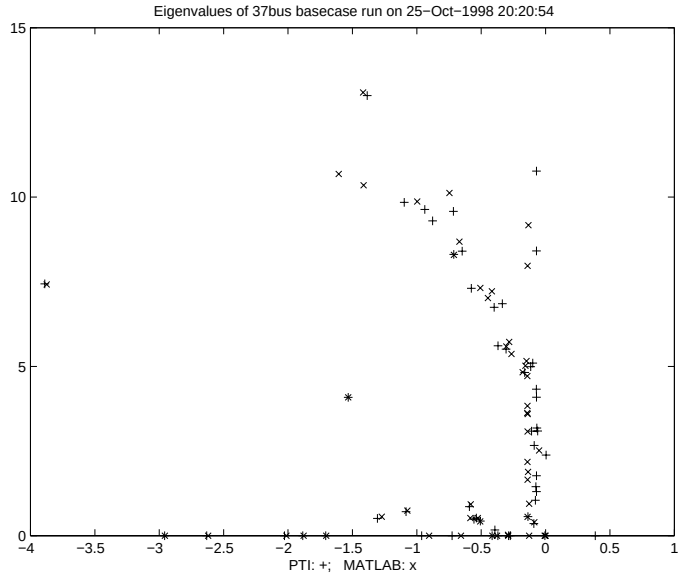

Figure 8: Eigenvalue comparison for 37 bus test system

4 Eigenvalue sensitivity

4.1 Stabilizing the equilibrium

The project takes a simple approach to suppressing or avoiding oscillations. In the case of a stable operating point with a poorly damped oscillatory mode, the objective is to increase the damping of that mode. That is, the power system linearization at the operating point is modified. (Operator actions such as redispatch often modify the operating point to do this.) The effect of this is that transients near enough to the operating point will decay more quickly. However, the analysis does not attempt the more difficult study of large signal transients. The existence of a stable operating point is of course necessary for system security, but there is no guarantee that large signal transients will result in operation at that operating point.

In case of a sustained oscillation, there is typically a power system equilibrium nearby that is oscillatory unstable. The objective is to stabilize this equilibrium by modifying the power system linearization at the equilibrium. Then a transient can occur to restore the power system to the equilibrium, which is now a stable operating point. This is a likely outcome, but other transient behaviors are possible. The project methods seek to stabilize the equilibrium to obtain an operating point that is sufficiently small signal stable and do not attempt to make more extensive changes to the system dynamics.

4.2 Challenges for eigenvalue sensitivity

A previous project [66] derived formulas for eigenvalue sensitivity with respect to a wide range of power system parameters, including parameters which can be changed by operator actions. The formulas take full account of changes in the operating point and are in a form suitable for sparse matrix computations. This project has improved these formulas by more accurately modeling the time scales involved.

Suppose that the power system has a poorly damped or unstable oscillatory mode. This mode is called a critical mode. If the critical mode and corresponding eigenvalue and eigenvectors can be found, then the sensitivity of the modal damping to a range of power system parameters or controls can be computed and used to select an operator control to effectively damp the mode and hence avoid or suppress the oscillation.

It is also desirable to be able to identify modes that are sufficiently damped, but sensitive to parameter variations so that they could rapidly become unstable. Eigenvalue sensitivity calculations can distinguish such modes so that control action can be taken to prevent oscillations.

The main potential obstacles to doing this seem to be:

- A good power system dynamic model is needed. The robustness of the selected controls to modeling uncertainty needs to be quantified. Errors due to uncertainty in the load models may be particularly important. A method for quantifying robustness is presented in sections 3.8, 3.9, and 4.7.

- Locating the critical mode(s) among the many lightly damped modes. Sensitivities can identify lightly damped modes which can become unstable when parameters vary. The use of measurements to help detect or predict critical modes is discussed in section 9.

- Computational speed in a large system. Computational speed is addressed in section 5.

- Nonlinearity in the eigenvalue movement. It is possible for nearby eigenvalues to interact in such a way that they move nonlinearly and with extreme sensitivity when the modes are near a strong resonance. This project made a major advance in describing this phenomenon and this is documented in sections 7 and 8.

- The requirement to simultaneously stabilize several critical modes. It is possible that a control action stabilizing one critical mode will destabilize another critical mode. A specific mechanism for this was found when the modes are near a strong resonance and this is documented in section 7.

4.3 Static and dynamic time scales

The power system can be modeled by separate equations for different time scales. The equations that are used to detect an oscillation (transient time scale) are different than those for the operator actions used to suppress the oscillation (steady state time scale). This subsection discusses these time scales and the corresponding power system modeling.

Although this separation of the power system model into separate equations for different time scales is not always explicitly stated, it does correspond to the standard practice of solving a loadflow to determine an operating point (solving steady state equations) but using a detailed dynamic model for the faster transient time scale. In any case the distinct modeling at the two time scales is fundamental for the project work.

The distinction between variables and parameters is important. Parameters are set or assumed external to the equations whereas variables assume values imposed by solution of the equations. The choice of variable and parameter is time scale dependent.

The transient time scale (less than one second to tens of seconds) is the time scale for low frequency oscillations. The dynamic behavior of the power system over transient time scale is represented by the parameterized differential-algebraic equations

$$\dot{x} = f(x, y, p, q) \tag{26}$$
$$0 = g(x, y, p, q) \tag{27}$$

where

- x is the vector of dynamic state variables, mainly generator dynamic states (e.g. δ, ω, $E_q^{'}$)
- y is the vector of algebraic state variables, such as the generator dq currents.
- p is a vector of algebraic state variables specifying generator bus PV and load PQ and the slack bus (or distributed slack). p also includes constants in the static equations for which the eigenvalue sensitivity is required. For example, if the eigenvalue sensitivity with respect to a line admittance y_{12} with nominal value 3.3 is required, then y_{12} becomes a component of p, and an algebraic equation $0 = y_{12} - 3.3$ is included in (27).
- q is the vector of set points for each generator and complex current sources and impedances for each load.

Equations (26),(27) can also be rewritten as

$$I_o \dot{z} = G(z, q) \tag{28}$$

where

$$z = \begin{pmatrix} x \\ y \\ p \end{pmatrix} \tag{29}$$
$$I_o = \begin{pmatrix} I_{n_x \times n_x} & O_{n_x \times n_Y} \\ O_{n_Y \times n_x} & O_{n_Y \times n_Y} \end{pmatrix} \tag{30}$$

and

$$G(z, q) = \begin{pmatrix} f(x, y, p, q) \\ g(x, y, p, q) \end{pmatrix} \tag{31}$$

n_x is the number of dynamic states in the vector x and n_Y is the number of algebraic states in the vectors y and p.

Equation (28) represents the transient time scale behavior of the system as the dynamic and algebraic states fluctuate about their nominal equilibrium values. For example, system frequency deviate from synchronous speed, bus voltages and powers vary and the interarea flows vary around the scheduled transfers. However, the generator set points and complex current sources and impedances for each load are assumed to be constant in the transient time scale and therefore they are modeled as parameters. The Jacobian matrix G_z is singular because the transient model does not include equations that describe how the system frequency is returned to synchronous speed [1].

The time scale for the operator actions (minutes to hours) is longer than the transient time scale steady state and is represented by the steady state static equations

$$0 = H(x, y, p, q) = H(z, q) \tag{32}$$

In (32), x and y are variables. However, in (32) p is a parameter and q is a variable. Equation (32) considers the time scale in which generation is economically dispatched to meet the slowly evolving component of load fluctuation and the Automatic Generation Control (AGC) acts to maintain scheduled interchanges and restore system frequency. (32) includes equations that describe how q changes over extended periods of time to account for economic dispatch, interarea schedules, and AGC, and assumes that system frequency is synchronous speed.

For consistency between the models (32) and (28) it is important that solutions of the static equations (32) are equilibria of the dynamic equations (28):

$$H(z_0, q_0) = 0 \Rightarrow G(z_0, q_0) = 0 \tag{33}$$

The variables and parameters in the dynamic and static models are summarized in Table 6.

Now we give more detail of the generator modeling at the two time scales. Load modeling at the two time scales is presented in section A.2.2.

The electrical output of a generator is controlled by two inputs, the governor droop and the load reference set point. The governor droop determines how the generator responds to a change in frequency. The governor droop is a constant parameter, not a control parameter. The load reference set point determines the steady state power output of the generator. The load reference set point is a control

[1] The zero eigenvalue of the system Jacobian is not an artifact of an inaccurate model or an indicator that power systems are operated close to instability. The singularity of the linearized system is intentional and provides for the secure operation of the power system during severe disturbances. Specifically, the indeterminate linearized model reflects an additional degree of freedom that allows all generators to speed up over a short time duration. Over longer time durations, the system must be reset so that frequency is restored.

quantity	description	dynamic model G	static model H	example components
x	dynamic state	variable	variable	δ, ω, $E_q^{'}$, ψ_q, E_{fd}
y	algebraic state	variable	variable	I_d, I_q, P_L, Q_L
p	algebraic state	variable	parameter	generator PV, load PQ, Y_{bus}
q	set points	parameter	variable	V_{ref}, P_M, load conductance

Table 6: Variables and parameters in dynamic and static models

input that can be revised according to an economic dispatch and permits control through the AGC.

Immediately following a disturbance the transient response of each generator is determined by its electrical proximity to the disturbance. The system frequency a short time (a few seconds) after a disturbance, and the proportion of the disturbance "picked-up" by each generator, is determined by each generator's rotating inertia. Several seconds after a disturbance the system frequency and generator response is affected by each generator's governor and droop. The relative outputs of the generators when the system frequency is restored to synchronous speed is determined by each generator's load reference set point. The load reference set point is adjusted only every few minutes, not seconds [34]. Over transient time periods then, the load reference is a parameter. Over longer time periods that assume steady state operation at synchronous speed, the load reference set points are variables determined by the system conditions and dispatch policy. At steady state the load reference set points equal the generator power outputs.

4.4 Eigenvalue sensitivity formula derivation

This subsection derives and explains the eigenvalue sensitivity formula used in this project. Discussion of technical mathematical assumptions is postponed to the end of the section. The derivation combines together approaches from [21], [57], [40], [71], [66].

It is convenient to notate the combined algebraic states of (26) and (27) as

$$\Upsilon = \begin{pmatrix} y \\ p \end{pmatrix} \tag{34}$$

Differential equations can be obtained from the differential algebraic model (26) and (27) by eliminating the algebraic states Υ. Solving the algebraic equations (27) for Υ in terms of x yields a function

$$\Upsilon = h(x, q) \tag{35}$$

Substitution of $h(x,q)$ for Y in (26) yields the differential equations

$$\dot{x} = f(x, h(x,q), q) \tag{36}$$
$$= F(x,q) \tag{37}$$

Superscripts are used to indicate the ith component of a vector. For example the ith component of the vector x is x^i and the ith equation of (37) is

$$\dot{x}^i = F^i(x,q) \tag{38}$$

Since h was derived by solving the algebraic equations (27),

$$0 = g(x, h(x,q), q) \tag{39}$$

the Jacobian h_x of h with respect to x is obtained by differentiating (39):

$$0 = g_x + g_Y h_x \tag{40}$$
$$h_x = -g_Y^{-1} g_x \tag{41}$$

Now the system Jacobian F_x can be expressed in terms of f and g by differentiating (37):

$$F_x = f_x + f_Y h_x = f_x - f_Y g_Y^{-1} g_x \tag{42}$$

The system eigenvalues are the eigenvalues of the Jacobian matrix F_x. Let λ be one of these eigenvalues and let v and w be the right and left eigenvectors associated with λ. w is a row vector and v is a column vector.

Write

$$\bar{v} = \begin{pmatrix} v \\ h_x v \end{pmatrix} = \begin{pmatrix} v \\ -g_Y^{-1} g_x v \end{pmatrix} \tag{43}$$

Then, using (42)

$$G_z \bar{v} = \begin{pmatrix} f_x & f_Y \\ g_x & g_Y \end{pmatrix} \begin{pmatrix} v \\ -g_Y^{-1} g_x v \end{pmatrix} = \begin{pmatrix} (f_x - f_Y g_Y^{-1} g_x) v \\ 0 \end{pmatrix} = \begin{pmatrix} F_x v \\ 0 \end{pmatrix} = \lambda \begin{pmatrix} v \\ 0 \end{pmatrix} = \lambda I_o \bar{v} \tag{44}$$

Similarly, write

$$\bar{w} = \begin{pmatrix} w, & -w f_Y g_Y^{-1} \end{pmatrix} \tag{45}$$

and obtain

$$\bar{w} G_z = \begin{pmatrix} w, & -w f_Y g_Y^{-1} \end{pmatrix} \begin{pmatrix} f_x & f_Y \\ g_x & g_Y \end{pmatrix} = \begin{pmatrix} w(f_x - f_Y g_Y^{-1} g_x), & 0 \end{pmatrix} = \begin{pmatrix} w F_x, & 0 \end{pmatrix}$$
$$= \lambda \begin{pmatrix} w, & 0 \end{pmatrix} = \lambda \bar{w} I_o \tag{46}$$

The vector $\bar{v}$ defines the mode shape of both the differential and algebraic variables in the same way as the eigenvector v defines the mode shape of the differential variables. (The equation $G_z\bar{v} = \lambda I_o \bar{v}$ is called a generalized eigenvalue problem [26], [71].)

It is convenient to group together the variables in the static equations (32) as

$$e = \begin{pmatrix} x \\ y \\ z \end{pmatrix} \tag{47}$$

The operating point or equilibrium of the static equations (32) is

$$E(p) = \begin{pmatrix} X(p) \\ Y(p) \\ Q(p) \end{pmatrix} \tag{48}$$

and $E(p)$ satisfies

$$0 = H(X(p), Y(p), p, Q(p)) \tag{49}$$

The equilibrium $E(p)$ is a function of the parameter p. The sensitivity of $E(p)$ with respect to p is the vector

$$E_p = \begin{pmatrix} X_p \\ Y_p \\ Q_p \end{pmatrix} = \begin{pmatrix} \frac{\partial X}{\partial p} \\ \frac{\partial Y}{\partial p} \\ \frac{\partial Q}{\partial p} \end{pmatrix} \tag{50}$$

which can be evaluated by differentiating (49) and rearranging terms:

$$0 = H_x X_p + H_y Y_p + H_q Q_p + H_p \tag{51}$$

$$0 = H_e E_p + H_p \tag{52}$$

where $H_e = [H_x | H_y | H_q]$. The ith components of equation (51) can be written as

$$0 = \sum_j \left(\frac{\partial H^i}{\partial x^j} X_p^j + \frac{\partial H^i}{\partial y^j} Y_p^j + \frac{\partial H^i}{\partial q^j} Q_p^j \right) + \frac{\partial H^i}{\partial p} \tag{53}$$

Solving (52) gives

$$E_p = -(H_e)^{-1} H_p \tag{54}$$

For practical computation of E_p, explicit evaluation of the inverse $(H_e)^{-1}$ is avoided and sparse methods are used to solve (52).

In the differential-algebraic equations (28), G is a function of x, y, p and q. Therefore the Jacobian of the differential-algebraic equations $G_z(z, q) = G_z(x, y, p, q)$ is also a function of x, y, p and q. When the Jacobian of the differential-algebraic

equations is evaluated at the equilibrium $E(p)$, it can be regarded as function $J(p)$ of p:

$$J(p) = G_z(X(p), Y(p), p, Q(p)) \tag{55}$$

That is, J varies with the parameter p, not only because the entries of the Jacobian can depend directly on p but also because the equilibrium $E(p)$ varies with p and the Jacobian is evaluated at $E(p)$. Many parameters p of interest appear linearly in (28), and in this case, the entries of the Jacobian do not depend directly on p.

Evaluating (44) and (46) at $(Z(p), p)$ gives

$$J\bar{v} = \lambda I_o \bar{v} \tag{56}$$

$$\bar{w}J = \lambda \bar{w} I_o \tag{57}$$

and hence

$$0 = \bar{w}(J - \lambda I_o)\bar{v} \tag{58}$$

To obtain the eigenvalue sensitivity, differentiate (58) with respect to p to obtain

$$0 = \bar{w}(J_p - \lambda_p I_o)\bar{v} \tag{59}$$

(The other terms involving $\bar{v}_p$ and $\bar{w}_p$ vanish). Rearrangement of (59) and using $\bar{w} I_o \bar{v} = wv$ gives a formula for the eigenvalue sensitivity $\lambda_p = \frac{\partial \lambda}{\partial p}$ with respect to the parameter p:

$$\lambda_p = \frac{\bar{w} J_p \bar{v}}{wv} = \frac{\sum_{i,j} \bar{w}^i J_p^{ij} \bar{v}^j}{\sum_i w^i v^i} \tag{60}$$

It remains to express J_p^{ij} in terms of derivatives of G. The i, j component of equation (55) is

$$J^{ij}(p) = G_z^{ij}(X(p), Y(p), p, Q(p)) = \frac{\partial G^i}{\partial z^j}(X(p), Y(p), p, Q(p)) \tag{61}$$

Differentiate (61) with respect to p to obtain

$$J_p^{ij} = \sum_k \left(\frac{\partial^2 G^i}{\partial z^j \partial x^k} X_p^k + \frac{\partial^2 G^i}{\partial z^j \partial y^k} Y_p^k + \frac{\partial^2 G^i}{\partial z^j \partial q^k} Q_p^k \right) + \frac{\partial^2 G^i}{\partial z^j \partial p} \tag{62}$$

$$= \sum_k \frac{\partial^2 G^i}{\partial z^j \partial e^k} E_p^k + \frac{\partial^2 G^i}{\partial z^j \partial p} \tag{63}$$

and substitute in (60) to finally obtain the eigenvalue sensitivity formula

$$\lambda_p = \frac{\sum_{i,j,k} \bar{w}^i \frac{\partial^2 G^i}{\partial z^j \partial e^k} E_p^k \bar{v}^j + \sum_{i,j} \bar{w}^i \frac{\partial^2 G^i}{\partial z^j \partial p} \bar{v}^j}{\sum_i w^i v^i} \tag{64}$$

The first term in (64) describes first order changes in the eigenvalue λ due to changes in p affecting the equilibrium position at which the Jacobian is evaluated and the second term describes first order changes in λ due to changes in p affecting the entries of the Jacobian directly.

There are some technical assumptions required to make the derivation above rigorous:

- f and g are assumed to be locally smooth functions. In particular, the power system should not be at a boundary where a hard limit is encountered.
- The construction of the function h in (35) requires g_Y to be assumed invertible. According to the implicit function theorem, h is well defined locally if g_Y is invertible. The construction of $\bar{w}$ and $\bar{v}$ also requires g_Y to be invertible.
- The eigenvalue λ is assumed to be unique and simple (that is, the system is not exactly at a strong or weak resonance). The simplicity of λ ensures that $wv \neq 0$ so that the division by wv in (64) is valid. The uniqueness of λ ensures that w and v are unique up to scaling by a constant.
- The computation of E_p requires that H_e is invertible (see (54)).

4.5 Sensitivity formula requirements

This section summarizes what needs to be computed to evaluate the eigenvalue sensitivity formula (64) with respect to the parameter p.

- the extended left and right eigenvectors $\bar{w}$ and $\bar{v}$ corresponding to the eigenvalue.
- the Hessian $\frac{\partial^2 G}{\partial z \partial e}$ of the dynamic equations.
- the equilibrium sensitivity E_p with respect to p.
- the Hessian $\frac{\partial^2 G}{\partial z \partial p}$ of the dynamic equations (vanishes if the parameter p does not appears explicitly in the Jacobian)

We have identified two possible mechanisms for oscillation modes becoming unstable:

1. A critical mode becomes unstable with little or no interaction with other modes
2. A critical mode becomes unstable as a result of an interaction with another mode.

The first mechanism allows a straightforward application of the sensitivity formulas to a single critical mode once the critical mode was identified. The second mechanism is more complicated and precludes a straightforward application of the sensitivity formulas because of the nonlinearity of the eigenvalue movement. The project devised a method to predict the eigenvalue movement in this case which is described in section 7.4.2.

4.6 Optimum redispatch to best improve critical mode damping

A formula for the best movement of the operating point to improve critical mode damping is stated and discussed to illustrate one approach to applying eigenvalue sensitivity methods. The formula could be used to help deduce a generator redispatch which effectively damps the critical mode.

Let the eigenvalue of the critical mode be λ. The critical mode damping is described by λ^r, the real part of λ. It is convenient to scale the right and left extended eigenvectors so that

$$\sum_i w^i v^i = 1 \tag{65}$$

Then taking the real part of the (64), the sensitivity of the critical mode damping with respect to the operating point is given by the vector u where

$$u^k = \frac{\partial \lambda^r}{\partial z^k} = \text{Real}\left\{\frac{\partial \lambda}{\partial z^k}\right\} = \text{Real}\left\{\sum_{i,j,k} \bar{w}^i \frac{\partial^2 G^i}{\partial z^j \partial e^k} E_p^k \bar{v}^j\right\} \tag{66}$$

If the operating point changes by a linearized change ΔE then the linearized change $\Delta\lambda^r$ in the critical mode damping is

$$\Delta\lambda^r = \sum_k u^k \, \Delta E^k \tag{67}$$

If ΔE is fixed at size one so that

$$1 = |\Delta E| = \sqrt{\sum_k \Delta E^k \, \Delta E^k} \tag{68}$$

then the direction of operating point change giving the maximum amount of modal damping is

$$\Delta E^k = \frac{-u^k}{|u|} \tag{69}$$

and the resulting best change in damping is

$$\Delta\lambda^r = -|u| \tag{70}$$

If the desired change in damping has magnitude $|\Delta\lambda^r_{\text{desired}}|$, then best change in operating point to achieve this to first order is

$$\Delta E^k = \frac{-u^k}{|u|^2} |\Delta\lambda^r_{\text{desired}}| \tag{71}$$

Suppose that we want to improve the critical mode damping by changing the operating point by redispatching the generators. Then we could proceed as follows:

1. Find the critical mode.
2. Compute the extended eigenvectors $\bar{w}$ and $\bar{v}$ of the critical mode.
3. Compute the best operating point change ΔE to first order with (66) and (71).
4. Compute the practical redispatch which best approximates the change in operating point ΔE.

Observations:

- The computation only requires the extended eigenvectors of the critical mode.
- The computation of the best operating point change ΔE only depends on quadratic terms of the power system equations (28). Linear terms in the power system equations do not affect the answer. This shows that the approach exploits the nonlinear parts of the power system equations. (Also components of $\bar{v}$ corresponding to variables which enter the power system equations linearly do not affect the answer and components of $\bar{w}$ which correspond to a linear equation in the power system equations do not affect the answer.)
- Step 4 requires only the static power system equations.

4.7 Quantifying eigenvalue uncertainty

A crucial factor in large and detailed power system dynamic models is the effects of various sorts of uncertainty in the model. This can be addressed by using sensitivity calculations to identify critical parameters and investigating the robustness of the eigenvalues to parameter uncertainty.

The eigenvalue is some function $\lambda(p_1, p_2, ..., p_m)$ of the uncertain parameters $p_1, p_2, ..., p_m$. The parameters p_i are chosen to satisfy the following conditions:

1. The uncertainty in the parameters is modeled by regarding each parameter p_i as a random variable with known mean $\mu(p_i)$ and known variance $\sigma^2(p_i)$.

2. The parameters are statistically independent.

3. There are sufficiently many parameters.

The uncertainty U of the eigenvalues due to the uncertainty in all the parameters is:

$$U = \lambda(p_1, p_2, ..., p_m) - \lambda(\mu(p_1), \mu(p_2), ..., \mu(p_m)) \tag{72}$$

The mean value of the uncertainty is zero:

$$\mu(U) = 0 \tag{73}$$

Approximating the changes in λ linearly in (72) gives

$$U \approx \sum_{i=1}^{m} \frac{\partial \lambda}{\partial p_i}(p_i - \mu(p_i)) \tag{74}$$

$\frac{\partial \lambda}{\partial p_i}$ is the sensitivity of λ to the parameter p_i evaluated at the nominal values $\mu(p_1)$, $\mu(p_2)$,...,$\mu(p_m)$.

Since the parameters are assumed to be independent,

$$\sigma^2(U) = \sum_{i=1}^{m} \sigma^2 \left(\frac{\partial \lambda}{\partial p_i} (p_i - \mu(p_i)) \right) \tag{75}$$

$$= \sum_{i=1}^{m} \left(\frac{\partial \lambda}{\partial p_i} \right)^2 \sigma^2(p_i) \tag{76}$$

and the standard deviation of U is

$$\sigma(U) = \sqrt{\sum_{i=1}^{m} \left(\frac{\partial \lambda}{\partial p_i} \right)^2 \sigma^2(p_i)} \tag{77}$$

Under conditions on the parameters stated above (and further discussed at the end of the section), the uncertainty U is approximately a normal random variable with mean zero and standard deviation given by (77). Thus (77) quantifies the uncertainty of λ in terms of the parameter standard deviations and the eigenvalue sensitivities. The formula (77) is simple and quick to evaluate.

We end this section by briefly stating the mathematics underlying the calculation. Let $X_1, X_2, ..., X_m$ be independent, zero mean random variables and write $s_m^2 = \sum_{k=1}^{m} \sigma^2(X_k)$ for the variance of $\sum_{k=1}^{m} X_k$. The approximate normality of $\sum_{k=1}^{m} X_k$ requires a central limit theorem. (Note that the most straightforward version of the central limit theorem does not apply because we do not assume that

$X_1, X_2, ..., X_m$ are identically distributed.) A special case of the Lindeberg theorem [10] states that if

$$\lim_{m\to\infty} \sum_{k=1}^{m} \frac{1}{s_m^2} \int_{|X_k|>\epsilon s_m} X_k^2 \, dF = 0 \tag{78}$$

holds for all positive ϵ then $\frac{1}{s_m} \sum_{k=1}^{m} X_k$ converges in distribution to a normal random variable of mean zero and variance unity. In our case it is reasonable to assume that the density function of each X_k vanishes uniformly outside a compact set, then the Lindeberg condition is easily justified. So, the uncertainty U is approximately a normal random variable if we have sufficiently many (say > 10) random variables of each general form of distribution.

4.8 Margin to oscillations and margin sensitivity

Suppose that the power system is operating stably and the objective is to measure how close the system is to oscillations. The closeness of the power system to oscillation can be measured by a margin which is the change in one of the parameters required for the system to be at the onset of oscillation. There are several useful choices of parameter to measure the margin with. For example, it might be appropriate to choose the margin as the change in a critical interarea flow. In this case, the margin describes the increase in this interarea flow which would lead to the onset of oscillations. Alternatively, system loading could be used as a margin by picking a specific pattern of load increase and then defining margin to be the amount of load increase in that specific pattern which would lead to the onset of oscillations.

The margin to the onset of oscillations can be measured by a continuation method. The main idea of a continuation method is to repeatedly calculate equilibrium solutions as the parameter varies in small steps. The parameter variation continues until the onset of oscillations is reached. The value of the parameter at the onset of oscillations then determines the margin.

Once the margin has been computed, it is useful to compute the sensitivity of the margin to a wide range of power system parameters and controls. For example, if the margin is too small, then the sensitivities to controls can be used to help select controls which are effective in increasing the margin. Also, if there is uncertainty about some of the model data or assumptions, then the sensitivity of the margin with respect to that data can be used to estimate the effect on the margin of the uncertainty.

It turns out that the computation of the margin sensitivity is an easy variant of an eigenvalue sensitivity computation performed at the onset of the oscillations [66]. Thus the margin sensitivity computation is no more difficult than the eigenvalue sensitivity computation once the onset of oscillations is found by continuation.

The advantage of the margin sensitivity concept is that it yields information in a form directly useful to the analyst or operator. For example, if the margin is chosen to be the increase in tie line real power until the onset of oscillations, then the sensitivity of this margin with respect to a redispatch can be used to estimate the additional tie line power capacity available if the redispatch is done (this assumes that the tie line power capacity is determined by oscillations).

5 Scaling of eigenvalue computation time with system size

Computational speed is a key limiting factor to computing operator actions to suppress oscillations using eigenvalue computations. This section examines the scaling of computational speed with system size for advanced algorithms. Special models with scalable size approximating realistic models for computational purposes are devised and tested. This approach provides estimates of computation time for realistic size models within the project resources without the enormous effort of setting up large system models.

Eigenvalue determination has been an integral component of the analysis of power systems for many years [20, 78]. While efficient methods for eigenvalue determination have evolved over the years, no systematic study of the growth in computation for the most important algorithms seems to have been undertaken. Results on computational efficiency have been based on case-by-case analysis. This chapter studies in a systematic way the growth of computational time in the determination of eigenvalues and eigenvectors for very large power systems and attempts to predict how computational time grows as systems increase in size and complexity.

The chapter considers both simple and multiple eigenvalue determination for a small subset of eigenvalues near specified complex-plane locations. The solution of the eigenvector problem follows quite readily from the eigenvalue problem, and is not discussed here.

The chapter begins with a review of selected topics and methods for eigenvalue computation in the context of power systems. It then considers computability issues associated with multiple eigenvalues (an appendix discusses the special case of eigenvalue determination in the presence of Jordan blocks). The chapter then performs a variety of numerical experiments and illustrates the results these numerical experiments. The experiments and examples considered include:

- A radial network of identical ideal machines, as illustrated in Figure 9. For this case the chapter determines only one eigenvalue. Computation time as a function of number of generators is considered.
- A more complex random-structure prescribed-density network interconnecting ideal (second-order) machines. The ideal machines all have slightly different, random characteristics. Five distinct eigenvalues closest to prescribed eigenvalue locations are determined in these experiments. Again, the results illustrate computing time as a function of number of generators.
- A more complex random-structure prescribed-density network interconnecting machines, where the machines are represented by seventh-order dynamic mod-

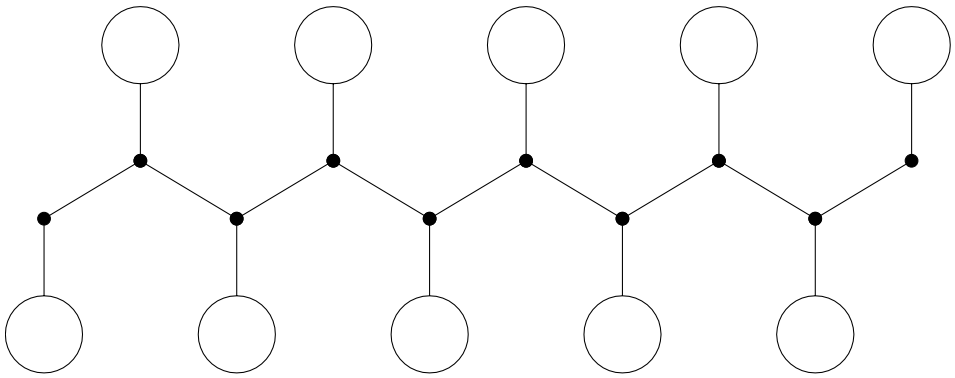

Figure 9: The structure of the radial test system interconnecting ideal second-order machines.

els. Five distinct eigenvalues are determined closest to prescribed eigenvalue locations.

- A study of the effect of network size is undertaken. The number of generators is kept constant as the size of the interconnecting network is varied.
- A study of the effect of network degree of interconnnectivity is undertaken. Both the number of generators and the number of nodes is held constant, but the density (interconnectivity) of the network is increased.

5.1 Computation of eigenvalues in electromechanical systems

We begin with an overview of the computation of eigenvalues for electromechanical systems. Electromechanical systems are characterized by sets of algebraic and differential equations of the general form:

$$\dot{x} = f(x, y, p) \tag{79}$$

$$0 = g(x, y, p) \tag{80}$$

where x is a vector of state variables. As a minimum, the x vector corresponds to machine angles and speeds, but numerous other variables associated with field

currents, fluxes and controls are also components of this vector. The vector y corresponds to purely algebraic variables, usually consisting of network voltages and angles at all network nodes. The vector y often includes other algebraic variables within the control loops of generators and other dynamic components. The scalar or vector p corresponds to a parameter or set of parameters of interest (such as the degree of loading of the system).

The equilibrium conditions (or operating point) are determined from a solution of a set of nonlinear algebraic equations based on the above, for a given value of p. Stability conditions associated with the steady state equilibrium point are determined from an analysis of the eigenvalues of the above equations, linearized around the operating point (x_0, y_0). The stability of the equilibrium conditions is obtained from an analysis of:

$$\begin{bmatrix} \Delta\dot{x} \\ 0 \end{bmatrix} = \begin{bmatrix} J_1 & J_2 \\ J_3 & J_4 \end{bmatrix} \begin{bmatrix} \Delta x \\ \Delta y \end{bmatrix} \tag{81}$$

where J_1, J_2, J_3 and J_4 are corresponding Jacobian components evaluated around the equilibrium point.

Early efforts for the computation of eigenvalues in power systems relied in the reduction of the problem above:

$$\Delta\dot{x} = A\Delta x \tag{82}$$

where $A = J_1 - J_2 J_4^{-1} J_3$ is the conventional reduced system matrix. For early efforts that rely on this computation, refer to [78]. Recent papers that do not focus on computational issues but rather on theoretical developments (such as [49]) continue to rely on this reduced formulation.

A slightly more general formulation of the original problem considers a version that is implicit (rather than explicit) in the state variables:

$$\begin{bmatrix} M_1\Delta\dot{x} \\ 0 \end{bmatrix} = \begin{bmatrix} J_1 & J_2 \\ J_3 & J_4 \end{bmatrix} \begin{bmatrix} \Delta x \\ \Delta y \end{bmatrix} \tag{83}$$

or alternatively:

$$\begin{bmatrix} M_1 & 0 \\ 0 & 0 \end{bmatrix} \begin{bmatrix} \Delta\dot{x} \\ 0 \end{bmatrix} = \begin{bmatrix} J_1 & J_2 \\ J_3 & J_4 \end{bmatrix} \begin{bmatrix} \Delta x \\ \Delta y \end{bmatrix} \tag{84}$$

If this implicit formulation is used, the expression for the explicit system matrix A in (82) becomes $A = M_1^{-1}\left(J_1 - J_2 J_4^{-1} J_3\right)$.

Efficient computation of eigenvalues for large scale problems requires that:

1. It be recognized that only certain modes are significant from the perspective of stability (i.e., solving the complete eigenproblem is not necessary), and

2. Sparsity be preserved throughout the computation.

Proper preservation of sparsity requires that the entire problem be formulated as an augmented problem. That is, equation (84) is to be preferred over equation (82). (This type of model is sometimes also referred to as a structure-preserving model.)

One of the first efforts in this regard was the AESOPS algorithm [11]. This algorithm was limited to electromechanical modes of a system. This algorithms finds the modes associated with each and every machine in turn by exciting the machine with a torque after shifting the system state matrix A. This algorithm works well because the electromechanical modes are generally the most important modes as far as electromechanical stability is concerned. Other algorithms that work on selected electromechanical modes include [55, 58].

The computationally difficult step in each and every eigenvalue algorithm mentioned above is the same: all methods require the solution of a shifted set of linear equations, where the amount of the shift is the best guess of the eigenvalue or eigenvalues of interest. Some algorithms are based on the use of multiple shifts. In every case, however, the key problem of interest consists of a sparse linear equation solution. If the reduced formulation is used, the linear set of equations that must be solved repeatedly is:

$$(A - qI)\, x = b \tag{85}$$

Sparsity preservation requires the use of the augmented formulation [50]. In this case, the equations of interest are:

$$\begin{bmatrix} (J_1 - qI) & J_2 \\ J_3 & J_4 \end{bmatrix} \begin{bmatrix} x \\ y \end{bmatrix} = \begin{bmatrix} b \\ 0 \end{bmatrix} \tag{86}$$

In both these cases, the "shift" q varies from iteration to iteration and according to the method used. The shift is generally complex (and purely imaginary in many cases), while the Jacobian matrices themselves are real. This often leads to the need for hybrid real/complex computations [45], or, if one is wishing to simplify matters, purely complex computation throughout.

The use of participation factors and sensitivity analysis has also been in widespread use in the power industry for the design of power system controls [57, 51]. Sensitivity analysis of eigenvalue locations is also a well-established topic in the numerical analysis literature and in other fields [68].

Ordinary transient stability studies consider parameters to be fixed. The impact of parameters (such as system loading) can be, however, dramatic. In fact, it can lead to qualitative changes in performance of the system. For example, the effect of reactive power limits on stability can lead to immediate instability points that are not evident at lower loading levels [22].

5.2 Second order models and a radial network

The first study considers a radial system with up to 5000 machines. For some eigenvalue algorithms (particularly those algorithms that rely on the construction of the explicit system state matrix A), the growth of computational complexity made it impossible to solve the above problem in reasonable time for anything but small systems. For the best algorithms tested the above sizes represented no significant problem.

In this section every machine is represented by the following model:

$$\dot{\delta}_i = \omega \tag{87}$$

$$\dot{\omega}_i = -B_i'\delta_i - D_i\omega_i + B_i'\theta_i \tag{88}$$

The linearized version of the network equations assumes that a nodal susceptance matrix $\mathbf{B}$ is available. The equations describing the network are thus given by:

$$\mathbf{B}\theta = 0 \tag{89}$$

where θ is a vector of nodal voltage angles. This equation presumes the use of a DC power flow approximation. However, similar computational results are obtainable for the general case if the Jacobian entries replace the above matrices and incremental variables replace actual variables. For our purposes, it is sufficient to consider this case.

Consider a system with n_g generators and n nodes. The model has $2n_g$ state variables and n additional network variables. This leads to $2n_g + n$ by $2n_g + n$ unreduced matrices $\mathbf{J}$ and $\mathbf{M}$ and a general problem structure of the form:

$$\underbrace{\begin{bmatrix} \mathbf{M}_{11} & 0 \\ 0 & 0 \end{bmatrix}}_{\mathbf{M}} \begin{bmatrix} \dot{\mathbf{x}} \\ 0 \end{bmatrix} = \underbrace{\begin{bmatrix} \mathbf{J}_{11} & \mathbf{J}_{12} \\ \mathbf{J}_{21} & \mathbf{J}_{22} \end{bmatrix}}_{\mathbf{J}} \begin{bmatrix} \mathbf{x} \\ \mathbf{y} \end{bmatrix} \tag{90}$$

where $\mathbf{J}$ is a Jacobian matrix and $\mathbf{M}$ is generally (but not always) a diagonal matrix of time constants. Figure 10 illustrates the topology of the $\mathbf{J}$ matrix and Figure 11 illustrates the topology of $\mathbf{M}$ for the case where $n_g = 10$ and $n = 10$.

5.3 Arbitrary topology networks

In order to experimentally test the growth in computation for large systems, we investigate what happens to the computational algorithms as networks grow in size and the number of machine increases. In order to perform these experiments, a program has been developed that permits us to test the computability of eigenvalues in ever-larger systems when the system topology is not purely radial. This program works as follows:

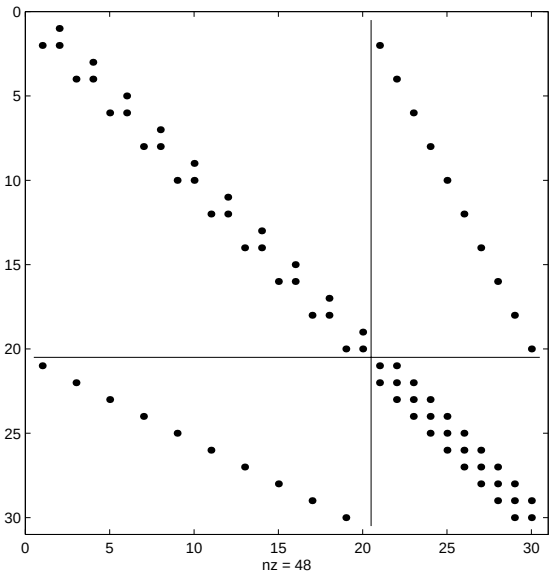

Figure 10: Topology of the **J** matrix for the case $n_g = 10$ and $n = 10$.

- A given number of nodes are randomly interconnected to form a tree.
- A given number of links are added to convert the tree structure into a network structure.
- Generators are added at a given number of random locations.

Figure 12 illustrates an example of the matrix topology that results from such an structure.

5.4 Arbitrary topology networks with high order machine models

The model for the machine was also expanded to a 7-th order model, based on the following equations:

$$\begin{aligned}
T'_{doi}\frac{dE'_{qi}}{dt} &= -E'_{qi} - (X_{di} - X'_{di})I_{di} + E^f_{di} \\
T'_{qoi}\frac{dE'_{di}}{dt} &= -E'_{di} + (X_{qi} - X'_{qi})I_{qi} \\
\frac{d\delta_i}{dt} &= \omega_i - \omega_s \\
\frac{2H_i}{\omega_s}\frac{d\omega_i}{dt} &= T_{Mi} - E'_{di}I_{di} - E'_{qi}I_{qi} - (X'_{qi} - X'_{di})I_{di}I_{qi} - D_i(\omega_i - \omega_s)
\end{aligned}$$

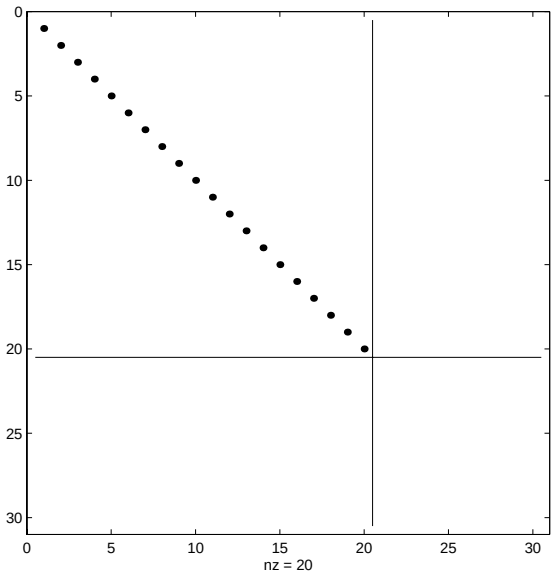

Figure 11: Topology of the $\mathbf{M}$ matrix for the case $n_g = 10$ and $n = 10$.

$$
\begin{aligned}
T_{Ei}\frac{dE'_{di}}{dt} &= -(K_{Ei} + S_{Ei})E'_{di} + V_{Ri} \\
S_{Ei} &= S_{eKi}\exp(S_{ePi}E'_{di}) \\
T_{Fi}\frac{dR'_i}{dt} &= -R'_i + \frac{K_{Fi}}{T_{Fi}}E'_{di} \\
T_{Ai}\frac{dV_{Ri}}{dt} &= -V_{Ri} + K_{Ai}R'_i - \frac{K_{Ai}K_{Fi}}{T_{Fi}}E'_{di} + K_{Ai}(V_{refi} - V_i) \\
T_{CHi}\frac{dT_{Mi}}{dt} &= -T_{Mi} + P_{SVi} \\
T_{SVi}\frac{dP_{SVi}}{dt} &= -P_{SVi} + P_{Ci} - \frac{1}{R_{Di}}(\frac{\omega_i}{\omega_s} - i)
\end{aligned}
$$

The algebraic equation corresponding to saturation (S_{E1}) is neglected in this section.

In addition to these differential equations, it is necessary to have two additional algebraic equations that relate the machine stator variables to the network variables:

$$
\begin{aligned}
E'_{di} - V_i\sin(\delta_i - \theta_i) - R_{si}I_{di} + X'_{qi}I_{qi} &= 0 \\
E'_{qi} - V_i\cos(\delta_i - \theta_i) - R_{si}I_{qi} - X'_{di}I_{di} &= 0
\end{aligned}
$$

The network for these experiments was also a lossless random arbitrary topology

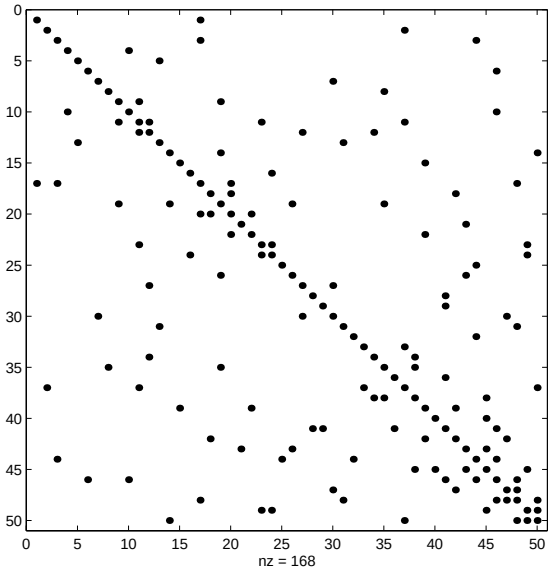

Figure 12: Topology of a random-structure interconnection admittance matrix for a 50 node network.

network. The system was assumed to be at equilibrium at no-load or low-load conditions. Within the network equations, the machine is connected to the system by including a term on the machine equations that corresponds to the power (active and reactive) delivered by the machine to the system (a similar term is added to represent loads). The following are the algebraic power equations used for the terminal nodes of the machine (for other nodes simply omit the power injection term).

$$\underbrace{I_{di}V_i\sin(\delta_i-\theta_i)+I_{qi}V_i\cos(\delta_i-\theta_i)}_{P_{Gi}}+P_{Li}(V_i)-\sum_{k=1}^{n}V_iV_kY_{ik}\cos(\theta_i-\theta_k-\alpha_{ik})=0$$

$$\underbrace{I_{di}V_i\cos(\delta_i-\theta_i)-I_{qi}V_i\sin(\delta_i-\theta_i)}_{Q_{gi}}+Q_{Li}(V_i)-\sum_{k=1}^{n}V_iV_kY_{ik}\sin(\theta_i-\theta_k-\alpha_{ik})=0$$

The initialization of the model for nonzero initial conditions proceeds as follows:

- A power system solution is obtained. This solution gives all values of voltage magnitudes V_i and voltage angles θ_i everywhere on the network.
- For each machine in turn, the solution of the following five simultaneous equa-

tions yields the solution for three of the internal state variables (δ_i, E'_{di} and E'_{qi}), along with two algebraic variables (I_{di} and I_{qi}):

$$I_{di}V_i\sin(\delta_i-\theta_i)+I_{qi}V_i\cos(\delta_i-\theta_i)=P_i \tag{91}$$
$$I_{di}V_i\cos(\delta_i-\theta_i)+I_{qi}V_i\sin(\delta_i-\theta_i)=Q_i \tag{92}$$
$$E'_{di}-V_i\sin(\delta_i-\theta_i)+R_iI_{di}+X_{qi}I_{qi}=0 \tag{93}$$
$$E'_{qi}-V_i\cos(\delta_i-\theta_i)-R_iI_{qi}+X_{di}I_{di}=0 \tag{94}$$
$$-E'_{di}+(X_{qi}-X'_{qi})I_{qi}=0 \tag{95}$$

- The remaining variables for the machine are then determined in turn from the appropriate equations:

$$E_{fd}=E'_{qi}+(X_{qi}+X'_{qi})I_{di} \tag{96}$$
$$\omega_i=\omega_s \tag{97}$$
$$V_{Ri}=-K_EE_{fd} \tag{98}$$
$$\text{etc.} \tag{99}$$

5.5 The eigenvalue solution methods

A number of eigenvalue computation methods were considered and tested. In the end, we settled on the following two methods:

- A simple inverse iteration method.
- The simultaneous iteration method.

These methods require that the problem be in standard form:

$$\dot{\mathbf{x}}=\mathbf{J}\mathbf{x} \tag{100}$$

or in generalized form:

$$\mathbf{M}\dot{\mathbf{x}}=\mathbf{J}\mathbf{x} \tag{101}$$

Converting the above problem to reduced form requires the use of the reduction formula:

$$\mathbf{A}=\mathbf{J}_{11}-\mathbf{J}_{12}\mathbf{J}_{22}^{-1}\mathbf{J}_{21} \tag{102}$$

Application of this formula to the above example results in the matrix topology structure illustrated in Figure 13, which after reordering yields the structure illustrated in Figure 14. Observe that a dense n by n corner of the matrix is obtained.

The use of this reduction formula makes it possible to use any ordinary method for eigenvalue computation, since there is no longer an issue associated with a non-full rank **M** matrix. However, doing this is highly discouraged as a result of the loss of sparsity. The result of using the reduced system matrix will generally be a quadratic (at least) growth in the computational characteristics of almost any eigenvalue determination method.

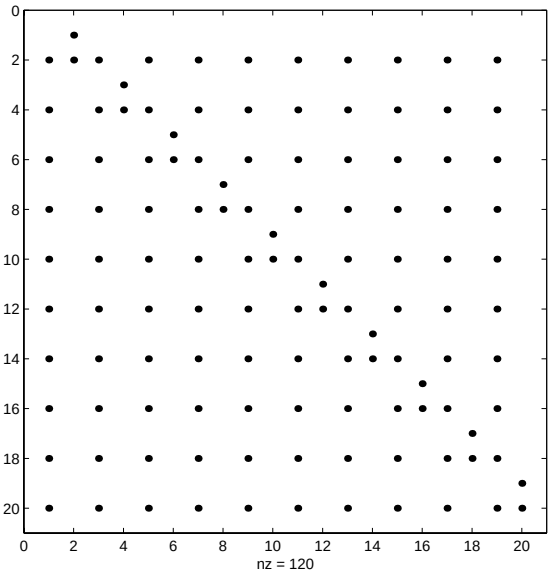

Figure 13: Topology of the reduced system **A** matrix for the case $n_g = 10$ and $n = 10$ (before reordering).

The most significant difference comes when one considers augmented methods for the solution of the eigenvalue problem. In the augmented method, no a-priori reduction takes place. Instead, we use a method based on the use of an augmented formulation, where no matrix is reduced.

The following specific methods and algorithms were considered:

1. Use of the reduced formulation and the full-matrix version of the Matlab eigensolver.

2. Use of the augmented generalized version of the full-matrix Matlab eigensolver. This solver finds all eigenvalues. Several of the eigenvalues are at infinity, which causes some problems with the algorithm, but successful solutions were obtained in all cases.

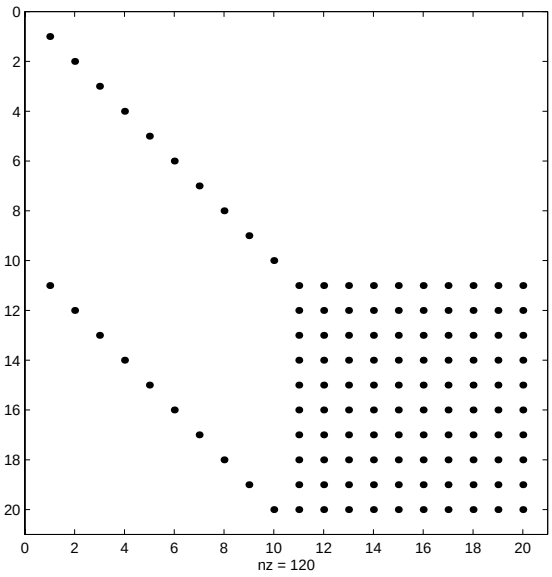

Figure 14: Topology of the *reordered* reduced **A** matrix for the case $n_g = 10$ and $n = 10$. The fact that **A** is now dense becomes evident.

3. Use of the sparse Matlab eigensolver on a sparse version of the *reduced* problem. The matrix **A** to which this method is applied can becomes dense.

4. Use of the sparse generalized Matlab eigensolver on the *unreduced* augmented matrix **J**.

5. Use the augmented inverse iteration algorithm with complex shifts on the reduced matrix, based on Matlab's linear solver.

6. Use the augmented inverse iteration algorithm with complex shifts on the augmented matrix, based on Matlab's linear solver.

7. Use of the augmented version of the simultaneous iteration method with a complex shift. The Matlab solver is used, along with Matlab's dense eigensolver to solve the reduced eigenproblem that result from the simultaneous iteration method.

8. Use of the augmented simultaneous iteration method with a vector of complex shifts. Multiple shift methods were not, however, tested.

The code for the simultaneous iteration method used in this work is supplied in section 5.8.

5.6 Numerical experiments on eigenvalue computation

We describe now the sequence of numerical experiments that were used to study how the growth in computing time increases with network size and other parameters.

The first case considered uses second order models for all machines and a radial network structure. It uses the inverse iteration method to obtain a single eigenvalue closes to a specified shift point. Figure 15 illustrates the growth in computation time and the eigenvalue as determined by the augmented inverse iteration method for this case. In this and all other examples, the times correspond to actual times on a 233 MHz Pentium II computer running Matlab version 5, and using the Windows 95 operating system.

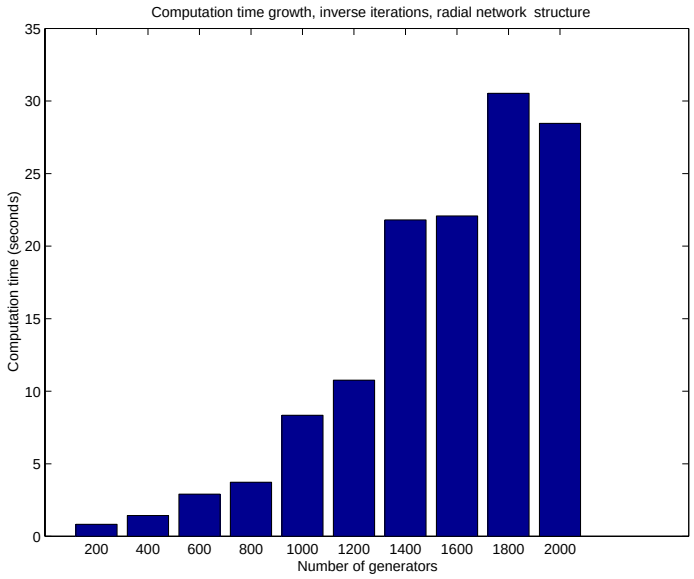

Figure 15: Growth in computation time for eigenvalue computation based on the augmented sparse inverse iteration method for radially-connected second order machines. Variability observed is due to variations in number of iterations to convergence.

The second experiment illustrates the growth in computation time for a random structure network interconnecting a set of second order machines. Figure 16 illustrates the growth in computation as a result of the inverse iteration version of the augmented eigensolver and applying it to the random structure low order model. The network itself is constructed as indicated earlier: first a random tree is constructed, then a specified number of links are added to the network. The number of links added increases as the network size increases. The size of the network (number

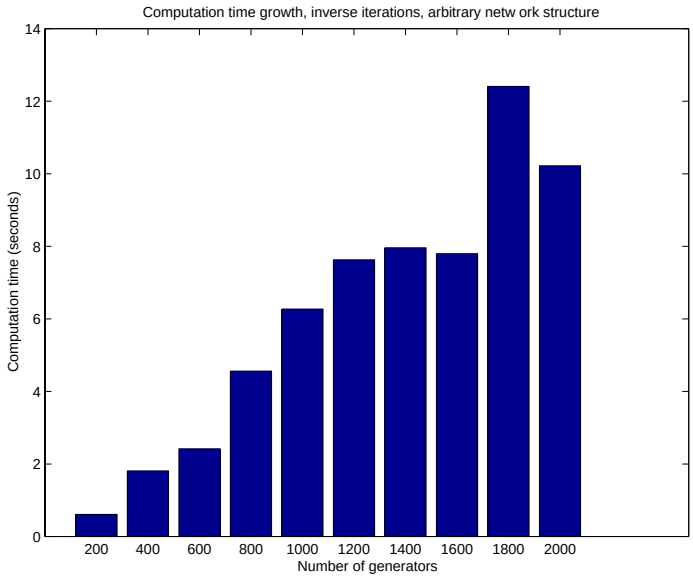

Figure 16: Growth in computation time for eigenvalue computation based on the augmented sparse inverse iteration method for network-connected second order machines. Variability observed is due to variations in number of iterations to convergence.

of network nodes) is a fixed multiple of the number of generators (in the case of these experiments, three).

In comparing these two cases, we observe that the radial network structure (which has a greater network "diameter") leads to greater computational growth.

The next two experiments compare the same two cases as above, but with two differences: first, the simultaneous iteration method is used instead of the inverse iteration method to obtain five eigenvalues, and second, the number of iterations to convergence has been standardized to prevent spurious variations in computation time (all subsequent studies compare times based on a fixed number of iterations to convergence). Figure 17 illustrates the growth in computation for the radial network case and Figure 18 illustrates the growth in computation time based on the use of an arbitrary non-radial network structure.

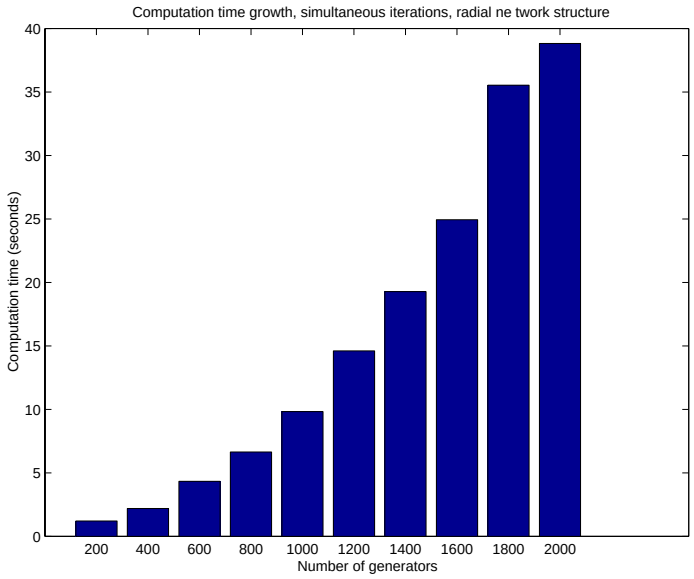

Figure 17: Growth in computation time for eigenvalue computation based on the augmented sparse simultaneous iterations for radially-connected second order machines. The number of iterations has been standardized.

The next set of experiments considers the use of more detailed generator models and the use of non-radial network structures. Figure 19 illustrates the matrix topology of the model for the augmented matrix **J** for a three-generator random-structure system using seventh order generator models. As networks grow larger, the structure of the diagonal entries for the generators stays the same (although the numbers themselves depend on the characteristics assumed for each unit). Figure 20

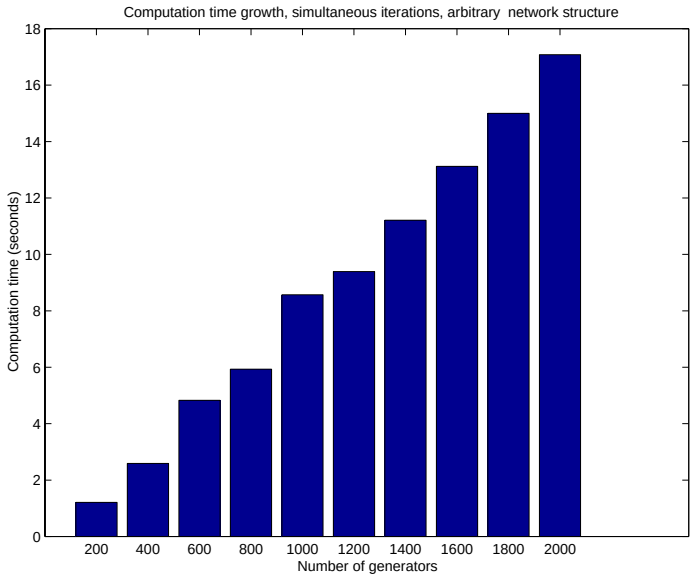

Figure 18: Growth in computation time for eigenvalue computation based on the augmented sparse simultaneous iteration method for network-connected second order machines. Variability observed is due to variations in number of iterations to convergence.

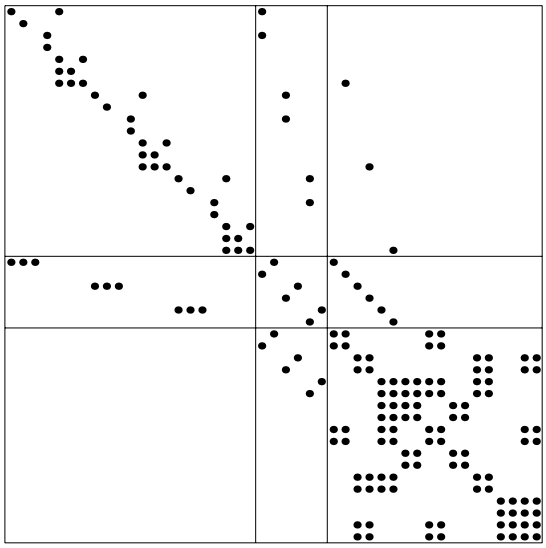

Figure 19: Topology for a three-generator nine-node random structure system.

illustrates the complete topology for the matrix for the 200 generator case using a seventh order model for each of the machines.

The results of the numerical growth in computation as a function of the number of generators for the seventh-order machine models are illustrated in Figure 21. Five eigenvalues closest to a given shift were determined using the simultaneous iteration algorithm.

The next experiment conducted corresponds to the study of the effect of network size on computability of eigenvalues. In the next set of experiments, 300 generators were represented as seventh-order models, but the number of nodes in the interconnected network was allowed to increase from one node per generator to 10 nodes per generator. Still, the five eigenvalues closest to a set of given shifts were determined as a function of interconnecting network size. The density of the interconnecting network measured as the number of links added to the network tree was increases as a square-root function of the network size. The results of these experiments are illustrated in Figure 22.

The last set of experiments corresponds to the study of the effect of network density. A 300 generator network was considered, each generator represented as a seventh order model. The network was assumed to consists of 900 nodes. The density of the network was allowed to increase from 50 links to 400 links. The growth in the computational time for the eigenvalue determination using the simultaneous

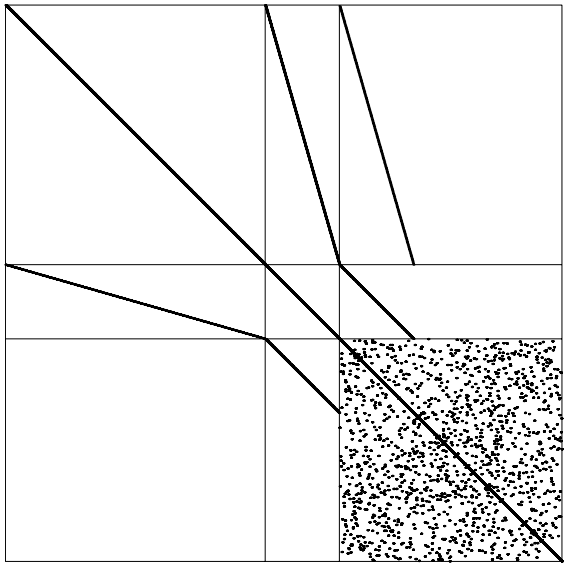

Figure 20: Topology for a 200 generator system interconnected by means of a 2000 node random structure network. The upper left portion of this matrix, which appears to be diagonal, is not. Each diagonal entry corresponds to a block with a sparsity structure corresponding to the machine differential equation model for one machine.

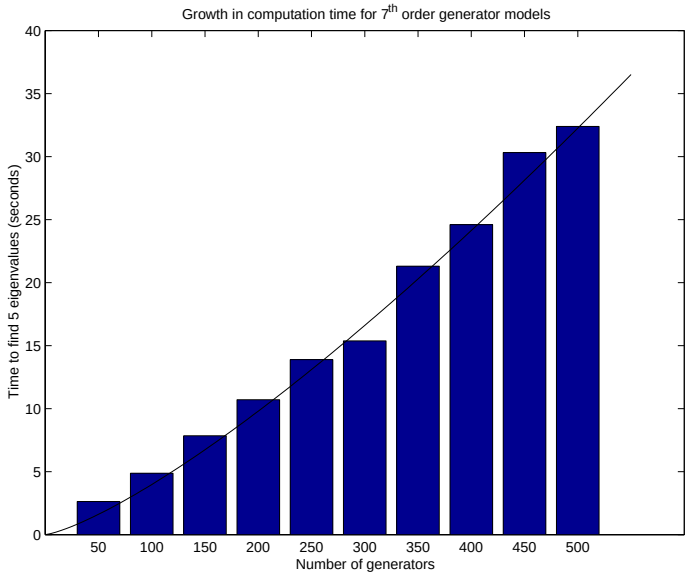

Figure 21: Growth in computation time for eigenvalue computation based on augmented sparse simultaneous iteration. A seventh order model for each of the machines was used. The background line shown illustrates a growth order of $n^{1.3}$. This growth is consistent with earlier studies on computational complexity in power systems that suggest growth in the order of $n^{1.0}$ to $n^{1.4}$ [3], and much lower than quadratic growth.

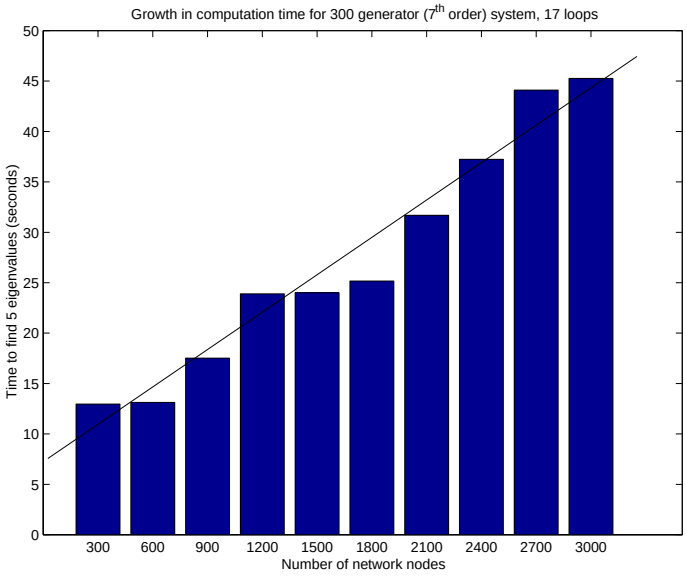

Figure 22: Growth in computation time for eigenvalue computation based on augmented sparse simultaneous iteration as a function of relative network size for a network with 300 generators with a fixed number of links. A seventh order model for each of the machines was used. The background line suggests linear growth in computation time.

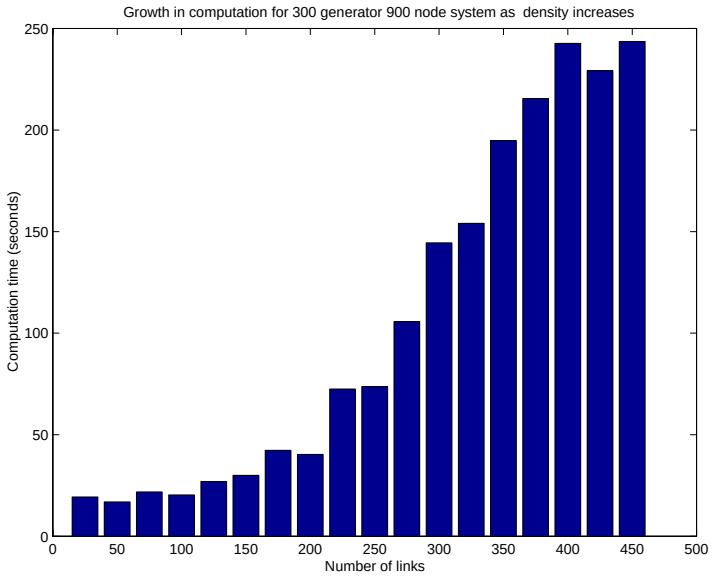

Figure 23: Growth in computation time for eigenvalue computation based on augmented sparse simultaneous iteration as a function of the density of the network interconnectivity (measured as the number of tree links in the network). A network with 300 generators was considered, and a seventh order model for each of the machines was used.

iteration method is illustrated in Figure 23. Observe that the growth in computing time for this case was greater than linear, leading to the observation that network density is perhaps the single most important determinant in eigenvalue computation time if proper sparsity methods are used in conjunction with the augmented formulation.

5.7 Jordan blocks

A key feature of eigenvalue computations is the inherent difficulty that occurs in the determination of eigenvalues associated with nontrivial Jordan blocks and non-diagonalizable matrices. A matrix is non-diagonalizable when it is similar to a Jordan block matrix according to the transformation:

$$A = XJX^{-1} \tag{103}$$

where J is a Jordan matrix of a certain order. A Jordan matrix of order n (or ascent n) is a matrix of the form:

$$J = \begin{bmatrix} \lambda & 1 & 0 & \cdots & 0 \\ 0 & \lambda & 1 & \cdots & 0 \\ \vdots & & & \ddots & 0 \\ 0 & 0 & \cdots & \lambda & 1 \\ 0 & 0 & \cdots & 0 & \lambda \end{bmatrix} \tag{104}$$

Jordan forms correspond to a defective multiple eigenvalue. It is important to indicate that not all multiple eigenvalues are defective. Only defective multiple eigenvalues give rise to serious computational difficulties. This chapter, for example, illustrates the computation of an eigenvalue of multiplicity about 5000 without any computational difficulties. On the other hand, an defective eigenvalue of multiplicity as low as 5 or less can become virtually incomputable in finite arithmetic. However, while computability of an eigenvalue location in exact arithmetic becomes impossible for such situations, the use of spectral analysis techniques makes it possible to compute a continuous spectrum that describes the behavior of the cluster of eigenvalues associated with the Jordan block. Thus, rather than attempting exact computation it is preferable to attempt to find a bound for the spectra of multiple defective eigenvalues.

5.8 The simultaneous iteration code

This section illustrates Matlab code used in the determination of multiple eigenvalues using the simultaneous iteration method. At the core of the code is the

determination of all eigenvalues of a reduced-dimension matrix. The size of the reduced matrix is equal to the number of desired eigenvalues. The amount of computation required for this step is generally quite trivial, unless a large number of eigenvalues are desired. Here is the code:

```
function lambda=simiter(A,q,m,M)
% Find m eigenvalues by sparse inverse simultaneous iteration
% Usage: lambda=simiter(A,q,m,M)
%   A single shift q is used
%   m is the desired number of eigenvalues (default is one)
%   If M is nonzero, a generalized eigenproblem is solved
n=size(A,1);
if nargin<3, m=1; end
if nargin<4, M=speye(n); end
ng=size(M,1);  % Number of state variables
z=sparse(i*rand(ng,m));
U=[z;sparse(n-ng,m)];
Vt=M*((A-speye(n)*q)\U);
Bt=(U'*U)\(U'*Vt);
[Pt,thetat]=eig(full(Bt));
oldTheta=0*diag(thetat);
for kk=1:50,
   V=M*((A-speye(n)*q)\U);
   B=(U'*U)\(U'*V);
   [P,theta]=eig(full(B));
   newTheta=diag(theta);
   if norm(oldTheta-newTheta,Inf)<=1e-4, break; end
   oldTheta=newTheta;
   U=V*P;
end
disp([int2str(kk) ' iterations']);
lambda=1./newTheta+q;
```

5.9 Concluding remarks

The numerical aspects of large scale computing of eigenvalues seems to not represent a significant technical challenge provided the augmented formulation is used. The methods used in the computation of large eigenvalues using sparse matrix methods scale close to linearly with matrix size.

No computational difficulties associated with Jordan blocks were encountered in

these experiments, in spite of the fact that many of the machines had identical characteristics. However, none of the systems considered were operating under extreme loading conditions.

A rather important remark concerns sparsity preservation issues. As is usually the case, sparsity preservation requires a careful consideration of the computational implications of every step of the computational process. It is very easy to end up with computational complexity that becomes quadratic or worse as a result of any one of a number of possible computational errors:

- If a key vector or matrix is accidentally declared to be dense, or otherwise becomes dense in the computational process. It is important to treat dense vectors (such as voltages) as sparse to preserve the sparsity of the overall computations.
- In languages such as Matlab, vectorization is quite critical to efficiency.
- Steps such as the construction of the Jacobians can, if not done carefully, overwhelm the rest of the computation.
- Steps that involve aggregation of matrices can, in some systems, become very slow. The use of profiling of programs is strongly recommended. For example, in languages such as Matlab, certain practices (such as operations involving selected rectangular portions of a sparse matrix) are to be avoided.

6 Directions in automated software for large dynamic models

This section describes the software which implements the eigenvalue calculations on the test systems and the scaling calculations and the lessons learned. This software tested several innovations in applying computer algebra to organize the equations, automatically derive Jacobians and Hessians, and automatically produce Matlab code. An approach to advanced, computer algebra assisted software for large systems is outlined based on the experience gained.

6.1 Software for 9 and 37 bus test systems

The software for 9 and 37 bus test systems was chosen for research flexibility, compatibility and use of standard software, ability to be validated and to try out some new approaches for power system software.

We made the following choices for the software implementing the 9 and 37 bus test systems:

- The test systems run in Matlab and the PTI program PSS/E. Matlab is needed for its flexibility, quick prototyping, some good numerical routines, its portability and for compatibility with other PSerc projects. The Matlab routines were developed by the project. PSS/E results are needed to validate the Matlab results and to encourage industry to believe the results. The approximate match between PSS/E results and Matlab results is shown in section 3.10. The Matlab routines find a succession of operating points and compute eigenvalues and eigenvalue sensitivities. PSS/E finds operating points, compute eigenvalues, and compute dynamical trajectories to illustrate the oscillations.

- The most difficult and time consuming aspect of setting up the test systems is specifying the same dynamic data for the machine models to both PSS/E and Matlab and validating the Matlab models. PTI format is our base standard for specifying the dynamics and statics of the test systems. Each machine requires a choice of the various generator, exciter, stabilizer and governor models and the appropriate parameters.

- The following procedure is used to pass the machine and other system data in PTI format to Matlab: The block diagrams of the models in the PTI manuals are used to write equations for the PTI models. These equations, together with the more straightforward network and load equations are entered into a Mathematica notebook. Executing the Mathematica notebook organizes the equations and also uses symbolic differentiation to produce the Jacobian and

Hessian of the entire system. The output of the Mathematica notebook is Matlab functions which are executed in a Matlab environment to evaluate the static or dynamic system equations and the system Jacobian and Hessian. Thus Mathematica is used to automatically write Matlab functions which incorporate the system equations and data and are used in the usual way within Matlab. This approach was chosen to exploit the organizational and symbolic capabilities of Mathematica while yielding stand-alone Matlab functions. We think that this approach is more flexible and reliable than direct coding of the test cases into Matlab.

- The Matlab functions require static equations to compute load flows and dynamic equations to compute the eigenvalues. The issue arises for the project because we are considering the effect of operating point changes on the dynamics. The static and dynamic equations are explained in section 4.3. Separate Matlab functions containing the static and dynamic equations are produced.

One purpose of the software was to explore the use of computer algebra in generating Jacobians and Hessians for realistic power systems models.

The conventional approach to generating power system Jacobians uses numerical differencing. To explain numerical differencing, suppose that the power system state is z and the power system differential-algebraic equations are

$$I_o \dot{z} = G(z) \tag{105}$$

We show a numerical differencing calculation for $G_z|_*$, the power system Jacobian evaluated at some operating point z_*. Let e_j be a column vector with 1 in the jth row and zeros elsewhere. The jth column of the Jacobian G_z is computed using the approximation

$$G_z[\cdot, j]|_* \approx (G(z_* + \Delta e_j) - G(z_*))/\Delta \tag{106}$$

The power system equations are evaluated with one state incremented slightly, the base case equations are subtracted, and then the result is divided by the increment.

The project represented the system equations symbolically, analytically differentiated the system equations using computer algebra and automatically produced code for evaluating the Jacobian and Hessians.

We compare the numerical differencing and computer algebra approaches:

- Accuracy. Computer algebra is more accurate. Accuracy is more significant when Hessians are computed by applying the differentiating procedure twice.

- Simplicity. Numerical differencing is simpler to program.

- Speed. Most current implementations of numerical differencing do not exploit sparsity. Sparsity is essential for practicality and can be exploited in the computer algebra approach.

- Handling of limits. The power system equations frequently change their form when limits are met. For example, excitation systems commonly include hard limits which constrain a dynamic variable to a constant or include continuous saturation functions. Numerical differencing handles limits without any elaboration in the code and this is a major advantage of numerical differencing. The hard limits cause programming complexity for computer algebra to account for the changes in the equations. The derivatives, and especially the second derivatives of continuous saturation functions are long algebraic expressions which can result in much unneeded computation.

- The symbolic representation of the model equations necessary for computer algebra allows the equations used for each component to be output for checking.

One important practical barrier to quick and accurate set up of power system dynamical models is the large amount of data in a variety of formats due to the various models used, particularly in the generator models. Checking the models and the data is a major task. For example, when directly coding dynamic models, it can be time consuming to get vector indices correct and to ensure that the input data can be output in a form which makes checking for data errors easy. One of the purposes of using the Mathematica computer algebra package was to allow the model equations to be written in a form close to ordinary mathematical notation, to allow more flexible assembly of the equations and vectors of quantities and to make data checking easier.

6.2 Software for eigenvalue scaling

To perform the eigenvalue computation time scaling in section 5, the project developed and used prototype symbolically-assisted numeric solving methods that permit the handling of arbitrary dynamic machine models. Thus many of the equations used in section 5 were automatically generated by this code, rather than manually entered. This approach was necessary to obtain a consistent set of equations with sufficiently realistic properties for meaningful computational growth results.

The automatic model and equation assembly process operated as follows:

- A network structure was generated. This required the construction of a synthetic network. Both fixed-structure networks and "random" structure networks were created. The simplest networks were simply and purely radial. The

values of the impedances connecting the radial nodes could be a fixed value or a variable value. This type of network model results in a tridiagonal nodal admittance matrix. The alternative model used a random structure model. Because truly random structure models lead to highly unrealistic statistical properties of the underlying matrices, the method used to generate random structures consisted of two steps: first, a random-structure *tree* was produced. Subsequently, a limited number of interconnections among the tree nodes was permitted. This resulted in a mostly networked system, with a few radial branches.

- At a number of locations within the artificially generated grid, a number of generators were placed. The properties (size, complexity of model, model parameters) for each of this generators were also controlled. Both the case of identical or similar machine models was considered, along with cases where the variables and the structure of the model used for the machine was varied randomly. The machines could include control systems or could be represented with models as simple as a second order model.

- A set of initial conditions was established. Having a steady-state conditions that is in (stable or unstable) equilibrium is essential for the analysis. Two approaches to the establishment of appropriate initial conditions were used: (a) Establishment of appropriate voltage/angle patterns and then computing the corresponding power flows and initial machine angles that lead to this result, or (b) solving in effect a power flow, based on the random specification of machine power outputs and/or load values, and then computing the internal machine and control system conditions.

Many alternatives to this system generation process remain to be investigated. In particular, it would be of interest to create the random networks either (a) by extrapolation of actual physical networks, where an automatic "expansion" procedure is considered, or (b) by interconnection of sets of smaller physical networks, or finally (c) by creating network growth by adding refinements and/or detail to existing physical models (for example, representing lower portions of the grid in greater detail). A combination of these methods is also permissible.

All these methods for the study of the performance of algorithms on ever-larger networks required the creation of an environment where the user had complete freedom on the equations to be used to model the system, including the ability to add new types of models and new types of controls to these models. Thus, it was difficult to do these studies using the more rigid model structure imposed by "classic" simulation environments such as those provided by PSS/E. However,

within the limited computer algebra system restrictions used in this project, it was also difficult to incorporate variable structure models.

Parts of the automatic and flexible assembly of power system model equations for assessing computational speed could be adapted and developed in future work to flexibly specify large dynamic power networks in a form suitable for applying advanced computer algebra methods.

6.3 Lessons learned

- The project reinforced our belief in the importance of data structures and software and model organization. Effective dynamic model software tools depend on being able to easily and flexibly specify and check dynamic models and their parameters.

- Validation of new software with existing software was very time consuming, partly because of the difficulty of reproducing exactly the models used in the commercial software. The large number of variants in machine dynamic modeling cause difficulties in comparing results.

- The issue of variable structure and control system limits is the main barrier to applying computer algebra methods. Better computer algebra models should, however, resolve this difficulty.

6.4 Advanced software concepts for large dynamic models

Based on the experience with the dynamic models described above, we outline some of the key issues for a new generation of dynamic power system models. The models are aimed towards oscillation problems, but many of the features would be of more general use in any dynamical investigation.

- The overall conception is a flexible set of tools to organize and assemble models and data into equations that can then be processed by any desired algorithm rather than a monolithic piece of software for a fixed purpose.

- Specification and checking of models and data. The model specifications should align with any emerging standards and be as compatible as possible with standard commercial packages to allow validation and transfer of cases. The software must produce easily legible output defining the models and parameters input so that they can be easily checked and updated. For example, parameter output must be labeled with the parameter names and subsets of the equations used should be accessible to the user.

- Hard limits and variable structure. This aspect requires a comprehensive approach. For example, a minimal set of basic operators for specifying hard limits and look up tables and case dependent functions could be developed. These operators would be used to specify variable structure and limits in the component models for input and internally in the code. The differentiation of the basic operators would be computable so that computer algebra could be used to automatically differentiate equations including the operators. The modeling and equation representation need to be designed for efficiency and for exploitation of sparsity. Alternative or similar concepts arising from automatic differentiation of functions defined by computer code containing conditional branching statements should be reviewed.

- Automatic assembly of equations. The software should automatically assemble equations in a form easily accessible to algorithms with flexibility in the choices of vectors of states and parameters.

- The use of matrix and vectorization concepts within symbolic algebra packages for purposes of efficiency needs to be further explored.

7 A new mechanism leading to oscillations

The power system linearization and its modes vary as power transfers, redispatch or other power system parameters change. We suggest a new mechanism for interarea power system oscillations in which two oscillatory modes interact near a strong resonance to cause one of the modes to subsequently become unstable. The two modes are near resonance when they have nearly the same damping and frequency. The possibility of this mechanism for oscillations is shown by theory and computational examples. Theory suggests that passing near strong resonance could be expected in general power system models. The mechanism for oscillations is illustrated in 3 and 9 bus examples with detailed generator models.

7.1 Introduction

This chapter considers how changes in power system parameters could cause low frequency oscillations. One example of parameter changes is power transactions which change the power system operating point and hence change the system modes and possibly cause oscillations. The main contribution of the chapter is to suggest, analyze and illustrate a mathematical mechanism for low frequency oscillations. Describing mechanisms which cause oscillations is an essential step in developing sound methods of operating the power system up to but not at the onset of oscillations.

The power system linearization and its modes vary as power system parameters change. Damped oscillatory modes can move close together and interact in such a way that one of the modes subsequently becomes unstable. An ideal version of this phenomenon occurs when two damped oscillatory modes (two conjugate complex pairs of eigenvalues) coincide exactly. This coincidence is called a resonance, or, especially in the context of Hamiltonian systems, a 1:1 resonance. If the linearization is not diagonalizable at the resonance, the resonance is called a *strong* resonance [68]. Otherwise, if the linearization is diagonalizable at the resonance, the resonance is called a *weak* resonance. Here we are most interested in strong resonance. At a strong resonance, the modes typically become extremely sensitive to parameter variations and the direction of movement of the eigenvalues turns through a right angle. For example, an eigenvalue that changes in frequency before the resonance can change in damping after the resonance and become oscillatory unstable as the damping changes through zero. The resonance is a precursor to the oscillatory instability in the sense that the resonance causes the eigenvalues to change the size and direction of their movement in such a way as to produce instability.

In practice the power system will not experience an exact strong resonance, but will pass close to such a resonance and the qualitative effects will be similar: the eigenvalues will move quickly and change direction as they interact and this can

lead to oscillatory instability. Note that although the eigenvalues move nonlinearly in the complex plane as power system dispatch varies, we are describing how a *linearization* of the power system model changes; we are not examining nonlinearities in the power system model at a fixed power system dispatch as in the normal form analysis recently applied to power systems [46, 72].

Previous power systems work related to the resonance phenomenon studied here includes analysis of the 1:1 resonance in Hamiltonian power system models by Kwatny [43], observation of mode patterns changing by Van Ness [74], the use of repeated poles to improve Prony analysis by Trudnowski et al. [73], and the studies of interarea oscillations at Ontario Hydro [39] and of the WSCC system [39, 52]. Seyranian has studied strong resonance in mechanics [68, 69]. These and other previous works are discussed in section 7.5.

7.2 Illustration of strong eigenvalue resonance

Two pairs of complex conjugate eigenvalues are exactly in resonance when they have exactly the same frequency and damping. Exact resonance is an unusual occurrence, but if it does occur, then the eigenvalues can be very sensitive to system changes and, if the resonance is strong, the eigenvalues move through a right angle at the resonance. This section illustrates strong resonance and near resonance in eigenvalues of parameterized matrices.

7.2.1 Example 1 (resonance of 2 real eigenvalues)

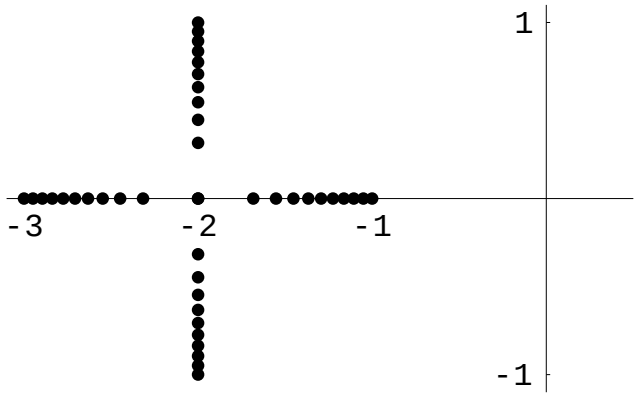

Figure 24: Resonance of two real eigenvalues

Before considering the strong resonance of complex eigenvalues, it is helpful to review the strong resonance of two real eigenvalues. Consider the matrix M_1

parameterized by the real number α:

$$M_1 = \begin{pmatrix} -2 & -1 \\ \alpha & -2 \end{pmatrix} \tag{107}$$

The eigenvalues of M_1 are $\lambda = -2 \pm \sqrt{-\alpha}$. The movement of the eigenvalues as α increases from -1 to 1 is shown in Figure 24. At $\alpha = -1$, the eigenvalues are -3 and -1. As α increases the eigenvalues approach each other until at $\alpha = 0$ the eigenvalues coincide at -2. As α increases through zero, the eigenvalues change direction by a right angle and move into the complex plane. At $\alpha = 1$, the eigenvalues are the complex pair $-2 \pm j$. The eigenvalue movement is fast near the strong resonance at -2; indeed, exactly at -2 the eigenvalues are infinitely sensitive to parameter variation.

This eigenvalue movement is familiar in control courses as the root locus obtained by increasing feedback gain on a second order plant with two real poles. In this context the point of strong resonance is called critical damping. The strong resonance point is also called a node-focus point and has been studied in power systems by Ajjarapu [2] and DeMarco [19]. Although the convergence of two system modes changes from monotonic to oscillatory at strong resonance, strong resonance is not generally a bifurcation (there is generally no change in topological equivalence or stability).

7.2.2 Example 2 (resonance of 2 complex pairs)

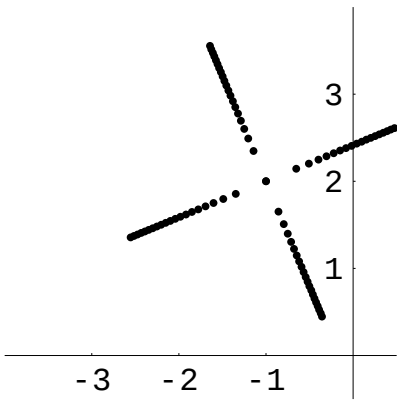

Figure 25: Exact resonance of two complex pairs

Consider the matrix M_2 parameterized by the real number α:

$$M_2 = \begin{pmatrix} -1+2\,j & 1+j & 0 & 0 \\ \alpha & -1+2\,j & 0 & 0 \\ 0 & 0 & -1-2\,j & 1-j \\ 0 & 0 & \alpha & -1-2\,j \end{pmatrix}$$

M_2 is a complex matrix, but it is structured to be similar to a real matrix (note that the 2×2 submatrices are complex conjugate). That is, a coordinate change T transforms M_2 into a real matrix:

$$T\,M_2\,T^{-1} = \begin{pmatrix} -1 & 1 & 2 & 1 \\ \alpha & -1 & 0 & 2 \\ -2 & -1 & -1 & 1 \\ 0 & -2 & \alpha & -1 \end{pmatrix}$$

$$\text{where} \quad T = \begin{pmatrix} 1 & 0 & -1 & 0 \\ 0 & 1 & 0 & -1 \\ j & 0 & j & 0 \\ 0 & j & 0 & j \end{pmatrix}$$

The eigenvalues of M_2 and $TM_2\,T^{-1}$ are the same.

At $\alpha = -2$, the eigenvalues of M_2 are $-1.64 \pm 3.55j$ and $-0.36 \pm 0.45j$. As α varies from -2 to 2, two of the eigenvalues of M_2 vary as shown in Figure 25 (these eigenvalues are $-1 + 2\,j \pm \sqrt{1+j}\,\sqrt{\alpha}$). Each eigenvalue shown in Figure 25 has a complex conjugate which moves correspondingly below the real axis. As α increases through zero, the eigenvalues change direction by a right angle. At $\alpha = 0$ the eigenvalues coincide at the strong resonance at $-1+2j$. M_2 is not diagonalizable at the resonance. The eigenvalue movement is fast near the resonance; indeed, exactly at the resonance the eigenvalues are infinitely sensitive to parameter variation. Note how one of the eigenvalues becomes unstable after the resonance.

7.2.3 Example 3 (near resonance)

Example 2 is not typical because an exact strong resonance is encountered. It is more typical to come close to strong resonance as the parameter is varied. Example 3 considers a matrix M_3 which is a perturbation of matrix M_2:

$$M_3 = M_2 + \begin{pmatrix} 0 & 0 & 0 & 0 \\ 0 & 0 & 1 & 0 \\ 0 & 0 & 0 & 0 \\ 1 & 0 & 0 & 0 \end{pmatrix} \tag{108}$$

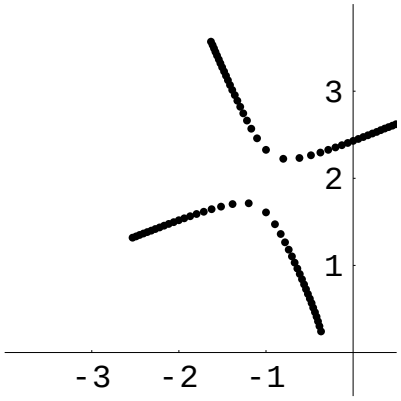

Figure 26: Near resonance of two complex pairs

The eigenvalues of M_3 vary as shown in Figure 26 as α varies from -2 to 2. Note how the eigenvalues come close together and quickly turn approximately through a right angle. There is a marked effect of coming close to the resonance.

7.2.4 Example 4 (near resonance)

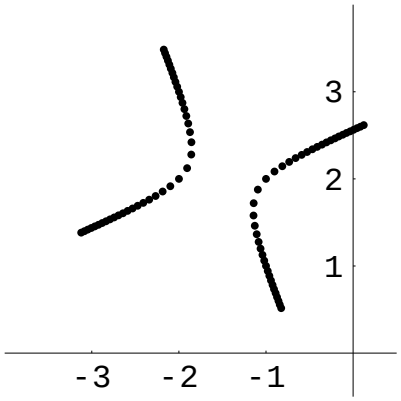

Figure 27: Near resonance of two complex pairs

Example 4 shows a different way in which example 2 can be perturbed:

$$M_4 = M_2 + \begin{pmatrix} 0 & 0 & 0 & 0 \\ 0 & -1 & 0 & 0 \\ 0 & 0 & 0 & 0 \\ 0 & 0 & 0 & -1 \end{pmatrix} \tag{109}$$

The eigenvalues of M_4 vary as shown in Figure 27 as α varies from -2 to 2. The eigenvalue movements in Figures 26 and Figure 27 are both close to the eigenvalue movement in Figure 25, but a different eigenvalue becomes unstable in Figures 26 and Figure 27.

7.3 Power system simulation results

This section shows examples of 3 bus and 9 bus power system models passing near strong resonance as parameters are changed.

7.3.1 3 bus system

We have found an oscillatory instability caused by strong resonance in the 3 bus system described in section 2.2.1. The 3 bus system consists of generators at bus 1 and bus 3 and a constant power load at bus 2. The generator models are tenth order and the system parameters are reported in section A.1. As the generator dispatch is varied to increase the power supplied by bus 3, two damped complex eigenvalues vary as shown in Figure 28. The eigenvalues are initially at $-0.4 \pm 8.3j$ and $-0.9 \pm 4.3j$ and are stable. As the power supplied by bus 3 increases, the two eigenvalues approach one another, interact, and then one of the eigenvalues crosses the imaginary axis and becomes unstable.

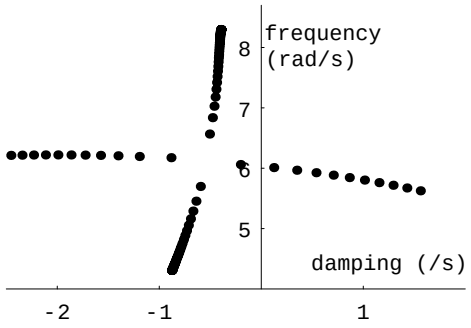

Figure 28: Eigenvalues as dispatch varies; $V_{ref} = 1.07$

The case shown in Figure 28 is adjusted to show the eigenvalues coming close together and has $V_{ref} = 1.07$, where V_{ref} is the voltage reference set point of the generators at buses 1 and 3. Rerunning the case for decreased and increased V_{ref} is shown in Figures 29 and 30. Figures 29 and 30 show typical perturbations of the

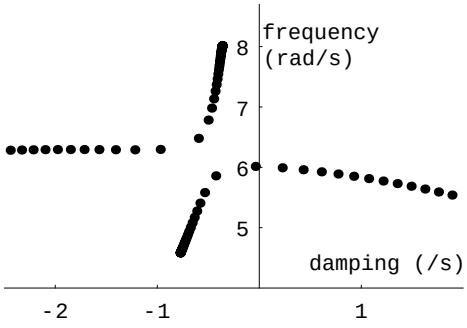

Figure 29: Eigenvalues as dispatch varies; $V_{ref} = 1.03$

strong resonance. Observe that if one attempts to stabilize the unstable eigenvalue of Figure 29 by raising V_{ref}, then this eigenvalue is indeed stabilized, but that the other eigenvalue becomes unstable as shown in Figure 30. This shows the importance of examining both pairs of eigenvalues near strong resonance when trying to stabilize the system.

7.3.2 9 bus system

The form of the 9 bus system is based on the WSCC system from the text of Sauer and Pai [67]. There are 3 generators with 2 axis models and IEEE Type I exciters. More details may be found in sections 2.2.2 and A.2. Figure 31 shows the eigenvalue movement when real power generation at bus 2 is varied from 1.5 pu to 2.10 pu in steps of 0.05. Real power generation at bus 3 is fixed at 1.5 pu.

The eigenvalues pass near resonance and then one of the eigenvalues becomes oscillatory unstable. Note that the eigenvalues initially move together by a change mostly in frequency. It is the resonance which transforms this movement into a change in damping and hence instability. The eigenvalues move quickly near the resonance.

7.4 Theory results

This section gives an informal account of the theoretical results. The mathematics to support these results is presented in section 7.7.

As power system parameters vary, the Jacobian matrix M describing the linearization of the power system at the operating point also varies. The system modes

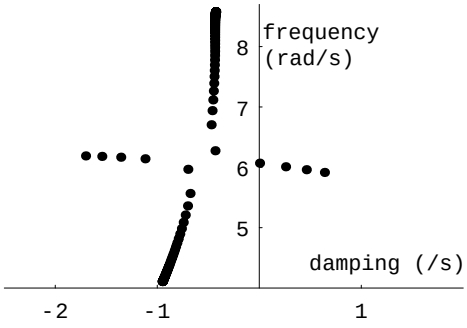

Figure 30: Eigenvalues as dispatch varies; $V_{ref} = 1.11$

are described by the eigenvalues and eigenvectors of the Jacobian M. The theory describes how two oscillatory modes of the Jacobian M vary when they are near a resonance in which two complex eigenvalues coincide in frequency and damping.

7.4.1 Strong resonance

We now describe the situation near a strong resonance. Near strong resonance the Jacobian M is similar to a matrix which includes a 4×4 submatrix M'_C describing the modes of interest:

$$M'_C = \begin{pmatrix} \lambda & 1 & 0 & 0 \\ \mu & \lambda & 0 & 0 \\ 0 & 0 & \lambda^* & 1 \\ 0 & 0 & \mu^* & \lambda^* \end{pmatrix} = \begin{pmatrix} M_C & 0 \\ 0 & M_C^* \end{pmatrix} \tag{110}$$

Here λ and μ are complex numbers which are functions of the power system parameters. The star symbol * stands for complex conjugate. The eigenvalues of M'_C are the same as the eigenvalues of the Jacobian M corresponding to the two oscillatory modes of interest.

The behavior of M'_C is governed by the submatrix

$$\boxed{M_C = \begin{pmatrix} \lambda & 1 \\ \mu & \lambda \end{pmatrix}} \tag{111}$$

It is straightforward to calculate that the eigenvalues of M_C are

$$\lambda_1 = \lambda + \sqrt{\mu} \qquad \text{and} \qquad \lambda_2 = \lambda - \sqrt{\mu} \tag{112}$$

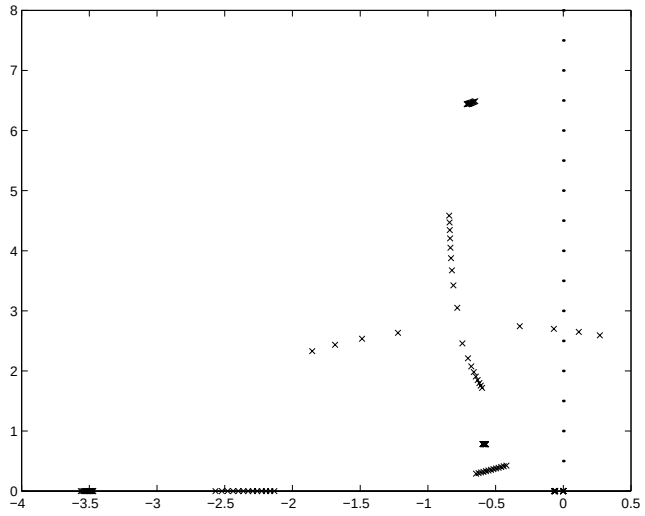

Figure 31: 9 bus eigenvalues as dispatch varies

Therefore the eigenvalues of M_C' are

$$\lambda \pm \sqrt{\mu} \quad \text{and} \quad (\lambda \pm \sqrt{\mu})^*$$

and these are the eigenvalues of the Jacobian M corresponding to the modes of interest. The idea is to study these modes by examining the eigenvalues and eigenvectors of M_C.

The eigenvalues of M_C coincide at λ when $\mu = 0$ and this is the condition for resonance. M_C is nondiagonalizable at resonance (alternative terms for 'nondiagonalizable' are 'nonsemisimple' and 'nondefective'). The sensitivity of these eigenvalues to the real or imaginary part of μ is $\dfrac{\pm 1}{2\sqrt{\mu}}$, which tends to infinity as μ tends to zero. As μ moves in the complex plane on a smooth curve through 0 with nonzero speed, the argument of $\sqrt{\mu}$ jumps by 90^o so that the direction of the eigenvalue movement changes by 90^o.

The right and left eigenvectors of M_C are

$$\begin{pmatrix} 1 \\ \pm\sqrt{\mu} \end{pmatrix} \qquad \text{and} \qquad (\pm\sqrt{\mu}, \quad 1)$$

At the resonance at $\mu = 0$, the eigenvectors are infinitely sensitive to changes in μ and the right and left eigenvectors are orthogonal. At the resonance at $\mu = 0$, there is a single right eigenvector together with a generalized right eigenvector. As μ tends

to zero and the resonance is approached, the two right eigenvectors become aligned and tend to the right eigenvector at $\mu = 0$. Thus the system modes approach each other as μ tends to zero. The dependence of this approach on $\sqrt{\mu}$ shows that this approach is initially slow and then very quick near $\mu = 0$.

7.4.2 Predicting eigenvalue movement near strong resonance

Let λ_1 be a lightly damped system eigenvalue. Formulas to compute the first order eigenvalue sensitivity $\frac{\partial \lambda_1}{\partial p}$ with respect to changes in any parameter p are very useful in determining the robustness of λ_1 and in detecting whether λ_1 is a critical mode that can readily become unstable as parameters change. (For the parameters such as redispatch considered here, the effect of the equilibrium movement must be accounted for by Hessian terms in the formulas computing these sensitivities.)

Now suppose that λ_1 and λ_2 are close to a strong resonance. Then the nonlinear and rapidly changing movement of the eigenvalues near the resonance will make $\frac{\partial \lambda_1}{\partial p}$ and $\frac{\partial \lambda_2}{\partial p}$ very poor estimates of the eigenvalue movements for any sizable changes in p. This subsection shows how better estimates can be obtained.

An important general observation is that λ and μ of (111) can be calculated from numerical eigenvalue results. Inversion of (112) yields

$$\lambda = (\lambda_1 + \lambda_2)/2 \tag{113}$$

$$\mu = (\lambda_1 - \lambda_2)^2/4 \tag{114}$$

λ is the average eigenvalue and μ describes the detuning from exact strong resonance.

Figure 32 shows how λ and μ computed from (114) vary for the case shown in Figure 33. The approximately linear variation of λ and μ in Figure 33 motivates the following method of estimating eigenvalue movement. The sensitivity of λ and μ with respect to p can be calculated from the sensitivities of λ_1 and λ_2:

$$\frac{\partial \lambda}{\partial p} = \frac{1}{2}\left(\frac{\partial \lambda_1}{\partial p} + \frac{\partial \lambda_2}{\partial p}\right) \tag{115}$$

$$\frac{\partial \mu}{\partial p} = \frac{\lambda_1 - \lambda_2}{2}\left(\frac{\partial \lambda_1}{\partial p} - \frac{\partial \lambda_2}{\partial p}\right) \tag{116}$$

First order estimates of the changes in λ and μ are made using (115) and (116) and then estimates of the eigenvalue movements are obtained using (112). Figure 33 shows a good match between the estimated and actual eigenvalue movements.

7.4.3 Strong resonance in the frequency domain

We examine the time and frequency domain solutions at strong resonance when $\mu = 0$. Assume that $\lambda = \sigma \pm j\omega$ with $\sigma < 0$. The time domain solutions to the

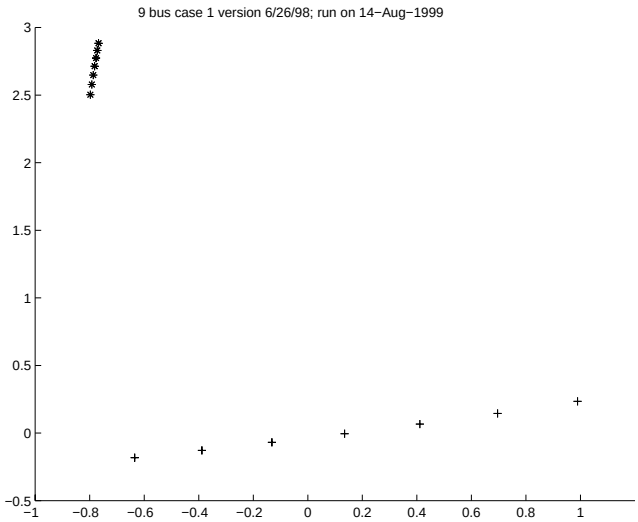

Figure 32: Variation in λ and μ near strong resonance; $* = \lambda$, $+ = \mu$.

linear differential equations with matrix (110) are linear combinations of $te^{\sigma t}\cos\omega t$, $te^{\sigma t}\sin\omega t$, $e^{\sigma t}\cos\omega t$ and $e^{\sigma t}\sin\omega t$. Some perturbations mainly excite the $te^{\sigma t}\cos\omega t$ and $te^{\sigma t}\sin\omega t$ solutions and these perturbations will cause oscillations that grow before exponentially decaying to zero. The frequency domain description may be shown in block diagram form:

Observe the input/output combination passing vertically down the page in Figure 34 in which the output of the first damped oscillator feeds the second damped oscillator. This mode coupling, which is characteristic of the strong resonance, has interesting consequences for the power system behavior.

Consider two modes which initially are local to separate areas of the power system. The modes are initially decoupled so that disturbances in one area will only affect the mode in that area. Now suppose that parameters change so that the two modes interact by encountering a strong resonance. As the strong resonance is approached, the mode eigenvectors will converge so that the modes are no longer confined to their respective areas. Moreover, at the strong resonance, a disturbance in one of the areas (say area 1) can excite the mode of area 2. We expect that qualitatively similar mode coupling effects can occur for systems that pass near strong resonance.

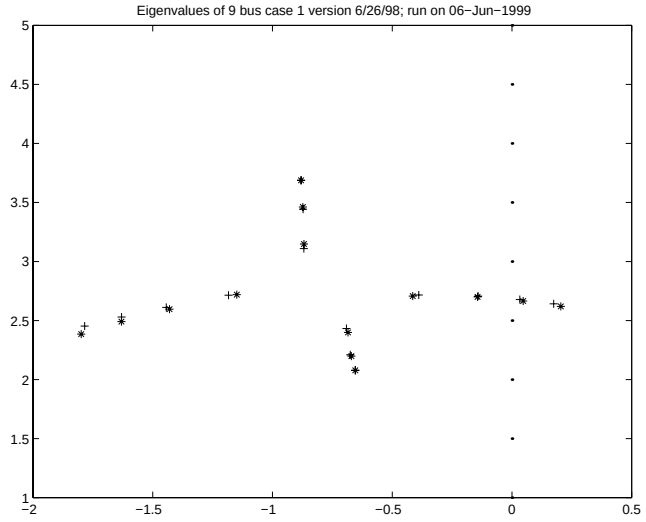

Figure 33: Predicting eigenvalue movement near resonance; +=predicted eigenvalues, *= actual eigenvalues.

7.4.4 Genericity of strong resonance

The theory also describes how typical strong resonance is in a generic set of differential equations such as those which might be expected when modeling a power system with no special structure. Consider a generic set of equations with two real parameters (this could be obtained from a power system model by letting only two of the power system parameters vary). Each point in the parameter plane yields an operating point and a Jacobian. The generic situation is that every point in the parameter plane will yield a diagonalizable Jacobian except for isolated points at which strong resonance occurs. Weak resonance does not generically occur in the parameter plane. (The meaning of a situation being generic is that the situation is robust to small perturbations of the equations and that any exceptional cases in which more exotic events occur can be perturbed with a small perturbation so that the situation obtains.) Now suppose that the two parameters vary as a function of another parameter t; this describes a curve in the parameter plane. It should be clear that, generically, this curve will not pass through any of the isolated resonance points. That is, as t is varied, the system will not typically encounter an exact strong resonance. However, it is quite possible that the curve passes *near* one of the strong resonances as t is varied.

More generally, we can examine the rarity of strong resonance using the concept of codimension. The rarity of an event can be described by the number of inde-

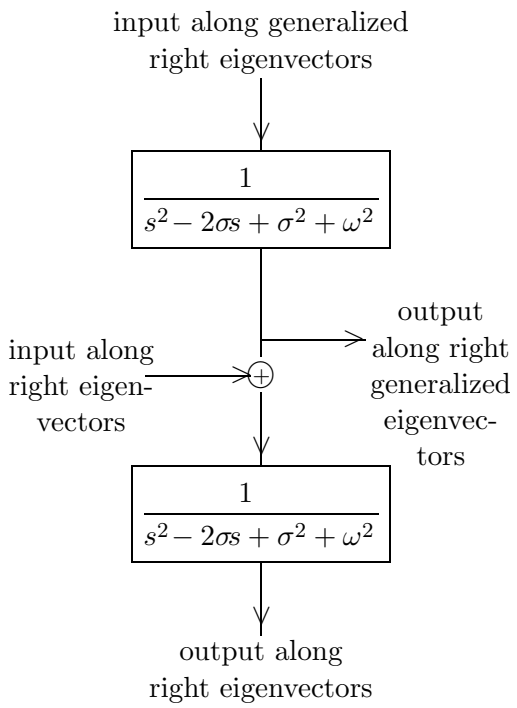

Figure 34: Modes at strong resonance

pendent parameters that need to be varied to typically encounter the event; this number is called the *codimension* of the event. For example, in a power system, the event that flow on a particular line is *not* exactly 500 MW typically occurs without any independent parameters varying and is codimension 0. The event that flow on a particular line is exactly 500 MW typically requires one parameter to be varied and is codimension 1. For example, the dispatch of a single generator could be changed so that the flow on a particular line is exactly 500 MW. The event that flow on a particular line is exactly 500 MW *and* the voltage angle at bus 27 is exactly 30$^{\text{o}}$ typically requires two parameters to be varied and is codimension 2. The dispatch of two generators could be changed so that flow on a particular line is exactly 500 MW *and* the voltage angle at bus 27 is exactly 30$^{\text{o}}$.

Events of higher codimension are successively rarer. A codimension 0 event can typically happen at any time in a power system. As the power system is operated during the day, it is parameterized by the single parameter time, so that codimension 1 events can typically happen during one day of operation. For example, the flow on a particular line being exactly 500 MW could be a typical occurrence at

some time during the morning load pick up. Note that a codimension 1 event need not necessarily happen every day, but that it is in some sense typical when it does happen. Oscillatory modes becoming unstable and voltage collapse are other examples of codimension 1 events: either instability can typically occur as a single loading parameter is increased.

The coincidence of two pairs of complex eigenvalues of a matrix at $\lambda = \sigma \pm j\omega$ typically happens with Jordan canonical form

$$\begin{pmatrix} \lambda & 1 & 0 & 0 \\ 0 & \lambda & 0 & 0 \\ 0 & 0 & \lambda^* & 1 \\ 0 & 0 & 0 & \lambda^* \end{pmatrix} \tag{117}$$

A strong resonance of the form (117) without regard to the value of λ occurs in the matrix (110) when the complex parameter $\mu = 0$. Since this requires both the real and imaginary part of μ to be zero, this is a codimension 2 event. (On the other hand, the occurrence of a strong resonance of the form (117) for a *particular* value of $\lambda = \lambda_0$ requires both $\lambda = \lambda_0$ and $\mu = 0$ and is a codimension 4 event.)

A strong resonance with two oscillatory modes exactly coinciding is a codimension 2 event. Thus it can be typically encountered when varying two parameters. Strong resonance will not be typically encountered when varying one parameter, but it is still possible to pass near to strong resonance and in this case the nearness would have a significant effect on the system behavior. In particular, if the system is near strong resonance, then the following is typical:

- The eigenvalues and eigenvectors are very sensitive to parameter variations
- A general parameter variation causes the direction of eigenvalue movement in the complex plane to turn quickly through approximately a right angle.
- The right and left eigenvectors are nearly orthogonal.
- The right eigenvectors of the two modes are nearly aligned. This implies that the pattern of oscillation of the two modes is similar.

7.4.5 Weak resonance

There is a further possibility when two complex eigenvalues coincide that the Jacobian is diagonalizable. That is, at resonance the Jacobian M is similar to a matrix which includes a 4×4 submatrix

$$\begin{pmatrix} \lambda & 0 & 0 & 0 \\ 0 & \lambda & 0 & 0 \\ 0 & 0 & \lambda^* & 0 \\ 0 & 0 & 0 & \lambda^* \end{pmatrix} \tag{118}$$

This type of eigenvalue resonance is called weak resonance and is not generic in two parameter equations. (Indeed it is a codimension 6 event.) Thus we do not expect weak resonance to occur in a generic set of equations such as those that might be expected when modeling a power system with no special structure. However, weak resonance can occur with some special structure: For example, consider two power systems which are not connected together by any tie lines. The eigenvalues of the entire system belong to either one power system or the other. If parameters vary so that an eigenvalue of one power system coincides with an eigenvalue of the other power system, then these two eigenvalues will not interact as parameters vary and this is weak resonance. Another example of special structure which can yield weak resonance is when a power system study is done with a bilaterally symmetric power system model.

At weak resonance, there is ambiguity in associating eigenvectors with one of the modes that is resonating because any nontrivial combination of the eigenvectors is also an eigenvector. Moreover, the eigenvectors and eigenvalues are ill conditioned in that some parameter changes cause sudden changes in the eigenvectors and eigenvalues. In particular, there are strong resonances arbitrarily close to a weak resonance.

We examine the time and frequency domain solutions at diagonalizable resonance. Assume that $\lambda = \sigma \pm j\omega$ with $\sigma < 0$. The time domain solutions to the linear differential equation with matrix (118) are linear combinations of $e^{\sigma t}\cos\omega t$ and $e^{\sigma t}\sin\omega t$. The frequency domain description may be shown in block diagram form:

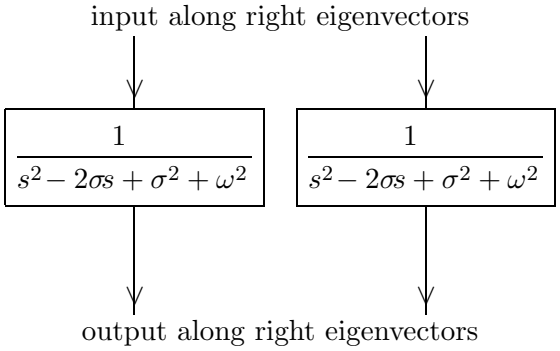

Figure 35: Modes at diagonalizable resonance

Observe that one mode does not feed the other mode as in Figure 34.

Suppose that two modes which are local to separate areas of the power system and thus decoupled encounter a weak resonance. Then the modes remain decoupled

at the weak resonance. For example, a disturbance confined to one area will only excite the local mode of that area. (This follows from the invariance of any linear subspace of the eigenspace corresponding to the coincident eigenvalues.)

7.4.6 Typical resonance in power system models

Suppose that a power system model is a generic set of parameterized differential equations such as those that might be expected when the power system has no special structure. Then the theory of the previous subsections shows that the resonance that is most typically encountered is the strong resonance. If a single parameter of the power system model were varied, the system would not be expected to encounter exact strong resonance, but it could well pass near strong resonance. If two parameters of the power system model were varied, then a strong resonance could be typically encountered.

This analysis raises the question of the extent to which practical power system models are generic or have 'special structure'. It seems clear that special structure such as bilateral symmetry or perfect decoupling due to the power system areas being completely disconnected is not expected in practical power systems models. Moreover, a sensible initial working assumption is that practical power system models are generic. However, it is a possibility that in some cases there could be sufficient decoupling between power system areas to make the areas approximately decoupled. In these cases the power system could pass near to a weak resonance. This would also imply passing near a strong resonance, since there are strong resonances arbitrarily close to a weak resonance. However, not all perturbations of the weak resonance involve the strong resonance and, moreover, it is possible that the strong resonance could be observed only in a detailed analysis whereas the weak resonance would determine the approximate overall behavior. More work is needed to clarify whether a weak resonance is likely to occur in a practical power system model and what would be expected to be observed near a weak resonance.

Another consideration is the genericity of the parameter changes being considered. Parameter changes such as power redispatch strongly affect the operating point and are expected to generically change the power system linearization. It is not clear whether changing a control system gain corresponds to a generic parameter change. Control systems are designed to affect particular modes and changes in control gains often have little or no effect on the operating point.

7.5 Previous Work

This section describes previous work and its relation to the resonance phenomenon.

Kwatny [43, 44] studies the flutter instability in power system models with

Hamiltonian structure. A stable equilibrium of a Hamiltonian power system model necessarily has all eigenvalues on the imaginary axis. One generic way for stability to be lost as a parameter varies is the flutter instability, or Hamiltonian Hopf bifurcation. In the flutter instability, two modes move along the imaginary axis, coalesce in an exact strong resonance, and split at right angles to move into the right and left halves of the complex plane. The Hamiltonian power system model in [43] represents electromechanical mode phenomena with simple swing models for the generators. Kwatny [43] gives a 3 bus example of the flutter instability and emphasizes that the flutter instability is generic in one parameter Hamiltonian systems. It is also possible to add uniform damping to the conservative model in order to shift the Hamiltonian eigenvalue locus a fixed amount leftwards in the complex plane [44]. Then two eigenvalues (necessarily of the same damping) approach other in frequency, coalesce in an exact strong resonance and then split apart in damping. One of these eigenvalues can then cross the imaginary axis in a Hopf bifurcation to cause an oscillation. This is clearly a special case of strong resonance causing an oscillation. The Hamiltonian plus uniform damping model structure constrains the eigenvalues to move either vertically along the line of constant damping or horizontally and causes the resonance to be exact.

Van Ness [74] analyzes a 1976 incident of 1 Hz oscillations at Powerton station with a 60 machine model of the Midwestern American power system with 9 machines represented in detail. The paper seems successful in reproducing the essential features of the incident by eigenanalysis of the model. Figure 7 of [74] examines the effect of a variation of power and excitation at Powerton unit 6. The eigenvector associated with a dominant eigenvalue shows significant changes near the instability that are attributed to a resonant interaction with another nearby mode. Movement in the real part of close eigenvalues when the excitation is lowered 'seems to be due to a coupling effect which has been observed in the model'. Unfortunately the data is sparse; only one change in each of the power or excitation is presented and firm conclusions about the nature of the resonant interaction cannot be made. However, the features shared between the account of the eigenanalysis of [74] and the strong resonance are suggestive.

Klein and Rogers et al. at Ontario Hydro [39] analyze local modes and an interarea mode in a symmetric power system model with 2 areas and 4 machines. The symmetry is bilateral: each of the 2 areas has the same machines and transmission lines. However, the base case is a stressed case with area 1 exporting power to area 2 over a single weak tie line. The two local modes have eigenvalues that are practically equal, and each of the computed local modes has substantial components across the entire system. A small decrease in the machine inertias in area 2 causes the local modes to change substantially to have significant components only in their respective areas. Klein and Rogers attribute these results to the nonunique-

ness of eigenvectors associated with a weak resonance. Although similar eigenvector changes could be found near a strong resonance, one can argue that a weak resonance is expected here because of the high degree of system symmetry. We do not expect bilateral symmetry in a practical power system. The assumption of a perfect bilateral symmetry would cause a weak resonance and exclude strong resonance.

Hamdan [28] studies the conditioning of the eigenvalue and eigenvectors of a system very similar to that of [39]. The eigenvectors become ill conditioned near resonance and singular value measurements of the proximity to a weak resonance ('sep' function) suggest that the system does pass near a weak resonance.

Klein and Rogers et al. [39] also discuss the modes near 0.7 Hz of the Western North American power system. The Kemano generating unit in British Columbia can have high participation not only in a local mode of 0.77 Hz but also in modes involving the Southwest United States of 0.74 and 0.76 Hz. Klein and Rogers regard this modal interaction as unusual, distinguish it from the phenomenon observed in their symmetric power system model and conclude that 'Oscillations in one part of the system can excite units in another part of the system due to resonance'. Mansour [52] shows large oscillations at Kemano due to disturbances in the the Southwest United States. It would be interesting to determine if this modal interaction can be explained by a nearby strong resonance.

Trudnowski, Johnson, and Hauer [73] use a strong resonance assumption to improve Prony analysis identification of transfer functions from noisy ringdown data. Closely spaced poles with large residues of nearly opposite sign are replaced by two poles in an exact strong resonance at the average of the previous pole positions. Trudnowski et al. show that this improves the estimates of the pole positions in a 27 bus, 17 generator example which captures some features of the WSCC system. This result is supportive of the occurrence of strong resonance in power systems.

DeMarco [19] describes how increased loading of tie lines can cause a low frequency mode to decrease in frequency until the complex conjugate eigenvalues coalesce at the real axis and then split along the real axis so that one eigenvalue passes through the origin and steady state stability is lost in a collapse. In this situation, the coalescing of the complex conjugate eigenvalues is a strong resonance of two real eigenvalues (see section 7.2.1) which is a precursor to the steady state loss of stability. DeMarco demonstrates the phenomenon in a 14 bus system. Ajjarapu [2] also describes this phenomena, calling the real strong resonance a 'node-focus bifurcation' and demonstrates the phenomenon in a 3 bus system. We observe that this phenomenon follows the same pattern of resonance as a precursor to instability as the strong resonance in the complex plane causing oscillatory loss of stability.

There is a large amount of very useful previous work addressing the tuning of control system gains to avoid oscillations which we do not attempt to review here.

The strong resonance and its implications for stability is known in mechanics.

Seyranian [68] gives a perturbation analysis of eigenvalue movement caused by parameter changes near both strong and weak resonance. Of particular interest is the analysis showing how passage through a diagonalizable resonance can be perturbed to obtain nondiagonalizable resonances. Seyranian [69] considers strong resonance of a parameterized linear oscillatory system. The eigenvalue movements near resonance are shown to be hyperbolas to first order and a procedure for calculating the hyperbolas from the eigenstructure is given. The role of the resonance as a precursor to instability and in altering which mode goes unstable is described and two applications in mechanics are presented.

7.6 Discussion and Conclusion

This chapter demonstrates strong resonance as a precursor to oscillatory instability in 3 and 9 bus power systems as power dispatch is varied. Mathematical analysis confirms the observed qualitative features of the eigenvalue and eigenvector movement near strong resonance. Near strong resonance, eigenvalues move quickly and turn through approximately 90^o. Thus if the eigenvalues are initially approaching each other in frequency, then they will quickly separate in damping after the resonance. One of these eigenvalues can cross the imaginary axis and cause an oscillation. This new mechanism for power system oscillations can be seen as a generalization of Kwatny's flutter instability of Hamiltonian power system models [43, 44] to a general power system model.

The new mechanism for power system oscillations requires some change of perspective: instead of only examining the damping of a single complex conjugate pair of eigenvalues, one must also consider the possibility that two pairs of eigenvalues interact near a strong resonance to cause the oscillations. If two pairs do interact in this way, then attempting to explain and predict the eigenvalue movement or attempting to damp the oscillation by only examining the complex pair that crosses the imaginary axis can easily fail (see section 7.3.1). The new mechanism does not preclude the possibility of a single isolated complex conjugate pair of eigenvalues changing in damping as a cause of oscillations; rather, the new mechanism points out an alternative way in which the interaction of two pairs of eigenvalues causes one of the pairs of eigenvalues to reduce its damping and become unstable.

With the notable exceptions of the Hamiltonian work of Kwatny [43, 44] and the transfer function identification work by Trudnowski et al. [73], the possibility of strong resonance seems to have been neglected in power systems analysis. However, theory suggests that a typical power system model can pass close to strong resonance as a parameter is varied and that encountering strong resonance is more likely than encountering a weak resonance. More work is needed to determine whether practical power systems have any special structure that could make approximate

weak resonance more likely. Nevertheless, we do suggest that effects due to nearby strong resonance do occur in practical power systems. Artificially symmetric power system models may fail to give resonance results representative of practical power systems.

As two eigenvalues approach strong resonance, the corresponding eigenvectors also converge. This is one way to explain how power system modes which are initially associated with different power system areas become coupled. Moreover, near strong resonance one expects that disturbances in one mode can excite oscillations in another mode. It will be interesting to try to verify these explanations in power system examples such as the 0.7 Hz WSCC system modes in which some sort of resonance has long been suspected of causing 'anomalous' results.

Recent simulation work by Jones has shown strong resonance near 0.7 Hz of two well damped electromechanical modes of a 19 machine dynamic model of the WSCC system [36]. These results also illustrate the approximate coincidence of mode shapes (eigenvectors) near the strong resonance.

Is modal resonance a precursor to power systems oscillations? The initial work in this chapter strongly suggests that a strong resonance can be a precursor to oscillations and that nearby strong resonance is a possible explanation whenever power systems have closely spaced modes interacting.

7.7 Appendix: Generic structure near resonance

This appendix describes the generic structure of two modes of a general power system model near resonance using the matrix deformation theory explained in Wiggins [80] and Arnold [6].

We begin with a general dynamic power system model and obtain a parameterized real matrix $\hat{M}(\alpha)$ whose eigenvalues determine the small signal stability of the power system. Assume that the power system is modeled by parameterized differential-algebraic equations which are analytic in the state and the parameters $\alpha \in \mathbb{R}^p$. Further suppose that the derivative of the algebraic equations with respect to the algebraic variables is nonsingular at the operating point. Then we can locally solve the algebraic equations for the algebraic variables via the implicit function theorem and obtain analytic differential equations in a neighborhood of the operating point. Suppose that the Jacobian of the differential equations at the operating point is nonsingular. Then the equilibrium is an analytic function of the parameters and evaluating the Jacobian at the equilibrium yields a real parameterized matrix $\hat{M}(\alpha)$. $\hat{M}(\alpha)$ is an analytic function of the parameters $\alpha \in \mathbb{R}^p$ in some open set U.

Suppose that at $\alpha = \alpha_0 \in U$, exactly two complex eigenvalues coincide at $\lambda_0 = \sigma_0 + j\omega_0$, where $\omega_0 \neq 0$. It follows that the complex conjugates of these eigenvalues also coincide at $\lambda_0^* = \sigma_0 - j\omega_0$. We are interested in the eigenstructure

of $\hat{M}(\alpha)$ for α near to α_0. Since the eigenvalues of $\hat{M}(\alpha)$ are continuous functions of α, by shrinking the neighborhood U as necessary, the eigenvalues can be expressed as functions $\lambda_1(\alpha), \lambda_2(\alpha), \lambda_1^*(\alpha), \lambda_2^*(\alpha)$ for $\alpha \in U$ with $\lambda_1(\alpha_0) = \lambda_2(\alpha_0) = \lambda_0$. Here U is shrunk so that $\lambda_1(\alpha), \lambda_2(\alpha)$ lie inside a disk centered on λ_0 for $\alpha \in U$ and that there are, counting algebraic multiplicity, exactly two eigenvalues in the disk for $\alpha \in U$.

Now we reduce the matrix $\hat{M}$ to a 4×4 matrix M which has the eigenstructure corresponding to the four eigenvalues of interest. The projection $P(\alpha)$ onto the four dimensional right eigenspace spanned by the generalized right eigenvectors corresponding to $\lambda_1(\alpha), \lambda_2(\alpha), \lambda_1^*(\alpha), \lambda_2^*(\alpha)$ is an analytic function of α [15]. Also the projection $Q(\alpha)$ onto the corresponding four dimensional left eigenspace is an analytic function of α. Define $M = Q^T \hat{M} P$. $M(\alpha)$ is an analytic 4×4 matrix valued function of the parameters α for $\alpha \in U \subset \mathbb{R}^p$. $M(\alpha)$ has exactly the eigenstructure corresponding to the four eigenvalues of $\hat{M}(\alpha)$ of interest. In particular, $M(\alpha_0)$ has two complex eigenvalues coinciding at $\lambda_0 = \sigma_0 + j\omega_0$.

There are now two cases depending on whether $M(\alpha_0)$ is diagonalizable or not. In the diagonalizable, weak resonance case $M(\alpha_0)$ is similar to the matrix

$$\begin{pmatrix} \lambda_0 & 0 & 0 & 0 \\ 0 & \lambda_0 & 0 & 0 \\ 0 & 0 & \lambda_0^* & 0 \\ 0 & 0 & 0 & \lambda_0^* \end{pmatrix}$$

in Jordan canonical form. Arnold [6], section 6.30E shows that weak resonance is codimension 6 in real parameter space. However, strong resonance is codimension 2 in real parameter space. Therefore we regard weak resonance as less likely to occur than strong resonance in Jacobians of a generic set of parameterized differential equations and we proceed to analyze the strong resonance.

7.7.1 Strong eigenvalue resonance.

In the strong case $M(\alpha_0)$ is similar to the matrix M_{R0} in real Jordan canonical form

$$M_{R0} = \begin{pmatrix} \sigma_0 & -\omega_0 & 1 & 0 \\ \omega_0 & \sigma_0 & 0 & 1 \\ 0 & 0 & \sigma_0 & -\omega_0 \\ 0 & 0 & \omega_0 & \sigma_0 \end{pmatrix}$$

A miniversal deformation of M_{R0} is $M_R : \mathbb{R}^4 \to \mathbb{R}^{16}$ given by

$$M_R(\sigma, \omega, \mu_r, \mu_i) = \begin{pmatrix} \sigma & -\omega & 1 & 0 \\ \omega & \sigma & 0 & 1 \\ \mu_r & -\mu_i & \sigma & -\omega \\ \mu_i & \mu_r & \omega & \sigma \end{pmatrix} \tag{119}$$

This key result can be deduced from [80, 6]. The consequence of the miniversal deformation is that there exist real analytic functions written, with some abuse of notation, as $\sigma(\alpha)$, $\omega(\alpha)$, $\mu_r(\alpha)$, $\mu_i(\alpha)$ and a 4×4 real matrix valued coordinate transformation $T_R(\alpha)$ analytic in α such that

$$M(\alpha) = T_R(\alpha)\, M_R(\sigma(\alpha), \omega(\alpha), \mu_r(\alpha), \mu_i(\alpha))\, (T_R(\alpha))^{-1}$$

for α in some neighborhood $U_1 \subset U$ of α_0. Also $\sigma(\alpha_0) = \sigma_0$, $\omega(\alpha_0) = \omega_0$, $\mu_r(\alpha_0) = 0$, and $\mu_i(\alpha_0) = 0$. That is, a matrix similar to $M(\alpha)$ can be analytically parameterized via the four parameters σ, ω, μ_r, and μ_i. The "mini" in "miniversal" implies that four is the minimum number of parameters generally required.

The eigenvalues of $M_R(\sigma, \omega, \mu_r, \mu_i)$ are $\sigma + j\omega \pm \sqrt{\mu_r + j\mu_i}$. It is convenient to shrink U_1 if necessary to ensure that the eigenvalues of $M_R(\sigma(\alpha), \omega(\alpha), \mu_r(\alpha), \mu_i(\alpha))$ for $\alpha \in U_1$ are never real. Then it follows, for $\alpha \in U_1$, that the eigenvalues of $M_R(\sigma(\alpha), \omega(\alpha), \mu_r(\alpha), \mu_i(\alpha))$ coincide iff $\mu_r(\alpha) = \mu_i(\alpha)) = 0$.

It is convenient to also express this result in terms of a 2×2 complex matrix describing the two eigenvalues with positive frequency. Permuting the second and third basis elements yields a matrix M'_R similar to M_R:

$$M'_R(\sigma, \omega, \mu_r, \mu_i) = \begin{pmatrix} \sigma & 1 & -\omega & 0 \\ \mu_r & \sigma & -\mu_i & -\omega \\ \omega & 0 & \sigma & 1 \\ \mu_i & \omega & \mu_r & \sigma \end{pmatrix} = \begin{pmatrix} A_r & -A_i \\ A_i & A_r \end{pmatrix}$$

Applying a complex coordinate change to M'_R gives a 4×4 complex matrix

$$M'_C = \begin{pmatrix} I_2 & jI_2 \\ I_2 & -jI_2 \end{pmatrix} M'_R \begin{pmatrix} I_2 & jI_2 \\ I_2 & -jI_2 \end{pmatrix}^{-1} = \begin{pmatrix} M_C & 0 \\ 0 & M_C^* \end{pmatrix}$$

where

$$M_C(\lambda, \mu) = \begin{pmatrix} \lambda & 1 \\ \mu & \lambda \end{pmatrix}$$

and

$$\lambda = \sigma + j\omega$$
$$\mu = \mu_r + j\mu_i$$

The 2×2 complex matrix $M_C = A_r + jA_i$ is called the complexification of M'_R. The two eigenvalues of M_C are the two eigenvalues of M_R with positive frequency. Note that, setting $\mu = 0$, $M_C(\lambda, 0)$ is in Jordan canonical form and that for $\mu = 0$ and $\lambda = \lambda_0$, M'_C is the Jordan canonical form of $M(\alpha_0)$.

In terms of $M_C(\lambda, \mu)$, the consequence of the miniversal deformation is that there exist complex analytic functions written, with some abuse of notation, as $\lambda(\alpha)$, $\mu(\alpha)$, and a 4×4 complex matrix valued coordinate transformation $T_C(\alpha)$ analytic in α such that

$$M(\alpha) = \\ T_C(\alpha) \begin{pmatrix} M_C(\lambda(\alpha), \mu(\alpha)) & 0 \\ 0 & M_C^*(\lambda(\alpha), \mu(\alpha)) \end{pmatrix} (T_C(\alpha))^{-1}$$

for α in some neighborhood $U_1 \subset U$ of α_0. Also $\lambda(\alpha_0) = \lambda_0$ and $\mu(\alpha_0) = 0$.

Thus the study of the eigenstructure of $M(\alpha)$ reduces to the study of the eigenstructure of $M_C(\lambda(\alpha), \mu(\alpha))$. In particular, the eigenvalues of $M_C(\lambda(\alpha), \mu(\alpha))$ are the eigenvalues of $M(\alpha)$ with positive frequency and the real and imaginary parts of the generalized eigenvectors of $M_C(\lambda(\alpha), \mu(\alpha))$ are generalized eigenvectors of $M_R'(\sigma(\alpha), \omega(\alpha), \mu_r(\alpha), \mu_i(\alpha))$, which is similar to $M(\alpha)$.

7.7.2 Structure of matrices near $M(\alpha_0)$.

The miniversal deformation result above can be applied to determine the structure of all real 4×4 matrices near $M(\alpha_0)$ by a choice of the parameterization α. Let $\alpha \in \mathbb{R}^{16}$ be the entries of a real 4×4 matrix. That is, we parameterize 4×4 matrices by their own entries. Then $\mu(\alpha) = (\mu_r(\alpha), \mu_i(\alpha))$ may be regarded as an analytic map $\mu : U_1 \to \mathbb{R}^2$ where $U_1 \subset \mathbb{R}^{16}$. Since μ can be computed from the matrix eigenvalues (see (114)) and the eigenvalues of $M_R(\sigma_0, \omega_0, \mu_r, \mu_i)$ are $\sigma_0 + j\omega_0 \pm \sqrt{\mu_r + j\mu_i}$,

$$\mu(T_R(M(\alpha_0))^{-1} M_R(\sigma_0, \omega_0, \mu_r, \mu_i) T_R(M(\alpha_0))) = (\mu_r, \mu_i)$$

Hence μ is regular near $M(\alpha_0)$. Therefore $\Gamma = \mu^{-1}((0,0))$ is an analytic codimension 2 submanifold of the real 4×4 matrices near $M(\alpha_0)$. Γ is the set of real 4×4 matrices near $M(\alpha_0)$ which are similar to $M_R(\sigma, \omega, 0, 0)$ for some values of σ and ω.

Every matrix N in U_1 is similar to $M_R(\sigma(N), \omega(N), \mu_r(N), \mu_i(N))$ and the eigenvalues of N and $M_R(\sigma(N), \omega(N), \mu_r(N), \mu_i(N))$ are $\sigma(N) + j\omega(N) \pm \sqrt{\mu_r(N) + j\mu_i(N)}$. Since U_1 is assumed to be shrunk so that these eigenvalues are never real, N has coincident eigenvalues iff $\mu_r(N) = \mu_i(N) = 0$. Hence Γ is the set of matrices in U_1 which have a coincident complex conjugate pair eigenvalues away from the real axis. Moreover, each matrix in Γ is not diagonalizable.

A generic two parameter system of differential equations will have Jacobians which are diagonalizable except at isolated points at which strong resonance occurs (see the first corollary in Arnold [6] chapter 6, section 30E).

8 Oscillatory precursors to angle/voltage collapse and the Hamiltonian approximation

This section describes how a low frequency electromechanical swing mode can reduce in frequency, pass through a strong resonance, and then cause instability by the operating point vanishing. (The detail of the eigenvalue movement is that a complex pair first coalesces on the negative real axis (strong resonance), splits, and then a single real eigenvalue crosses into the right half plane.) The dynamic consequences of this instability would be a dynamic voltage collapse, or rather, an "angle collapse" since the electromechanical origins of the instability suggest that the angles typically collapse faster than the voltages. The analysis uses a modified Hamiltonian formulation of swing dynamics to approximate the power system dynamics and exploits the structure of this model to gain insight and computational simplification. The phenomenon is illustrated on a version of the IEEE 14 bus system. The analysis and example clarifies a way in which increasing a power system transfer can make a low frequency oscillation evolve to cause a system collapse. The algorithm for computing the critical point is shown to be quite simple to implement.

This instability mechanism could be practically important in the evolving competitive utility environment, in which large active power transfers across transmission corridors will be increasingly common and variable. Should this prove true, we believe that this type of instability will warrant further study, as it will impose an important constraint on available transmission capability.

This section complements section 7 nicely: in both instabilities an oscillatory mode or modes pass near or through a strong resonance, and their interactions causes instability. In section 7, two oscillatory modes interact near a strong resonance as a precursor to an oscillatory instability whereas in this section, one oscillatory mode pass though a strong resonance or node-focus on the negative real axis as a precursor to a monotonic collapse instability as a single eigenvalue crosses into the right half plane through zero. The two types of strong resonance are explained by examples in section 7.2.

This section also clarifies a relationship between voltage collapse and electromechanical oscillatory modes. However, most recent voltage collapse research has focussed on collapses with a relatively large involvement of voltage magnitudes in the collapse and the associated right eigenvector and the electromechanical instability studied here seems to have a relatively large involvement of angles in the collapse and the associated right eigenvector. [2]

[2]The question of identifying "most significant" components of an eigenvector when the states have different physical units and normalization schemes can sometimes be difficult [75]. However, for the simple dynamic model to be employed here, a naive interpretation of "significance" based

8.1 Structural features of linearized models for electromechanical dynamics

Strong structural features that arise in linearized dynamics of power systems relate to the fact that power system models consist roughly of second order oscillators coupled through the non-linear power flow of the network. When linearized, the important effects of the coupling show up in a matrix structure closely related to that of a nodal admittance matrix. A number of authors (for example, [65] [13]) have summarized these features in various ways. With this "admittance-like" matrix describing the coupling, one manner in which a zero eigenvalue can be introduced is for a cutset of branches to have zero coefficients (in the graph associated with the admittance matrix). This simple idea is the foundation of the instability mechanism to be studied in this paper. For completeness, and development of notation, we shall review some results on model structure [18].

Consider an augmented power system network of n buses, with those numbered 1 through m representing the internal voltage of synchronous generators, and the remainder representing generator terminals and loads. The network is augmented in the sense that generator internal bus voltages are explicitly represented, with an appropriate series reactance (transient reactance of the synchronous machine) connecting the internal bus to terminal bus; a simple classical representation of constant internal bus voltage magnitude is assumed. The equilibrium system frequency is equal to a known value of ω_0.

It will prove convenient to impose assumptions that yield a symmetric power flow Jacobian (provided reactive equations are normalized by voltage magnitude), as is done in stability studies that require existence of a path independent system energy function [56]. We initially neglect rotational damping/governor action, but will reintroduce this effect in our example. With these assumptions, the dynamic equations for the system will possess a modified Hamiltonian form, which yields a simple closed form relationship between real eigenvalues of a reduced dimension, symmetric problem, and eigenvalues of the full dimension, linearized dynamic equations.

To describe this model, let:
$V \in \mathcal{R}^n$, V = vector of bus voltage magnitudes;
$\delta \in \mathcal{R}^n$, δ = vector of bus voltage phase angles relative to an arbitrary synchronous reference frame of frequency ω_0 (no reference angle is deleted);
$\omega \in \mathcal{R}^m$, ω = vector of generator frequency deviations, relative to synchronous frequency ω_0;
$M \in \mathcal{R}^{m \times m}$, M = diagonal matrix of normalized generator inertias;
$P^I \in \mathcal{R}^n$, P^I = vector of net active power injection at each bus; assumed constant;
$Q^I : \mathcal{R}^{n-m} \rightarrow \mathcal{R}^{n-m}$, $Q^I(V)$ = vector valued function of net reactive power injec-

on relative magnitude of components of the right eigenvector is judged adequate.

tion at load buses, normalized by voltage magnitude;
L_1 = rows 1 through m of an $n \times n$ identity matrix;
L_2 = rows $m+1$ through n of an $n \times n$ identity matrix;
$P^N(\delta, V)$ = vector-valued function of active power absorbed by network at each bus;
$Q^N(\delta, V)$ = vector-valued function of reactive power absorbed by network at load buses, normalized by voltage magnitude.

Note that because we have chosen to maintain all voltage angles as states, the model that results is not a minimal realization. The linearization will have a fixed eigenvalue at zero associated with uniform translational motion of angles (see [56] for discussion of minimum versus non-minimum state models).

With the above notation, the resulting nonlinear model for the rotational dynamics of machines coupled through power exchange in the network may be written as follows:

$$\begin{aligned} M\dot{\omega} &= L_1(P^I - P^N(\delta, V)) \\ L_1\dot{\delta} &= \omega \\ 0 &= L_2(P^I - P^N(\delta, V)) \\ 0 &= Q^I(V) - Q^N(\delta, V) \end{aligned}$$

A linearization of these equation about an equilibrium $(0, \delta^e, V^e)$ is then given in the "singular system" form as

$$\tilde{E}\Delta\dot{x} = \tilde{R}\Delta x$$

with

$$\tilde{E} = \begin{bmatrix} M_{m\times m} & 0 & 0 \\ 0 & I_{m\times m} & 0 \\ 0 & 0 & 0_{2(n-m)\times 2(n-m)} \end{bmatrix}$$

$$\tilde{R} = \begin{bmatrix} 0 & -I_{m\times m} & 0 \\ I_{m\times m} & 0 & 0 \\ 0 & 0 & I_{2(n-m)\times 2(n-m)} \end{bmatrix}$$

$$S = \begin{bmatrix} I_{m\times m} & 0 & 0 \\ 0 & J_{11} & J_{12} \\ 0 & J_{21} & J_{22} \end{bmatrix}$$

$J : \mathcal{R}^n \times \mathcal{R}^{n-m} \to \mathcal{R}^{(2n-m)\times(2n-m)}$,

$$J = \begin{bmatrix} \frac{\partial P^N}{\partial \delta} & \frac{\partial P^N}{\partial V_L} \\ \frac{\partial Q^N}{\partial \delta} & \frac{\partial \{Q^N - Q^I\}}{\partial V_L} \end{bmatrix}$$

Next, let us consider a relationship between the generalized eigenvalue problem of interest, and a reduced dimension, symmetric generalized eigenvalue problem in which the power flow Jacobian enters in a direct way. In particular, consider the reduced generalized eigenvalue problem defined by (E, J), where

$$E = \begin{bmatrix} M & 0 \\ 0 & 0_{2(n-m)\times 2(n-m)} \end{bmatrix}$$

Proposition: Assume (E, R) has a finite generalized eigenvalue λ, with right eigenvector $v \in \mathcal{R}^{2n-m}, v = \left[v_1^T, v_2^T\right]$; i.e. $\lambda E v = Rv$. Then there exists a $w \in \mathcal{C}^{2n}$ such that (γ, w) satisfies $\gamma \tilde{E} w = \tilde{R} w$, with $\gamma = j\sqrt{\lambda}$.
Proof: Minor variation on that of Proposition 2 in [18].

Observation: The result of Proposition 2 indicates that if we wish to examine the behavior of eigenvalues with respect to operating point (e.g., bifurcation behavior) in the non-symmetric generalized eigenvalue problem of $(\tilde{E}, \tilde{R})$, we may do so in the context of the reduced dimension, symmetric generalized eigenvalue problem (E, J).

Consequences:

1. Suppose that (E, J) at an operating point of interest has all its finite generalized eigenvalues non-negative. All finite generalized eigenvalues of $(\tilde{E}, \tilde{R})$ must appear on the $j\omega$ axis. It is a straightforward exercise to show that if linear rotational damping is added in every generator component (which provides a very rough approximation to governor action), all finite eigenvalues save one are shifted to the left, and one finite eigenvalue remains fixed at zero.

2. Consider now a possible route to loss of stability, starting from a stable operating point with the properties assumed in 1. One could hypothesize a gradual change in operating point that would bring one of the positive, finite eigenvalues of (E, J) to the origin. In the full problem, $(\tilde{E}, \tilde{R})$, with small damping, one would have a complex pair of eigenvalues moving parallel to the $j\omega$ axis. Very near to the parameter values for which the eigenvalue of (E, J) reaches zero, a critical complex pair of $(\tilde{E}, \tilde{R})$ coalesces to a double real eigenvalue on the negative real axis. Precisely at the parameter values for which (E, J) has a new zero eigenvalue, $(\tilde{E}, \tilde{R})$ must also have an additional zero eigenvalue. As we will illustrate in the example to follow, this new zero eigenvalue in $(\tilde{E}, \tilde{R})$ comes about as the pair which coalesced on the real axis splits, sending one of the pair through the origin. Also note that if parameters move further, beyond the values which yield this singularity, the equilibrium at which the linearization was being evaluated typically ceases to exist.

3. Finally, note that the motion of this eigenpair will not be differentiable with respect to the parameters at the critical parameter value for which the complex pair coalesce to a repeated real root. Indeed, as we approach this point, the derivative of the eigenvalue motion with respect to parameters approaches infinity. This, of course, is typical in bifurcation problems, but it practical impact is important. The example to follow will illustrate.

The key insight into network structure that is used in our algorithm is quite simple, and may be summarized as follows. The critical complex pair of eigenvalues represents a low frequency swing mode. Our interest is in low frequency modes associated with large transfers of active power through a transmission corridor. Under these circumstances, the low frequency swing mode will be an inter-area mode, describing generators on one side of the transmission corridor "swinging" coherently relative to generators on the other side of the transmission corridor, which are also assumed to swing as a coherent group. In this scenario, the associated generalized right eigenvector of the full dynamic model, $(\tilde{E}, \tilde{R})$, has a special form. The components of the eigenvector associated with generator angles will show values 180 degrees out of phase on either side of the cutset formed by the transmission corridor. We assume that this structure of eigenvector persists to the point of bifurcation, were the complex pair has split, and one of the resulting real eigenvalues is zero. In other words, we will formulate a system of equations to solve that forces the system $(\tilde{E}, \tilde{R})$ to have an "extra" zero eigenvalue, with the generator angle components of the associated eigenvector having the special form described here.

8.2 Computational formulation and example

To formulate our problem precisely, we need additional piece of notation; to this end, let $P^M \in \mathcal{R}^m$ be the active power injections at generator buses. These are a subset of the $P^I \in \mathcal{R}^n$ vector introduced earlier, and will be the only components of P^I to be viewed as unknowns. For compactness, it is also useful to define the overall power mismatch function

$$f(\delta, V, P^M) := \left[((P^I - P^N(\delta, V))^T, (Q^I(V) - Q^N(\delta, V))^T\right]^T$$

Finally, we shall assume that we are seeking a right eigenvector of J, associated with a zero eigenvalue, that has generator angle components with values given by $[1^T, -\gamma 1^T]^T$, with γ a positive real scalar. This enforces the assumption of an inter-area swing mode, as described above. Note also that once we restrict our attention to solving for a zero eigenvalue, it does not matter whether we consider the generalized eigenvalue problem of (E, J), or simply enforce singularity in J itself. Given the dimensions of our partitioning scheme, specifying the generator angle components

of the eigenvector leaves $2n - 2m$ components of the eigenvector as unknowns. Let us denote these remaining eigenvector components as w. Then our problem may be succinctly stated as follows. Given load demand components of P^I, Q^I , solve for (δ, V, P^M, w) satisfying:

$$\begin{aligned} 0 &= f(\delta, V, P^M) \\ 0 &= J((\delta, V)[1^T, -\gamma 1^T, w^T]^T \end{aligned}$$

While this formulation is technically correct, the assumption of a lossless network implies linear dependence between equations. In particular, the sum of all active power equations components must be identically zero for any operating point. Given this dependence, we may discard one row of $f(\delta, V, P^M)$, and one row of $J((\delta, V)$. Moreover, the unknowns of the generation dispatch vector, PM, appear linearly in the associated components of the $f(\delta, V, P^M) = 0$ constraint, and may be computed as "outputs" after the desired (δ, V) is identified. Hence, all m rows of the $f(\delta, V, P^M) = 0$ corresponding internal generators buses may be deleted. Denote the resulting reduced dimension quantities respectively as $\tilde{f}$ and $\tilde{J}$. Finally, while it was convenient in Section 8.1 to develop the dynamic equations keeping all phase angles as variables, this is not convenient when formulating a Newton-Raphson algorithm to solve the equation set above. Rather, we follow the standard practice of selecting generator angle #1 as reference, and delete that angle from variables for which we solve; denote the reduced vector as $\tilde{\delta}$. In the reduced Jacobian, $\tilde{J}$, the eigenvector associated with the remaining zero eigenvalue can now take the form $[0, 1^T, \tilde{w}^T]^T$, rather than it original form of $[1^T, -\gamma 1^T, w^T]^T$. In this process, we eliminate the scalar γ as an unknown. With these modifications, we are left with the constraint equations:

$$\begin{aligned} 0 &= \tilde{f}(\tilde{\delta}, V) \\ 0 &= \tilde{J}((\tilde{\delta}, V)[0, 1^T, \tilde{w}^T]^T \end{aligned} \tag{120}$$

We now have a dimensionally consistent set of equations in the unknowns $(\tilde{\delta}, V, w)$. While we will not attempt to offer a proof of that the associated Jacobian is generically nonsingular, numerical experience to date suggests that a Newton-Raphson iteration for (120) is typically well-conditioned. Studies to date have employed a heuristic mix of human judgment in selecting an initial operating point, coupled with the Newton-Raphson algorithm to solve (120). An operating point is selected that produces a heavily loaded corridor in the system. A cutset is selected whose branches include all lines the transmission corridor, and which separates two subsets of generators, one on either side of the cutset. This identifies which components of generator angles are assigned values 0 or 1 in the eigenvector (0's for those generators on the same side of the cutset as the reference bus, 1's for those generators

Bus #	Original op. point voltage/phase(degs.)		Critical op. point voltage/phase(degs.)	
1	1.0600	0	1.0600	0
2	1.0450	-4.7545	1.0450	-3.3284
3	1.0800	-2.8056	1.0800	-6.4522
4	0.9196	-25.1819	0.8351	-28.9282
5	0.9476	-23.6900	0.8733	-26.8531
6	1.0200	-70.0082	1.0200	-84.2610
7	0.9514	-62.1503	0.8663	-79.5870
8	1.0400	-58.2712	1.0400	-79.4164
9	0.9407	-76.0226	0.8562	-94.5890
10	0.9426	-83.9820	0.8702	-103.0148
11	0.9852	-87.8051	0.9412	-105.1052
12	0.9478	-90.6433	0.9385	-105.5251
13	1.0056	-82.1261	0.9884	-97-3412
14	0.9960	-89.9647	0.9410	-108.4568

Table 7: Original & critical operating points

on the opposite side). An inverse power method is used to identify the smallest magnitude eigenvalue of $\tilde{J}(\tilde{\delta}, V)$, and its associated eigenvector. Those components of the eigenvector not associated with generator phase angles determine the initial guess for w.

To illustrate this process, consider a network that is a slightly modified version of the IEEE 14 bus system, illustrated below in Figure 36 (the synchronous condensers of that test case are here replaced with standard generators). Table 7 identifies the initial operating point selected, as well as the operating point obtained as the solution of (120).

To provide further insight into the dynamic interpretation of these results, we performed the following computations. A sequence of operating points were computed, corresponding to a linear interpolation between the generation dispatch for the two operating points identified in Table 1 (loads are unchanged between the two operating points). In a linearized swing dynamic model of the form described in section 8.1, with small rotational damping added at each machine, the finite eigenvalues were calculated for this sequence of operating points. The resulting locus of finite eigenvalues of the dynamic model is illustrated in Figure 37, with an expanded view of the critical eigenvalues in Figure 38. Note that, as predicted, the critical operating point is associated with a complex conjugate pair of eigenvalues coalescing on the negative real axis, splitting, with one of the resulting real eigenvalues moving

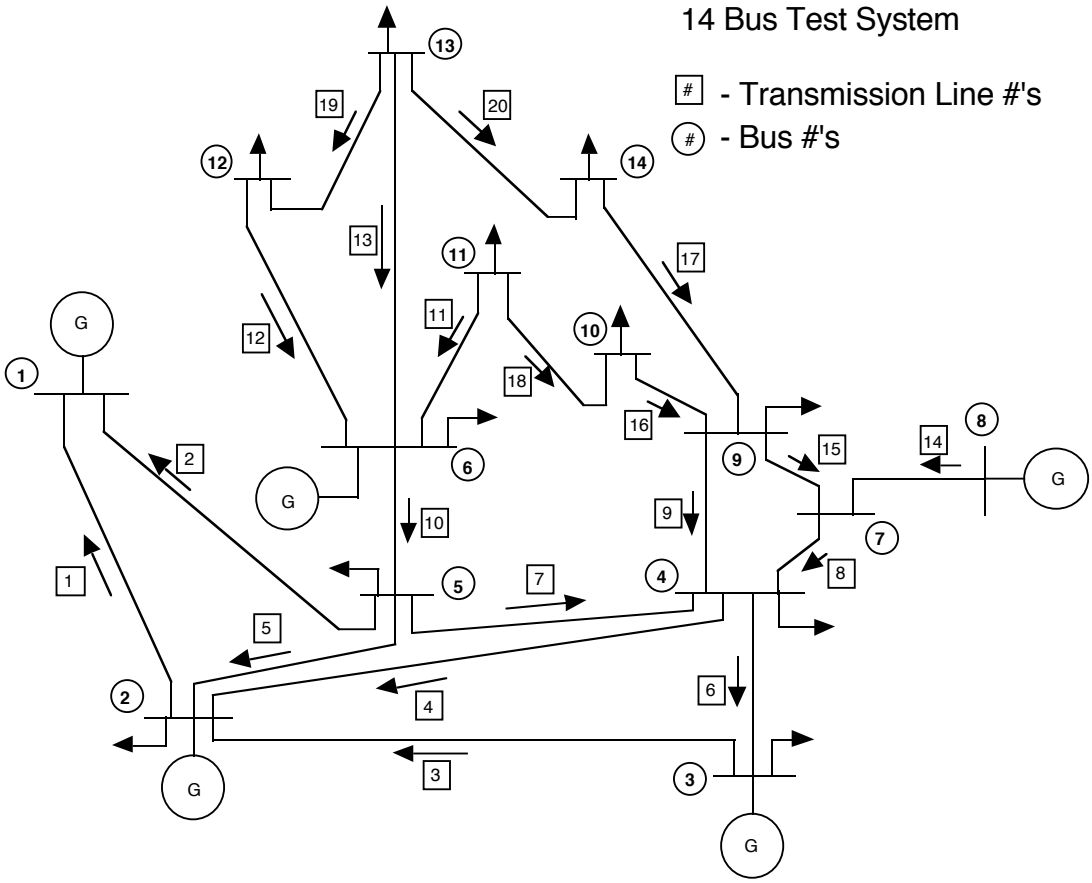

Figure 36: 14 Bus Test System

to the origin. As a final piece of information, the generalized eigenvectors associated with selected eigenvalues of interest are shown in Table 8, with a one shown for the original operating point, and several for the critical operating point.

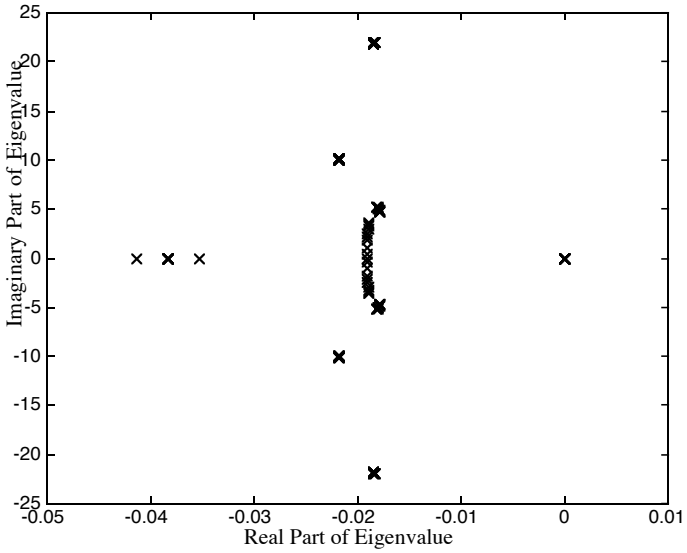

Figure 37: Scatter Plot of Eigenvalues

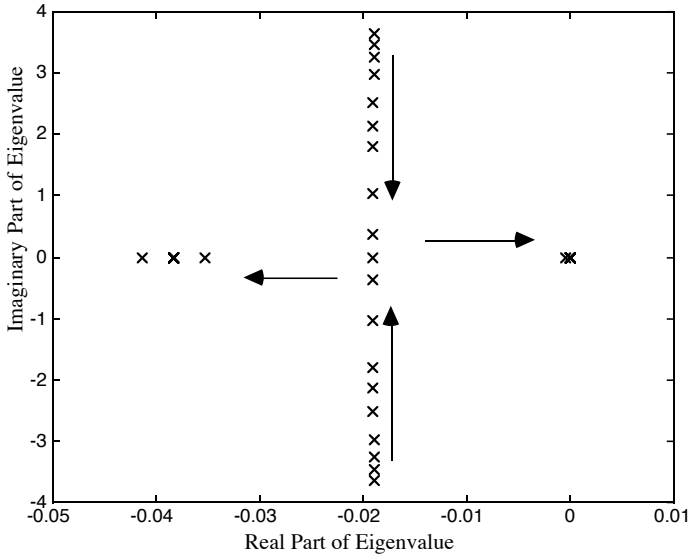

Figure 38: Expanded View Critical Eigenvalues

Eigenvector component	Original op. point Eigenvalue -0.0189 + 3.6342i	Critical op. point Eigenvalue -0.3957	Critical op. point Eigenvalue -0.2294	Critical op. point Eigenvalue 0 (original)	Critical op. point Eigenvalue 0 (new)
Freq@bus 1	-0.4033-0.0048i	-0.0181	-0.0000	0.0000	-0.0000
Freq@bus 2	-0.3917-0.0047i	-0.0181	-0.0000	0.0000	-0.0000
Freq@bus 3	-0.4287-0.0051i	-0.0181	-0.0000	0.0000	-0.0000
Freq@bus 6	0.3068+0.0026i	0.0000	-0.0103	0.0000	0.0000
Freq@bus 8	0.4964+0.0054i	0.0000	-0.0103	0.0000	0.0000
Angle@bus 1	-0.0007+0.1110i	0.4384	0.0000	0.2675	-0.2019
Angle@bus 2	-0.0007+0.1078i	0.4384	0.0000	0.2675	-0.2019
Angle@bus 3	-0.0008+0.1180i	0.4384	0.0000	0.2675	-0.2019
Angle@bus 6	0.0003-0.0844i	-0.0000	0.2924	0.2672	0.2359
Angle@bus 8	0.0008-0.1366i	-0.0000	0.2924	0.2672	0.2359
Angle@bus 4	-0.0005+0.0625i	0.3689	0.0463	0.2674	-0.1326
Angle@bus 5	-0.0005+0.0639i	0.3659	0.0484	0.2674	-0.1295
Angle@bus 7	0.0004-0.0868i	-0.0005	0.2928	0.2672	0.2364
Angle@bus 9	0.0005-0.1030i	-0.0799	0.3457	0.2671	0.3156
Angle@bus 10	0.0005-0.1130i	-0.1091	0.3652	0.2671	0.3448
Angle@bus 11	0.0004-0.1060i	-0.0745	0.3421	0.2671	0.3103
Angle@bus 12	0.0003-0.0895i	-0.0159	0.3030	0.2672	0.2517
Angle@bus 13	0.0003-0.0912i	-0.0218	0.3069	0.2672	0.2576
Angle@bus 14	0.0005-0.1136i	-0.1031	0.3612	0.2671	0.3388
Volt@bus 4	0.0003-0.0569i	-0.1401	0.0935	-0.0001	0.1399
Volt@bus 5	0.0003-0.0502i	-0.1251	0.0834	-0.0001	0.1249
Volt@bus 7	0.0003-0.0548i	-0.1492	0.0995	-0.0001	0.1490
Volt@bus 9	0.0003-0.0564i	-0.1549	0.1033	-0.0001	0.1546
Volt@bus 10	0.0003-0.0483i	-0.1341	0.0894	-0.0001	0.1339
Volt@bus 11	0.0002-0.0272i	-0.0793	0.0529	-0.0001	0.0791
Volt@bus 12	0.0000-0.0052i	-0.0159	0.0106	-0.0000	0.0159
Volt@bus 13	0.0001-0.0101i	-0.0302	0.0202	-0.0000	0.0302
Volt@bus 14	0.0002-0.0364i	-0.1021	0.0681	-0.0001	0.1020

Table 8: Selected generalized (right) eigenvectors of the full dynamic model; Angles are in radian and voltage magnitudes are in per unit.

9 Use of measurements

Instead of relying solely on real time computations with a dynamic power system model, some of the needed information could be measured from the power system as in WAMS [29, 59, 77, 73]. Indeed the combined use of power system measurements and model based software offers many opportunities for real time system control.

9.1 Modal information such as frequency

One promising suggestion is measuring the frequency of the critical oscillatory mode which is unstable or poorly damped. Some knowledge of the mode frequency would simplify the task of computing the critical mode in the power system model. In particular an estimate of the modal frequency, together with a assumption of small or zero damping, would supply a complex shift for the eigenvalue computational methods of section 5.

It might also be possible to measure the pattern or relative phases of the oscillation. This information would help in approximating the eigenstructure (more precisely, the right eigenvector) of the oscillation as discussed in section 8. (The eigenvalue and margin sensitivity formulas require the eigenstructure of the oscillatory mode.) Note that the new phasor measurement units would be able to estimate relative phases.

There are two cases to consider:

1. The sustained or transient oscillation is occurring and the objective is to suppress it. In this case it should be feasible to measure or estimate the oscillation frequency. It might also be feasible to obtain some information about the pattern of oscillation.

2. The system is close to oscillation but not actually oscillating and the objective is to avoid oscillations. This case is the more difficult task of obtaining measurements of the critical frequencies which reflect system weakness or potential weakness as regards oscillations. The spectral monitor described below might yield measurements indicating the modal frequency when the system is close to oscillations.

9.2 Measuring closeness to oscillation by peaks in the ambient noise

Suppose that the power system is at equilibrium but there is a poorly damped oscillatory mode. The problem is to detect the closeness to this condition by power system measurements, and estimate the frequency of the oscillatory mode

The motivation is that a poorly damped mode would cause a sizable poorly damped oscillation if there is a sizable disturbance. There is also a risk that the

mode could become unstable by gradual or sudden changes, leading to sustained oscillations. Knowing the closeness to this condition would allow remedial action to be taken. The mode frequency could be very helpful in selecting the remedial action.

The concept is that there is broadband ambient noise present on the power system from a variety of sources. A power system bus is chosen to observe the noise and the power spectral density of the noise at this bus can be estimated from real time measurements. The power spectral density of the observed noise should contain a peak at a frequency corresponding to a poorly damped mode. The size of the peak will increase as the modal damping decreases and can be used to give a relative measure of the closeness to oscillation.

Measurement of power spectral density of power system signals has been done by John Hauer and others for the purpose of estimating transfer functions for control design. The spectral monitoring application is easier than estimating transfer functions. We briefly review some work in this direction:

John Hauer et al. [29] briefly summarizes some results on the Western North American Power system showing spectral peaks obtained from real measurements. They suggest that 'changes in the spectral signature can be used to give warnings of system changes to system operators'. It seems clear that the method would give an estimate of the frequency of the mode which is becoming unstable.

Pierre and others [59] have analyzed measured power system ambient noise data and computed modal dampings and frequencies by constructing a whitening filter which reflects the poles of the power system transfer function. The whitening filter is found by solving Wiener-Hopf equations for linear prediction. The results agree with the modes found by Prony analysis of a ring down test. Wies and Pierre [77] test a Least Mean Square adaptive version of the whitening filter on simulated data to show that the method could be used to track changing modes in real time. Scottish utilities have experience in using online oscillations monitors [16].

We conclude that experts in power system measurements are already developing real time monitoring of oscillatory modes. These methods can be expected to provide valuable inputs to real time control, especially when combined with the model based controls suggested in this project.

10 Other ideas

This section records various ideas which were produced but not fully developed during the project.

10.1 Zero frequency approximation

The main idea is to suppress a low frequency oscillation by deriving controls which suppress an associated "zero frequency oscillation". That is, the low oscillation frequency is approximated as zero for the purpose of deriving controls. As explained below, a zero frequency oscillation has special properties which allow a suppressing control to be more easily obtained. It is clear that this approximation becomes better as the oscillation frequency decreases and that determining the range of usefulness of the approximation would be important.

First, what is a "zero frequency oscillation"? In general, the onset of an oscillation is characterized by the system linearization having a pair of eigenvalues on the imaginary axis at $\pm j\omega$, where ω is the oscillation frequency. A zero frequency oscillation occurs as a limiting case in which the system linearization has two zero eigenvalues. The presence of a zero eigenvalue causes the zero frequency oscillation to have characteristics of a voltage collapse (saddle node bifurcation) as well as being a limiting case of oscillations.

The zero frequency oscillation case is well studied in bifurcation theory and numerical analysis, where it is sometimes called a combined saddle node–Hopf bifurcation. It also has been studied in some simple power system models by Venkatasubramanian [35], but not in the context of exploiting its features to avoid real time oscillations. (There is some intricacy in its analysis since the Jordan block corresponding to the two zero eigenvalues is nontrivial and complicated dynamics can appear nearby.)

The following result suggests how a zero frequency oscillation is simpler than the low frequency oscillation it approximates:
Result: The following are equivalent conditions at the onset of oscillation:

1. Oscillation frequency is zero

2. Eigenvectors corresponding to the oscillation can be chosen to be real

3. All states in the linearized oscillation are either exactly in phase (phase difference = 0^o) or exactly in antiphase (phase difference = 180^o).

Thus a zero frequency oscillation approximates an oscillation in which the power system approximately splits into two areas swinging against each other in antiphase

with each area approximately in phase with itself. Given such an oscillation occurring in real time, the two areas (or their interface) could be identified from monitoring equipment. This would give information about the structure of the corresponding zero frequency oscillation which might then be exploited to try to devise a control to suppress the oscillation.

10.2 Heuristics

The network structure of the power flow ties in closely with the electromechanical dynamics of the system. It is frequently possible to develop efficient heuristics that approximately characterize both certain modes of the system (e.g., the zero frequency approximation above) and the relationship between operating point and lightly damped modes. A simple conjecture based on this type of reasoning may be briefly stated:

> Conjecture: If a low frequency interarea power oscillation is occurring so that the power system approximately splits into two areas swinging against each other with each area approximately in phase with itself, then decreasing the power transferred between the two areas will tend to suppress the oscillation.

Part of the work in establishing or disproving such a conjecture is defining its range of applicability: How low is low frequency? Does it also work for local area oscillations? How approximate can the split into two areas be? If the rule does not work can it be modified so that it does work? How close is this rule to the optimum control action determined by sensitivity methods using a detailed model?

10.3 Frequency domain approach to resonant complex eigenvalues

This subsection is an initial attempt to get insight into the resonance from a frequency domain point of view.

10.3.1 Transfer functions related to a mode

First think about a linear system $\dot{x} = Ax$ with an eigenvalue λ and corresponding left and right eigenvectors w and v respectively. w is a row vector and v is a column vector. We can choose an input $u(t)$ which only excites the mode v and an output $y(t)$ which measures the response of the mode:

$$\begin{aligned} \dot{x} &= Ax + vu \\ y &= wx \end{aligned} \tag{121}$$

That is, the input is v scaled by some time function and the output is the state x projected along the mode by w. The transfer function of this single input, single output system is

$$w(sI - A)^{-1}v = \frac{wv}{s - \lambda} \tag{122}$$

(This can be derived from $v = (sI - A)^{-1}(sI - A)v = (sI - A)^{-1}(s - \lambda)v$.)

In the case of complex λ which we are interested in, v is arbitrary up to multiplication by a complex constant; in particular, v can be rotated by an angle α in the eigenspace $< \Re e\{v\}, \Im m\{v\} >$ by multiplying by $e^{j\alpha}$. There is similar arbitrariness in the choice of w. These different choices will, however, lead to different input-output systems.

In the case of complex λ, v and w and the input-output system (121) and the transfer function (122) are complex. Let $v = v_r + jv_i$ and $w = w_r + jw_i$ and consider the input along v_r and the output obtained with w_r. This real input-output system is

$$\begin{aligned} \dot{x} &= Ax + v_r u \\ y &= w_r x \end{aligned} \tag{123}$$

The transfer function of (123) is

$$\begin{aligned} w_r(sI - A)^{-1}v_r &= \frac{1}{4}\left[(w + w^*)(sI - A)^{-1}(v + v^*)\right] \\ &= \frac{1}{4}\left[\frac{wv}{s - \lambda} + \frac{w^*v^*}{s - \lambda^*}\right] \end{aligned} \tag{124}$$

using (122) since $wv^* = w^*v = 0$.

10.3.2 Transfer functions related to a nonsemisimple mode

Consider a nonsemisimple mode with left and right eigenvectors w and v and left and right generalized eigenvectors w' and v'. The formulas derived above still apply for the input-output system defined by the eigenvectors. Consider the complex input-output system with input along v' and the output obtained with w':

$$\begin{aligned} \dot{x} &= Ax + v'u \\ y &= w'x \end{aligned} \tag{125}$$

The complex transfer function is

$$w'(sI - A)^{-1}v' = \frac{w'v'}{s - \lambda} + \frac{w'v}{(s - \lambda)^2} \tag{126}$$

(This can be derived from $Av' = \lambda v' + v$ and
$v' = (sI - A)^{-1}(sI - A)v' = (sI - A)^{-1}((s - \lambda)v' - v)$.)

Consider the real input-output system with input along v'_r and the output obtained with w'_r:

$$\begin{aligned} \dot{x} &= Ax + v'_r u \\ y &= w'_r x \end{aligned} \tag{127}$$

The transfer function can be derived similarly to (124) to be

$$w'_r(sI - A)^{-1}v'_r = \frac{1}{4}\left[\frac{w'_r v'_r}{s - \lambda} + \frac{w'_r v_r}{(s - \lambda)^2} + c.c.\right] \tag{128}$$

where *c.c.* stands for complex conjugate (The derivation uses $w'^* v$=0, which is obtained by considering $w'^* Av$, and $w^* v' = 0$, which is obtained by considering $w^* Av'$)

10.3.3 Transfer function as resonance is approached

Suppose we choose a single input and single output for the power system and obtain the transfer function $g(s)$. How does this transfer function change as the resonant nonsemisimple case is approached? Suppose

$$g(s) = h(s)\left[\frac{1}{(s - \lambda_1)(s - \lambda_2)} + c.c.\right] \tag{129}$$

where λ_1 and λ_2 are nearby complex poles which are not near poles of $h(s)$. Partial fraction expansion gives

$$g(s) = \text{other fractions} + \frac{1}{\lambda_1 - \lambda_2}\left[\frac{h(\lambda_1)}{(s - \lambda_1)} - \frac{h(\lambda_2)}{(s - \lambda_2)} + c.c.\right] \tag{130}$$

Neglecting the 'other fractions', we get

$$\frac{1}{\lambda_1 - \lambda_2}\left[\frac{(s - \lambda_2)h(\lambda_1) - (s - \lambda_1)h(\lambda_2)}{(s - \lambda_1)(s - \lambda_2)} + c.c.\right]$$

$$= \frac{1}{(s - \lambda_1)(s - \lambda_2)}$$

$$\left[\frac{h(\lambda_1) - h(\lambda_2)}{\lambda_1 - \lambda_2}\left(s - \frac{\lambda_1 + \lambda_2}{2}\right) + \frac{h(\lambda_1) + h(\lambda_2)}{\lambda_1 - \lambda_2}\left(\frac{\lambda_1 - \lambda_2}{2}\right) + c.c.\right]$$

$$\to \frac{Dh|_\lambda}{(s - \lambda)} + \frac{h(\lambda)}{(s - \lambda)^2} + c.c.$$

as λ_1 and λ_2 tend to a common limit λ.

11 Prospects for real time control of oscillations

Key barriers to real time control of oscillations are

1. Understanding mechanisms of oscillations
2. Identifying critical modes.
3. Selecting operator actions
4. Robustness to model data
5. Computational speed
6. Hybrid system/variable structure aspects

We first discuss each of these barriers and assess the prospects for overcoming each one. Then a staged approach to developing real time control for oscillations is discussed.

11.1 Understanding mechanisms of oscillations

One conception is that oscillations arise when the damping of a single oscillatory mode becomes insufficient due to a combination of factors in the power system as sketched in the last paragraph of section 1.2. This is perhaps the prevailing view of oscillations and there is little doubt that some oscillations can be understood in this general way. While much is known about tuning control gains to achieve stability at a given operating point, much less is known about predicting the stabilizing or destabilizing effects of operator actions such as redispatch or switching exciters to manual. The project has developed sensitivity methods of predicting the effects of these operator actions and these methods can provide results and formulas to improve the understanding of these effects. The project has also made some progress on heuristic or approximate methods to understand oscillations and the effects of operator actions. Experience shows that good physical insight or good approximations capturing the essential features of a phenomenon are often the basis of practical methods of controlling the phenomenon.

The project has demonstrated also demonstrated a new mechanism for interarea oscillations involving a strong resonance between two system modes. The existence of a plausible new mechanism suggests that interarea oscillations are not thoroughly understood. Special methods would be needed to avoid the strong resonance induced type of oscillation.

Overall it seems clear that further insights into interarea oscillations are needed in order to devise effective ways of suppressing and avoiding them.

11.2 Identifying critical modes

It is clearly impractical to blindly compute all the power system eigenvalues in a power system of realistic size. It is also necessary to distinguish the eigenvalues that are lightly damped and unlikely to move from those critical, lightly damped eigenvalues which can become unstable as conditions evolve.

Integration of real time power system measurements [29, 59, 77, 73] into control action computations can help solve these problems. In particular, measurements of the frequency of threatening oscillations could be made available from ambient spectral measurements before the oscillation occurs or by directly measuring the oscillation frequency once the oscillation occurs. An estimate of the oscillation frequency obtained from measurements can be used as a "complex shift" in eigenvalue computations which find eigenvalues closest to the complex shift. There are also possibilities of using information about the machines involved in the oscillation to estimate right eigenvectors of the critical mode to initialize eigenvalue computations as described in Section 8.

Once the approximate frequencies of concern have been identified from measurements (or by previous experience), the sensitivities of the lightly damped eigenvalues can be computed by evaluating the sensitivity formulas of section 4 to establish which eigenvalues are critical.

It might also be sufficient to track a set of critical modes found to be sensitive and troublesome in off line studies.

11.3 Selecting operator actions

There are two approaches to advising operators which actions will be effective in suppressing or avoiding oscillations. The first approach uses sensitivity computations on a dynamic power system model integrated with power system measurements as described in section 11.2. The second approach derives heuristic or approximate controls based on the understanding of the oscillations pursued in section 11.1. The controls can be derived by approximations to the model or sensitivity formulas or from physical insight gained. A combination of these approaches, singly and in combination, would increase the chances of devising a successful method. This aspect of the problem seems soluble, especially if progress can be made in understanding oscillations better.

11.4 Robustness to model data

Approaches that rely on detailed dynamic power system models are subject to problems of unknown or bad data. Dynamic generator data can be available if money is spent to determine it. However, deregulation and increased competition will tend

to limit access to the data of competitors. On the other hand, repeated blackouts involving dynamics and/or the threat of legislation could conceivably make some data public. A more fundamental problem occurs with dynamic load data, which is usually poorly known and could vary significantly with operating conditions. Overall, dynamic data can be expected to be to some extent uncertain, unreliable, or unknown.

The sensitivity formulas of section 4 can be used to quantify the importance of particular data to eigenvalue position as demonstrated in sections 3.8 and 3.9. Moreover, treating parameters as random variables, and exploiting the large number of power system parameters and a version of the central limit theorem yields estimates of the overall eigenvalue uncertainty in terms of the uncertainties in the data. Even better, if the oscillation is caused by increasing a bulk power transfer, then the uncertainty in the transfer limit can be quantified. Since the transfer limit represents money lost when a transaction is curtailed or not made available, this analysis quantifies the link between data uncertainty and money. (A larger uncertainty in transfer margin requires a larger TRM (transmission reliability margin) and hence a lower available transfer capability.) This quantification of eigenvalue uncertainty is an essential first step to finding out how much of a limiting factor data uncertainty is, which parameters are important, and how much knowing any parameter better is worth.

The issue of robustness to data also motivates the approximate or heuristic approaches to selecting controls discussed in section 11.3, since approximate or heuristic approaches require less data and are more robust.

An alternative to probabilistic handling of uncertainty is the use of interval methods for handling uncertainty [63, 64]. These methods, when properly applied, have as an objective to provide tight bounds to solution results in the face of uncertainty of parameters or even problem structure. However, careless application of interval methods can lead to gross overestimates of uncertainty intervals of solutions, proper methods can give tight enclosures for many types of problems. The complete interval enclosure problem for a most general class of problems has been recently shown to be NP-complete in terms of the number of independent variables (but only polynomial in terms of the order or complexity of the equations themselves) [17]. However, practical methods do exist for many important problems. Interval methods work best when combined with symbolic algebra solutions for many portions of the problem. See, for example, [79, 4, 54]. For a review of another approach to symbolic computation, refer also to [8].

Overall, there is some degree of reasonable doubt that an exact approach to the problem will be able to overcome the problem of availability and reliability of dynamic data. The project has devised means to assess the problem and has also begun work on approximate or heuristic approaches which would substantially

reduce the data robustness problems.

11.5 Computational speed

Computational speed could be a factor in obtaining real time controls, but advances in both hardware and algorithms are expected to solve these problems to a large extent in the time scale that this research is to be applied. Section 5 indicates the state of the art. In particular, one can typically compute 5 eigenvalues of a power system with 300 seventh order generator models in less than one minute using Matlab on a 233 MHz Pentium II. We view this result as encouraging progress towards using computed eigenvalues in real time control. Additional concepts that will help improve computational speed include the notion of continuously tracking eigenvalues, and the idea of distributed or parallel computation of eigenvalues.

11.6 Hybrid system/variable structure aspects

There are two aspects of the hybrid system/variable structure problem.

In the first aspect this variable structure (as, for example, in excitation system limits and look up tables) is a key feature of the power system data and needs to be systematically represented in data structures and algorithms, especially when computer algebra is applied. This aspect will yield good results from research and development effort.

In the second aspect, some of the controls or events associated with oscillations are variable structure as in the selection of exciters to be set to manual to suppress an oscillation and the prediction of oscillations if a transmission line trips. Both of these problems involve discrete changes in the equations modeling the system and are difficult to solve without the use of brute force computation exhaustively computing all the possibilities. Basic research to attempt to solve this aspect is indicated.

11.7 Staged approach to real time control of oscillations

A natural way to approach real time control of oscillations is to solve problems of increasing difficulty in stages. The suggested stages are

1. Off-line analysis tools

2. Real time suppression of ongoing oscillations

3. Real time avoidance of oscillations

Off line analysis is included since development of real time tools must pass through this stage for development and testing purposes and it allows value to be gained from partially developed real time methods. For example, the sensitivity methods developed in this project have many useful applications in off line studies.

Suppression of ongoing oscillations by operator actions is much easier than avoidance of oscillations because the system topology (fault condition) can be assumed to be known and the approximate oscillation frequency can be obtained from real time measurements. An approach to suppressing oscillations stressing both model based and heuristic or approximate methods and exploiting real time measurements is more likely to overcome the critical robustness to data problem discussed in section 11.4.

Real time avoidance of oscillations requires tackling the problem of predicting the effect of faults, a hybrid systems problem. This would require greater reliance on the dynamic model data and also more difficulty in estimating the frequency of potentially dangerous modes. Continuation and margin sensitivity techniques (section 4.8) could be applied to address such problems as transfer capability limited by oscillations.

All approaches would benefit from further advances in understanding oscillations and flexibly specifying and processing large dynamic power system models.

12 Project Management

This section presents the original project plan and its relation to the work done. Management problems solved during the project are also discussed.

12.1 Work statement/plan

This section reproduces the original project work statement annotated by references within square brackets [ ] to the section of this document which addresses that part of the plan.

12.1.1 Summary

Two complementary approaches will be pursued: The first approach exploits the eigenvalue and margin sensitivity formulas to select effective controls. The main challenges are identifying and controlling a set of critical modes in a large and nonlinear dynamic model, robustness to modeling errors, and computational efficiency. The second approach develops and tests approximate methods obtained by approximating the exact sensitivity computations or from heuristics. The main challenges are understanding the oscillations well enough to devise approximate methods and demonstrating that the approximate methods are effective. Basic to both approaches is devising scenarios of system oscillations to develop and test the proposed methods. Methods which can only work on small systems will not be pursued. Methods will be tested on the scenarios in order to assess whether the methods can be developed into tools of practical value in suppressing or avoiding oscillations in a real power system. Some of the methods may require supplementary observations or measurements (for example observing the oscillation frequency).

12.1.2 Tasks

1. Create test systems and test scenarios for power system oscillations on systems up to 37 buses [2.2,A]. The objective for the test systems is to develop sufficiently large and detailed power system dynamic models so that methods of avoiding and suppressing oscillations can be developed and their potential as a practical tool on much larger systems can be estimated. We plan to use systems of up to 37 buses to develop and assess methods. Issues to be addressed include detail of generator modeling (up to a dozen states per generator), assumptions about load modeling and possible ill conditioning due to algebraic equation singularity. The test scenarios will illustrate several ways in which an oscillation can arise [3]. For example, the oscillation could arise due to a increase in an interarea transfer or could be initiated by a line tripping. The

test scenarios should also include a case of multiple nearly critical oscillatory modes [7]. The planned software packages are Mathematica (very fast and flexible development of concepts), Matlab (good numerics and flexibility and compatibility with other PSerc projects) and PTI software (validation) [6.1].

2. Estimate feasibility of avoiding or suppressing oscillations by identifying and controlling critical oscillation modes using sensitivity formulas [11]. Demonstrate and evaluate methods on test scenarios [3,5]. Applying and efficiently computing the sensitivity formulas are important issues. Applying the formulas requires the critical modes to be identified and requires experiment with the range over which first order sensitivity formulas give useful estimates. A method to deal with multiple nearly critical oscillatory modes will be developed and assessed [7, 7.4.2]. Any problems in applying and computing the formulas will be identified and solved or assessed. Efficient computation will investigate and assess the use of state of the art algorithms exploiting sparsity. A key issue is computational time and its scaling with model size [5]. The use of measurements to supplement the computations will be investigated [9]. The robustness to model data will be assessed [3.8,3.9,4.7].

3. Develop approximate or heuristic methods to suppress oscillations [8,10]. Test and evaluate these methods on test scenarios [8]. The oscillations scenarios will be studied to improve understanding of the oscillations and their analyses with the objective of developing candidate methods of suppressing the oscillations. The effectiveness, justification and range of applicability of the candidate methods will be investigated. For example, approximations to exact calculations will be examined and analytical justification for heuristic methods will be attempted. The methods may use system measurements. The methods will be critically evaluated and tested on the oscillation scenarios to estimate their practical potential.

4. Write 6 month progress report outlining test scenarios and methods for suppressing or avoiding oscillations. [This item was addressed in part by writing a detailed progress report in November 1997 and providing regular summaries and presentations to the IAB as detailed in section 12.6.]

5. Write final report describing methods to suppress or avoid large scale power system oscillations, testing of the methods on oscillation scenarios and assessment of their potential to be developed into a practical tool [this report].

12.2 Deliverable

Final report describing methods to suppress or avoid large scale power system oscillations, testing of the methods on oscillation scenarios and assessment of their potential to be developed into a practical tool.

12.3 Budget and cash flow

Table 9: Project budget

Dobson	40,000
Alvarado	10,000
DeMarco	5,000
Sauer	5,000
Total	$ 60,000

The project was approved by the PSerc IAB in December 1996. The project work started in Fall 1997 with support from Dobson's NSF Presidential Young Investigator grant. PSerc funds were phased in as they became available and $55,000 of the project funding has been received to date as shown in Table 10.

Table 10: Project cash flow

Amount	Date received by UW/UIUC
25,000	August 1998
20,000	February 1999
20,000	July 1999
5,000	Not yet paid to UIUC

The project was originally planned to last one year, January - December 1997, but was extended in time with no extra cost. (The first portion of project funding was received in August 1998.) Partial support of the work in section 8 was also provided by the Western Area Power Administration.

The project work plan was ambitious in that it required both detailed modeling work based on industry data and the initial development of entirely new theoretical and software approaches. (Much project effort was spent preparing the 37 bus model equations and software in a form compatible with PSS/E and also on developing an initial understanding of new mechanisms for oscillations.)

In hindsight, the project was underfunded relative to the work done and the funding delays slowed progress and required inexperienced students to be trained.

These problems were solved by partial funding from other sources, mainly Dobson's NSF grant, and by considerable faculty overtime and by extending the period of performance. Thus the project goals were successfully achieved by the use of extra effort and resources.

12.4 Students

Graduate student Jianfeng Zhang is the principal student working on the project. Jianfeng Zhang started as a Masters student with a strong background in controls and developed his power systems expertise working on the project. Jianfeng Zhang is now working on his PhD at University of Wisconsin.

An experienced graduate student Scott Greene phased out of the project in Fall 1997 to work part time in industry and write up his PhD and graduated in 1998. Some of Scott's valuable expertise was transferred to others in the project team.

Undergraduate Henrik Engdahl assisted with setting up models and running PSS/E. Henrik was funded from Sweden and worked on the project from September 1997 to January 1998.

The turnover of students and the time spent training them on the project is a natural and expected consequence of the educational function of the university but has greatly slowed progress on the project. The available experienced PhD students used to estimate the project effort were largely unavailable by the time the project was approved and then funded.

12.5 Infrastructure

The project infrastructure included the use of two Power Macintoshes 7600 running at 132 MHz with 150 MB RAM and one external Jaz drive and a MMX Pentium PC running at 200 MHz with 48 MB RAM and an internal Jaz drive. The Macintosh software includes Mathematica and Matlab. The PC software includes Matlab and Pacdyn and the latest version of PSS/E software from PTI. The Power Macintoshes and PC purchase specifications were tailored to the project requirement to run the 37 bus system. (All these computers are now outdated). The project hardware and software was mainly funded by NSF.

12.6 Project reports and presentations

All reports and presentations, including this final report are available on the PSerc web site [60].

The reports and presentations to PSerc are

- brief work statement and slide presentation to PSerc IAB December 1996

- comprehensive project plan report June 1997
- slide presentation to PSerc IAB, Ithaca June 1997
- project plan and initial work report November 1997
- progress summary and slide presentation to PSerc IAB, IREQ June 1998
- progress summary and slide presentation to PSerc IAB, Vancouver December 1998
- progress summary and slide presentation to PSerc IAB, Madison June 1999
- progress summary for PSerc IAB, Tennessee October 1999
- this final report November 1999

The conference papers and talks to which the project contributed are

- I. Dobson, J. Zhang, S. Greene, H. Engdahl, P.W. Sauer, Is modal resonance a precursor to power system oscillations?, International symposium on Bulk power System Dynamics and Control-IV Restructuring, Santorini, Greece, August 1998, pp. 659-673.
- C.L. DeMarco, Identifying swing mode bifurcations and associated limits on available transfer capability, *Proceedings of the 1998 American Control Conference*, Philadelphia PA, June 1998, pp. 2980-2985.
- C.L. DeMarco, Network structure in swing mode bifurcations, *PSerc internet seminar*, 1998.

[Note added after original electronic publication: The project contributed to the following journal paper:

- I. Dobson, J. Zhang, S. Greene, H. Engdahl, P.W. Sauer, Is strong modal resonance a precursor to power system oscillations?, *IEEE Transactions on Circuits and Systems, Part 1*, vol. 48, no. 3, March 2001, pp. 340-349.]

A Detail of 3 bus and 9 bus models and test cases

A.1 3 bus test system

The dynamic model for both generators consists of a fourth-order synchronous machine (angle, speed, field flux, one damper winding) with an IEEE type I excitation system (third order), and a first-order model each for the turbines, boilers, and governors. The machine equations are (6.110–6.116), (4.98), (4.99), (6.118) and (6.121) in [67]. The limits on exciter voltage V_R and the steam valve P_{SV} are neglected.

All data is in per unit except that time constants are in seconds.

Three bus power system data

Generator	Exciter	Gov/Turbine
$T'_{do} = 5.33$	$K_A = 50$	$T_{RH} = 10.0$
$T'_{qo} = 0.593$	$T_A = 0.02$	$K_{HP} = 0.26$
$H = 2.832$	$K_E = 1$	$T_{CH} = 0.5$
$T_{FW} = 0$	$T_E = 0.78$	$T_{SV} = 0.2$
$X_d = 2.442$	$K_F = 0.01$	$R_d = 0.05$
$X_q = 2.421$	$T_F = 1.2$	$\omega_s = 120\pi$ rad/s
$X'_d = 0.830$	$S_E(E_{fd}) = 0.397\, e^{0.09E_{fd}}$	
$X'_q = 1.007$		
$R_s = 0.003$		

Load	Line 1-2	Line 2-3
$P_L = 1.0$	$R = 0.042$	$R = 0.031$
$Q_L = 0.3$	$X = 0.168$	$X = 0.126$
	$B = 2 \times 0.01$	$B = 2 \times 0.008$

The generator dispatch is controlled by a parameter α which specifies the proportion of power specified at the governors at buses 1 and 3:

$$P_{c1} = \alpha P_{ctotal}$$
$$P_{c3} = (1 - \alpha) P_{ctotal}$$

(P_{ctotal} is determined when the equilibrium equations are solved.) The base case has $\alpha = 0.5$ and the results are produced by decreasing α to 0.1 in steps of -0.1.

A.2 9 bus test system

The overall form of the 9 bus model is that of the WSCC system shown in Figure 7.4 of [67], except that PQ loads are added at buses one and two. The generators

are round rotor with IEEE Type 1 exciters. The generator dynamic equations are consistent with (6.173) to (6.181) of [67]. (Note that for (6.178), we omit T_{FW} and substitute T_M with $(w_s P_m - D(w - w_s))/w_s$, but this does not matter because D=0!) The generator algebraic equations are consistent with (6.186), (6.187) and (6.188) of [67]. The saturation function relations (131,132) in section A.2.1 are consistent with (6.189) to (6.193) of [67] and all the modeling in section A.2.1 is consistent with PSS/E.

The network data is given in Table 7.2 of [67]; other parameters are as follows. All data is in per unit except that time constants are in seconds.

Machine Data

Parameter	bus1	bus2	bus3
T'_{do}	8.96	8.5	3.27
T'_{qo}	0.31	1.24	0.31
T''_{do}	0.05	0.037	0.032
T''_{qo}	0.05	0.074	0.079
H	22.64	6.47	5.047
T_{FW}	0	0	0
X_d	0.146	1.75	2.201
X_q	0.0969	1.72	2.112
X'_d	0.0608	0.427	0.556
X'_q	0.0608	0.65	0.773
$X''_d = X''_q$	0.05	0.275	0.327
X_l	0.026	0.22	0.246
S_{GA}	0.898	0.911	0.825
S_{GB}	9.610	8.248	2.847

Exciter Data

Parameter	bus1,2,3
T_R	0
K_A	20
T_A	0.2
K_E	1.0
T_E	0.314
K_F	0.063
T_F	0.35
S_{EA}	2.5484
S_{EB}	0.5884

Load Data					
Parameters	bus1	bus2	bus5	bus6	bus8
P_L	1.80	0.50	0.25	0.25	1.0
Q_L	0.265	0	0.075	0.075	0.35

Bus 1 has a constant power load. The loads on buses 2,5,6,8 have real power loading of 40% constant current and 60% constant admittance and reactive power loads of 50% constant current and 50% constant admittance. Base MVA is 100 and the system frequency is 60 Hz. Bus voltage settings are $v1 = 1.02, v2 = 0.99, v3 = 1.005$.

The sources for the data are as follows: Exciter parameters are given in Table 7.3 of [67]. Data for bus 1 comes from [67]. Data for bus 2 comes from 37 bus system generator 5525; data for bus 3 comes from 37 bus system generator 3814. The following modifications were made: The values of X''_{d1} and X_{l1} for bus 1 were suggested by Graham Rogers. H_1 and H_3 were adjusted to obtain a case showing strong resonance.

A.2.1 Saturation

$$
\begin{aligned}
S_{fd} &= \frac{\psi''_d}{|\psi''|} S_{sm}(|\psi''|) \\
S_{1q} &= \frac{\psi''_q (X_q - X_l)}{|\psi''|(X_d - X_l)} S_{sm}(|\psi''|) \\
|\psi''| &= \sqrt{\psi''^2_d + \psi''^2_q} \\
\psi''_d &= \frac{(X''_d - X_l)}{(X'_d - X_l)} E'_q + \frac{(X'_d - X''_d)}{(X'_d - X_l)} \psi_d \\
\psi''_q &= \frac{(X''_q - X_l)}{(X'_q - X_l)} E'_d + \frac{(X'_q - X''_q)}{(X'_q - X_l)} \psi_q
\end{aligned}
$$

$$
S_{smi}(|\psi''|) = \begin{cases} 0 & \text{if} \quad |\psi''| \le S_{GA} \\ S_{GB}(|\psi''| - S_{GA})^2 & \text{if} \quad |\psi''| > S_{GA} \end{cases} \tag{131}
$$

$$
S_E(E_{fd}) = \begin{cases} 0 & \text{if} \quad E_{fd} \le S_{EA} \\ S_{EB}(E_{fd} - S_{EA})^2 / E_{fd} & \text{if} \quad E_{fd} > S_{EA} \end{cases} \tag{132}
$$

A.2.2 Loads

The load equations are

$$
P_L = (1 - \alpha_P - \beta_P) P_{L0} + irV + ggV^2 \tag{133}
$$

$$Q_L = (1 - \alpha_Q - \beta_Q)Q_{L0} + iiV + susV^2 \quad (134)$$
$$\alpha_P P_{L0} = irV \quad (135)$$
$$\beta_P P_{L0} = ggV^2 \quad (136)$$
$$\alpha_Q Q_{L0} = iiV \quad (137)$$
$$\beta_Q Q_{L0} = susV^2 \quad (138)$$

and the quantities used are presented in table 11.

quantity	description	dynamic model G	static model H	component of
V	voltage magnitude	algebraic variable	variable	y
P_L	total real power	algebraic variable	variable	y
Q_L	total reactive power	algebraic variable	variable	y
P_{L0}	load flow real power	parameter	parameter	p
Q_{L0}	load flow reactive power	parameter	parameter	p
ir	const. current coeff.(P)	parameter	variable	q
gg	conductance	parameter	variable	q
ii	const. current coeff.(Q)	parameter	variable	q
sus	susceptance	parameter	variable	q
α_P	fraction const. current(P)	constant	constant	
β_P	fraction impedance(P)	constant	constant	
α_Q	fraction const. current(Q)	constant	constant	
β_Q	fraction impedance(Q)	constant	constant	

Table 11: Load model quantities

On the transient timescale, V, P_L, Q_L are variables and ir, gg, ii, sus are parameters. On the steady state time scale, V, P_L, Q_L ir, gg, ii, sus are variables.

B Detail of 37 bus model and base case

The 37 bus system model is modified from a PSS/E format raw data of New York Power Pool as shown in Table 12. The 37 bus system model has 29 generators of 3 types(11 round rotor, 3 salient pole, 15 swing dynamics), 1 hydro governor, 12 exciters of 6 types, 6 stabilizers of 4 types, and 4 SVC of 2 types. In the project, only generators and exciters are modeled. Generator models GENROU, GENSAL, GENCLS and exciter model IEEET1, SEXS remain unchanged; other models are modified to these models. NYPP EXST1 model data effectively removed these exciters so that omission of these exciters from the project model is not an approximation. The equations of each model are in B.1. Exponential saturation is represented as in section A.2.1 but no hard limits are included. The load models are the same as in section A.2.2. The project model has 135 dynamic states, 289 algebraic states, and 120 parameters.

B.1 Model equations

GENROU

round rotor generator

$$
\begin{aligned}
T_{do}^{'}\dot{E}_{q}^{'} &= -E_{q}^{'} - (X_d - X_d^{'})(I_d - \frac{(X_d^{'} - X_d^{''})(\psi_d + (X_d^{'} - X_l)I_d - E_q^{'})}{(X_d^{'} - X_l)^2}) - S_{fd} + E_{fd} \\
T_{do}^{''}\dot{\psi}_d &= -\psi_d + E_q^{'} - (X_d^{'} - X_l)I_d \\
T_{qo}^{'}\dot{E}_{d}^{'} &= -E_{d}^{'} - (X_q - X_q^{'})(I_q - \frac{(X_q^{'} - X_q^{''})(\psi_q + (X_q^{'} - X_l)I_q + E_d^{'})}{(X_q^{'} - X_l)^2}) + S_{1q} \\
T_{qo}^{''}\dot{\psi}_q &= -\psi_q + E_d^{'} + (X_q^{'} - X_l)I_q \\
\dot{\delta} &= \omega_s n \\
2H\dot{n} &= \frac{1}{1+n}(P_M - Dn) - \frac{X_d^{''} - X_l}{X_d^{'} - X_l}E_q^{'}I_q - \frac{X_d^{'} - X_d^{''}}{X_d^{'} - X_l}\psi_d I_q - \frac{X_q^{''} - X_l}{X_q^{'} - X_l}E_d^{'}I_d - \\
&\quad \frac{X_q^{'} - X_q^{''}}{X_q^{'} - X_l}\psi_q I_d - (X_q^{''} - X_d^{''})I_d I_q
\end{aligned}
$$

GENSAL

salient pole generator

$$
\begin{aligned}
T_{do}^{'}\dot{E}_{q}^{'} &= -E_{q}^{'} - (X_d - X_d^{'})(I_d - \frac{(X_d^{'} - X_d^{''})(\psi_d + (X_d^{'} - X_l)I_d - E_q^{'})}{(X_d^{'} - X_l)^2}) - S_{sm}(E_q^{'}) + E_{fd} \\
T_{do}^{''}\dot{\psi}_d &= -\psi_d + E_q^{'} - (X_d^{'} - X_l)I_d
\end{aligned}
$$

PTI name	PTI ref	bus numbers	project modeling
		GENERATORS	
GENROU	V-29	51,136,1459,2855,3645,3814, 4305,5525,5890,5902,5903	modeled
GENSAL	V-33	2458,4895,6321	modeled
GENCLS	V-23	1,2812,2833,2834,2864,3517, 3520,3523,3814,4611,4656, 6597,6632,6659,6660	modeled
		GOVERNORS	
HYGOV	VI-91	4895	omitted
		EXCITERS	
EXAC3	VI-33	1459,3645	SEXS substituted
EXST1	VI-41	5890,5902,5903	omitted (see text)
EXST3	VI-47	2855	SEXS substituted
IEEET1	VI-49	51,136,3814,4895	modeled
IEEET5	VI-57	2458	approximated by IEEET1
IEEEX1	VI-59	6321	approximated by IEEET1
		STABILIZERS	
IEEEST	V-47	5890,5902,5903	omitted
PTIST1	V-51	4305	omitted
OEX12	VIII-117	5525	omitted
OSTAB5	VIII-125	5525	omitted
		SVC	
CHASVC	???	2473,2474	omitted
CSVGN1	V-11	4383, 9484	omitted

Table 12: NYPP 37 bus system models and their representation in project 37 bus system

$$
\begin{aligned}
T_{qo}^{''}\dot{\psi}_q &= -\psi_q + (X_q - X_q^{''})I_q \\
\dot{\delta} &= \omega_s n \\
2H\dot{n} &= \frac{1}{1+n}(P_M - Dn) - \frac{X_d^{''} - X_l}{X_d^{'} - X_l}E_q^{'}I_q - \frac{X_d^{'} - X_d^{''}}{X_d^{'} - X_l}\psi_d I_q - \frac{X_q - X_d^{''}}{X_q - X_l}\psi_q I_d
\end{aligned}
$$

GENCLS

swing equation generator

$$
\begin{aligned}
\dot{\delta} &= \omega_s n \\
2H\dot{n} &= \frac{1}{1+n}(P_M - Dn) - \frac{E_{fd}Vsin(\delta - \theta)}{X_s}
\end{aligned}
$$

IEEET1

IEEE type 1 exciter

$$
\begin{aligned}
T_E\dot{E_{fd}} &= -(K_E + S_E(E_{fd}))E_{fd} + V_R \\
T_F\dot{R_f} &= -R_f + K_F E_{fd} \\
T_A\dot{V_R} &= -V_R + \frac{K_A}{T_F}(R_f - K_F E_{fd})K_A(V_{ref} - V_T)
\end{aligned}
$$

SEXS

generic exciter

$$
\begin{aligned}
T_E\dot{E_{fd}} &= -E_{fd} + K(\frac{T_A}{T_B}(V_{ref} - V_T) + LL \\
T_B\dot{LL} &= -LL + (1 - \frac{T_A}{T_B})(V_{ref} - V_T)
\end{aligned}
$$

B.2 Base Case

bus number	Generator	Exciter	Pg	Load	Bus Voltage
1	GENCLS		30.8034	23.5072+12.3943i	0.9878
51	GENROU	IEEET1	33.42	20.5448+32.3948i	33.42
136	GENROU	IEEET1	31.13	52.0397+26.2982i	1.038
1377				27.1083+20.1042i	
1459	GENROU	SEXS	35.84		0.9834
2458	GENSAL	IEEET1	12.88	-14.9222+17.3697i	1.076
2812	GENCLS		235.0420	206.1759+47.5065i	1.0389
2833	GENCLS		234.6597	222.3754+49.5134i	1.0143
2834	GENCLS		235.0773	221.8341+49.3747i	1.0134
2855	GENROU	SEXS	74.35	166.0184+118.3536i	1.013
2864	GENCLS		235.7961	220.8136+49.3009i	0.9696
3517	GENCLS		231.7168	232.2607+51.8871i	1.0609
3520	GENCLS		233.8769	230.7088+52.6512i	0.9568
3523	GENCLS		229.0716	231.9886+55.0370i	1.0082
3645	GENROU	SEXS	6.417	3.2652+3.5105i	1.043
3814	GENROU	IEEET1	0.7641	230.3129+50.3509i	1.026
3814	GENCLS		230.4431		
3864				1.5749+0.9613i	
4305	GENROU		slack	7.1687+16.6267i	1.013
4383				2.4897+3.5288i	
4387				5.8764+8.0557i	
4611	GENCLS		223.0368	230+50i	1.0148
4656	GENCLS		223.6187	231.3877+51.2139i	1.0155
4895	GENSAL	IEEET1	23.57	15.8173+15.0123i	1.040
5506				19.7403+28.3319i	
5525	GENROU		61.71	10.0594+15.6871i	1.066
5685				37.1967+27.9934i	
5686				26.4481+22.5839i	
5890	GENROU		35.22		1.021
5902	GENROU		20.61		1.008
5903	GENROU		20.61		1.032
6188				15.3363+11.2270i	
6321	GENSAL	IEEET1	10.73		1.011
6597	GENCLS		227.4630	233.6991+52.4896i	0.9909
6632	GENCLS		227.1556	234.1364+55.2911i	1.0954
6659	GENCLS		230.9616	229.4764+49.8269i	1.0298
6660	GENCLS		230.9871	229.4807+50.1727i	1.0298
9484				2.2096+3.6136i	

Table 13: 37bus basecase

References

[1] E.H. Abed, P.P. Varaiya, Nonlinear oscillations in power systems, *International Journal of Electric Energy and Power Systems*, vol. 6, no. 1, Jan. 1984, pp. 37-43.

[2] V. Ajjarapu, B. Lee, A general approach to study both static and dynamic aspects of voltage stability, *Proceedings of the 31st Conference on Decision and Control*, Tucson, AZ, December 1992, pp. 2916-2919.

[3] F. L. Alvarado. Computational complexity in power systems. *IEEE Transactions on Power Apparatus and Systems*, 95(4), July/August 1976, pp.1028–1037.

[4] F.L. Alvarado, Z. Wang, Direct sparse interval hull computations for thin non-M matrices, *Interval Computations*, March 1993, pp. 5-28.

[5] G. Angelidis, A. Semlyen, Improved methodologies for the calculation of critical eigenvalues in small signal stability analysis, *IEEE Trans. Power Systems*, vol. 11, no. 3, Aug 1996, pp. 1209-1217.

[6] V.I. Arnold, *Geometrical methods in the theory of ordinary differential equations*, Springer-Verlag, NY, 1983.

[7] P.M. Anderson,A.A. Fouad, *Power System Control and Stability*, Iowa State University Press, Ames Iowa, 1977.

[8] R. Bacher: Automatic code differentiation applied to OPF code: An example of using a "symbolic" tool (ADIFOR) for advanced software development. Presentation at the IEEE/PES Winter Power Meeting, New York, February 1999.

[9] A.R. Bergen, *Power Systems Analysis*, Prentice-Hall, Englewood Cliffs NJ, 1986.

[10] P. Billingsley, *Probability and measure*, second edition, Wiley 1986, theorem 27.2, page 369.

[11] R. T. Byerly, R. J. Bennon, and D. E. Sherman. Eigenvalue analysis of synchronizing power flow. In *Power Industry Computer Applications Conference*, pages 134–142, 1981.

[12] C.A. Cañizares, Conditions for saddle-node bifurcations in AC/DC power systems, *Electrical Power & Energy Systems*, vol.17, no.1, 1995, pp. 61-68.

[13] *Time-Scale Modeling of Dynamic Networks with Applications to Power Systems*, J. H. Chow, ed., Springer-Verlag, Berlin, 1982.

[14] J. H. Chow, New Algorithms for Slow Coherency Aggregation of Large Power Systems, from *Systems and Control Theory for Power Systems*, J. H. Chow, P. V. Kokotovic, R. J. Thomas, ed., Springer-Verlag, New York, 1995.

[15] K.E. Chu, On multiple eigenvalues of matrices depending on several parameters, *SIAM Journal of Numerical Analysis*, vol. 27, no. 5, October 1990, pp. 1368-1385.

[16] Cigré Task Force 07 of Advisory Group 01 of Study Committee 38, Analysis and control of power system oscillations, Paris, December 1996.

[17] G. E. Coxson, Computing Exact Bounds on Elements of an Inverse Interval Matrix is NP-Hard, *Reliable Computing*, vol. 5, no. 2, 1999, pp. 137-142.

[18] C. L. DeMarco, J. J. Wasner, A generalized eigenvalue perturbation approach to coherency, pp. 605-610, *Proc. IEEE Conference on Control Applications*, Albany, NY, Sept. 28-29 1995.

[19] C.L. DeMarco, Identifying swing mode bifurcations and associated limits on available transfer capability, *Proceedings of the 1998 American Control Conference*, Philadelphia PA, June 1998, pp. 2980-2985.

[20] F. P. deMello and C. Concordia. Concepts of synchronous machine stability as affected by excitation control. *IEEE Transactions on Power Apparatus and Systems*, 88:316–329, April 1969.

[21] I. Dobson, Fernando Alvarado and C. L. DeMarco, Sensitivity of Hopf bifurcations to power system parameters, Proceedings of the 31st Conference on Decision and Control, Tucson, Arizona, December 1992.

[22] I. Dobson, L. Lu, Voltage collapse precipitated by the immediate change in stability when generator reactive power limits are encountered, *IEEE Transactions on Circuits and Systems, Part 1*, vol. 39, no. 9, Sept. 1992, pp. 762-766.

[23] I. Dobson, J. Zhang, S. Greene, H. Engdahl, P.W. Sauer, Is modal resonance a precursor to power system oscillations?, International symposium on Bulk power System Dynamics and Control-IV Restructuring, Santorini, Greece, August 1998, pp. 659-673.

[24] L.H. Fink, ed., Proceedings: Bulk power system voltage phenomena, voltage stability and security, ECC/NSF workshop, Deep Creek Lake, MD, Aug. 1991, ECC Inc., 4400 Fair Lakes Court, Fairfax, VA 22033-3899.

[25] I. S. Duff, J. A. Scott, Computing selected eigenvalues of sparse unsymmetric matrices using subspace iteration, *ACM Transactions on Mathematical Software*, vol. 19, No. 2, June 1993.

[26] G. Golub, C. VanLoan, *Matrix Computations*, Johns Hopkins University Press, Baltimore, 1983.

[27] J. Guckenheimer, P. Holmes, *Nonlinear Oscillations, Dynamical Systems, and Bifurcations of Vector Fields*, Springer-Verlag, NY, 1983.

[28] A.M.A. Hamdan, The SVD of system matrices and modal properties in a two-area system, *Electric Machines and Power Systems*, vol. 26, no. 7, Aug/Sept 1998, pp. 671-684.

[29] J. Hauer, D. Trudnowski, G. Rogers, B. Middlestadt, W. Litzenberger, J. Johnson, Keeping an eye on power system dynamics, *IEEE Computer Applications in Power*, vol. 10, no. 4, October 1997, pp. 50-54.

[30] I. Hiskens, D. Hill, Dynamic aspects of voltage collapse, in [24].

[31] IEEE Committee Report, Computer representation of excitation systems, *IEEE Transactions on Power Apparatus and Systems*, vol. PAS-87, no. 6, June 1968, pp. 1460–1470.

[32] IEEE Power system engineering committee, *Eigenanalysis and frequency domain methods for system dynamic performance*, IEEE Publication 90TH0292-3-PWR, 1989.

[33] IEEE Power Engineering Society Systems Oscillations Working Group, Inter-Area Oscillations in Power Systems, IEEE Publication 95 TP 101, October 1994.

[34] N. Jaleeli, et. al., Understanding automatic generation control, *IEEE Transactions on Power Systems*, vol. 7, no. 3, Aug. 1992, pp. 1106-1122.

[35] W.J. Ji, V. Venkatasubramanian, Dynamics of a minimal power system: Invariant tori and quasi-periodic motions *IEEE Transactions on Circuits and Systems Part I*, vol. 42,no. 12, December 1995, pp. 981-1000.

[36] L.E. Jones, *On zero dynamics and robust control of large AC and DC power systems*, PhD thesis, ISSN 1100-1607, Royal Institute of Technology, Stockholm, Sweden, 1999.

[37] K. Kim, H. Schättler, V. Venkatasubramanian, J. Zaborsky, P. Hirsch, Methods for calculating oscillations in large power systems, *IEEE Transactions on Power Systems*, vol. 12, no. 4, November 1997, pp. 1639-1648.

[38] M. Klein, G.J. Rogers, P. Kundur, A fundamental study of inter-area oscillations in power systems, *IEEE Transactions on Power Systems*, vol. 6, no. 3, August 1991, pp. 914-921.

[39] M. Klein, G.J. Rogers, S. Moorty, P. Kundur, Analytical investigation of factors influencing power system stabilizers performance *IEEE Transactions on Energy Conversion*, vol. 7, no. 3, Sept. 1992, pp. 382-390, also reprinted in [33].

[40] P. Kundur, G. J. Rogers, D. Y. Wong, L. Wang and M. G. Lauby, A comprehensive computer program package for small signal stability analysis of power systems, *IEEE Transactions on Power Systems*, vol. PWRS-5, no. 4, November 1990, pp. 1076-1083.

[41] P. Kundur, *Power System Stability and Control*, McGraw-Hill, NY, 1993.

[42] G.L. Kusic, *Computer-Aided Power Systems Analysis*, Prentice-Hall, Englewood Cliffs, NJ, 1986.

[43] H.G. Kwatny, X.-M. Yu, Energy analysis of load-induced flutter instability in classical models of electric power networks, *IEEE Trans. Circuits and Systems*, vol. 38, no. 12, December 1989, pp. 1544-1557.

[44] H.G. Kwatny, G.E. Piper, Frequency domain analysis of Hopf bifurcations in electric power networks, *IEEE Trans. Circuits and Systems*, vol. 37, no. 10, October 1990, pp. 1317-1321.

[45] L.T.G. Lima, N. Martins, and H.J.C.P. Pinto. Mixed real-complex factorization. *IEEE Transactions on Power Systems*, vol. 8, no. 1, February 1993, pp. 302-308.

[46] C.-M. Lin, V. Vittal, W. Kliemann, A.A. Fouad, Investigation of modal interaction and its effects on control performance in stressed power systems using normal forms of vector fields, *IEEE Transactions on Power Systems*, vol. 11, no. 2, May 1996, pp. 781-787.

[47] Y.V. Makarov, V. A. Maslennikov, D.J. Hill, Calculation of oscillatory stability margins in the space of power system controlled parameters, Proceedings Stockholm Power Tech, Stockholm, June 18-22, 1995, pp. 416-421.

[48] Y.V. Makarov, V. A. Maslennikov, D.J. Hill, Revealing loads having the biggest influence on power system small disturbance stability, *IEEE Transactions on Power Systems*, 11(4):2018–2023, November 1996.

[49] Yuri V. Makarov, Zhao Yang Dong, and David J. Hill. A general method for small signal stability analysis. *IEEE Transactions on Power Systems*, 13(3):979–985, August 1998.

[50] N. Martins, Efficient eigenvalue and frequency response methods applied to power system small-signal stability studies, *IEEE Transactions on Power Systems*, vol. PWRS-1, no. 1, 1986, pp. 217-226.

[51] Nelson Martins and Leonardo T. G. Lima. Eigenvalue and frequency domain analysis of small-signal electromechanical stability problems. In C. W. Taylor and R. G. Farmer, editors, *Eigenanalysis and Frequency Domain Methods for System Dynamic Performance*, pages 17–33. IEEE, Piscataway, New Jersey, 1990. Publication IEEE 90TH0292-3-PWR.

[52] Y. Mansour, Application of eigenanalysis to the Western North American Power System, in [32], pp. 97-104.

[53] *MATLAB User's Guide*, The MathWorks, Inc., Natick, MA, 1993.

[54] A. Neumaier, *Interval Methods for Systems of Equations*, (Encyclopedia of Mathematics and Its Applications 37), Cambridge University Press, 1990.

[55] Y. Obata, S. Takeda, and Suzuki. An efficient eigenvalue estimation technique for multimachine power systems. *IEEE Transactions on Power Apparatus and Systems*, 100:259–263, January 1881.

[56] M. A. Pai, *Energy Function Analysis for Power System Stability*, Kluwer Academic Publishers, Boston, 1989.

[57] F. Luis Pagola, Ignacio Pérez-Arriaga, and George Verghese. On sensitivities, residues and participations: Applications to oscillatory stability analysis and control. *IEEE Transactions on Power Systems*, pages 278–285, February 1989.

[58] I. J. Perez-Arriaga, G. C. Verghese and F. C. Schweppe, Selective modal analysis with applications to electric power systems, Part I and II, *IEEE Transactions on Power Apparatus and Systems*, vol. PAS 101, no. 9, 1982, pp. 3117-3134.

[59] J.W. Pierre, D.J. Trudnowski, M.K. Donnelly, Initial results in electromechanical mode identification from ambient data, *IEEE Transactions on Power Systems*, vol. 12, no. 3, August 1997, pp. 1245-1251.

[60] http://www.pserc.wisc.edu (click on "research" and then "avoiding and suppressing oscillations").

[61] G. Rogers, Demystifying power system oscillations, *IEEE Computer Applications in Power*, vol. 9, no. 3, July 1996, pp. 30-35.

[62] G. Rogers, Power system structure and oscillations, *IEEE Computer Applications in Power*, vol. 12, no. 2, April 1999, pp. 14-.

[63] J. Rohn, *SIAM J. Numer. Anal.*, vol. 30, 1993, pp. 864-870.

[64] J. Rohn, Cheap and tight bounds: The recent result by E. Hansen can be made more efficient, *Interval Computations* 4, 1993, pp. 13-21.

[65] P.W. Sauer and M.A. Pai, Power System Steady State Stability and the Load-Flow Jacobian, *IEEE Trans. on Power Systems*, vol. 5, no. 4, pp. 1374-1383, Nov. 1990.

[66] P. Sauer, M.A. Pai, S. Fernandes, I. Dobson, F. Alvarado, S. Greene, R.J. Thomas, H.-D. Chiang, Final Report, Empire State Electric Energy Research Corporation Project EP 95-11, *Real Time Control of Oscillations of Electric Power Systems*, September 1996.

[67] P. W. Sauer, M. A. Pai, *Power System Dynamics and Stability*, Prentice-Hall, Englewood Cliffs NJ, 1998.

[68] A. P. Seyranian, Sensitivity analysis of multiple eigenvalues, Mechanics of structures and machines, vol. 21, no. 2, 1993, pp. 261-284.

[69] A. P. Seiranyan, Collision of eigenvalues in linear oscillatory systems, Journal of Applied Mathematics and Mechanics, vol. 58, no. 5, 1994, pp. 805-813.

[70] R. Seydel, From equilibrium to chaos: practical bifurcation and stability analysis, Elsevier, New York OR the second edition Springer-Verlag, New York, 1994.

[71] T. Smed, Feasible eigenvalue sensitivity for large power systems, *IEEE Transactions on Power Systems*, vol. 8, no. 2, May 1993, pp. 555-563.

[72] S.K. Starrett, A.A. Fouad, Nonlinear measures of mode-machine participation, *IEEE Transactions on Power Systems* vol. 13, no. 2, May 1998, pp. 389-394.

[73] D. J. Trudnowski, J. M. Johnson, J. F. Hauer, SIMO system identification from measured ringdowns, Proceedings of the American Control Conference, Philadelphia, Pennsylvania, USA June 1998, pp. 2968-2972.

[74] J.E. Van Ness, F.M. Brasch, G.L. Landgren, S.T. Naumann, Analytical investigation of dynamic instability occurring at Powerton station, *IEEE Transactions on Power Apparatus and Systems*, vol. PAS-99, no. 4, July/Aug 1980, pp. 1386-1395.

[75] G.C. Verghese, I.J. Perez-Arriaga, F.C. Schweppe, and K.W-K. Tsai, Selective Modal Analysis in Power Systems, Electric power Research Institute Report 1764-8, January 1983.

[76] L. Wang and A. Semlyen, Application of sparse eigenvalue techniques to the small signal stability analysis of large power systems, *IEEE Transactions on Power Systems*, vol. 5, no. 2, May 1990, pp. 635-642.

[77] R.W. Wies, J.W. Pierre, Use of LMS adaptive filtering technique for tracking simulated low-frequency electromechanical modes of power systems, *North American Power Symposium*, Laramie, Wyoming, October 1997, pp. 354-358.

[78] J. E. Van Ness, F. M. Brasch, G. L. Landgren, and S. T. Naumann. Analytical investigation of dynamic instability occurring at powerton station. *IEEE Transactions on Power Apparatus and Systems*, 99:1386, 1980.

[79] Z. Wang, Sparsity Preservation in Matrix Interval Solutions within Power System Applications, PhD thesis, Dept. of Electrical and Computer Engineering, University of Wisconsin-Madison,1994.

[80] S. Wiggins, *Introduction to applied nonlinear dynamical systems and chaos*, Springer-Verlag, NY, 1990.

[81] A. J. Wood, B. F. Wollenberg, *Power Generation Operation & Control*, Wiley, NY 1984.

[82] D. Y. Wong, G. J. Rogers, B. Poretta and P. Kundur, Eigenvalue analysis of very large power systems, *IEEE Trans. Power Systems*, PWRS-5, no. 2, May 1990, pp. 635-642.

[83] EPRI Final Report, Application of taxonomy theory, Part I: Research Project 3573-10, April 1995, prepared by Washington University in St. Louis, System Science and Mathematics, St. Louis, Missouri.